UNIVERSITEIT VAN PRETORIA
UNIVERSITY OF PRETORIA
YUNIBESITHI YA PRETORIA

# Development of an approach to incorporate proportional hazard modelling into a risk-based inspection methodology for an optimal inspection policy

**by Nzita Alain Lelo**

Submitted in partial fulfilment of the requirements for the degree

**Philosophiae Doctor (Mechanics)**

in the

Department of Mechanical and Aeronautical Engineering

Faculty of Engineering Built Environment and Information Technology.

University of Pretoria

July 2024

## Abstract

Title: Development of an approach to incorporate proportional hazard modelling into a risk-based inspection methodology for an optimal inspection policy.

| | | |
|---|---|---|
| Author | : | Nzita Alain Lelo |
| Supervisor | : | Professor P.Stephan Heyns |
| Co-Supervisor | : | Professor J.Wannenburg |
| Department | : | Mechanical and Aeronautical Engineering |
| University | : | University of Pretoria |
| Degree | : | Philosophiae Doctor (Mechanics) |

Keywords: Risk-based inspection (RBI), proportional hazard model (PHM), probability of failure ($PoF$), the consequence of failure ($CoF$), boiling expanding vapour explosion (BLEVE).

The health and safety of pressure vessels are a concern in the power, chemical, petrochemical, and other industries handling gases or liquids at high temperatures. The content of a pressure vessel usually is at a substantially different pressure than the ambient pressure, and if not handled carefully it can lead to fatal accidents such as an explosion. Therefore, industry decision makers rely on a risk-based approach to perform inspection and maintenance on the pressure vessel.

According to the Risk-Based Inspection and Maintenance Procedures project (RIMAP) for the European industry, risk has two main components: the probability of failure ($PoF$) and the consequence of failure ($CoF$). As one of these risk drivers, a more accurate estimation of the $PoF$ will contribute to a more accurate risk assessment. Current methods to estimate the probability of failure are either time-based or founded on expert judgement. This work proposes enhancements to the quantitative risk assessment for the probability of failure ( $PoF$) and the consequence of failure ($CoF$) through the utilization of a newly proposed methodology.

The proposed methodology consists of incorporating the proportional hazard model (PHM), which is a statistical procedure to estimate the risk of failure for a component subject to condition monitoring, into the risk-based inspection (RBI) methodology so that the $PoF$ estimation can be enhanced to optimize inspection policies.

To achieve the overall goal of this work, case studies applying the PHM to determine the $PoF$ for real-time condition data components, are discussed. Also, considering the consequences of failure due to accidents which can occur in pressure vessels using steam and water as reference material, boiling expanding vapour explosions (BLEVEs) are especially important due to their severity and diverse effects such as overpressure, thermal radiation and missile ejection. By way of example this work considers only the overpressure due to BLEVE to model the $CoF$.

The first benefit of this work is that by incorporating PHM with the RBI approach, the PHM uses real-time condition data, to allow dynamic decision-making on inspection and maintenance planning. An additional advantage of the PHM is that where traditional techniques might not give an accurate estimation of the remaining useful life to plan an inspection, the PHM method can consider the condition as well as the age of the component.

Another benefit of this work is that risk-based inspection is presently one of the best methodologies to provide an inspection schedule and ensure the mechanical integrity of pressure vessels. RBI usually provides an inspection schedule based on calendar or usage time intervals. This work however optimizes the inspection schedule on pressure vessels, by incorporating proportional hazard modelling (PHM) into RBI methodology as stated above.

The work presented here comprises the application of the newly proposed methodology in the context of pressure vessels, considering the important challenge of possible explosion accidents due to boiling liquid expanding vapour explosion (BLEVE) as the consequence of failure calculations. The proposed risk management methodology incorporates a quantitative assessment of the Probability of Failure ($PoF$), based on Proportional Hazard Modelling (PHM), and the Consequence of Failure ($CoF$), of an explosion event. The unmitigated risk is thereby quantified by means of a risk matrix, which enables evaluating and deciding on suitable risk mitigation strategies.

## Acknowledgements

I would like to thank and acknowledge the following for their support and guidance in the completion of this work:

- My supervisors, Professor P.S. Heyns and Professor J. Wannenburg for their assistance, advice and guidance throughout my studies.
- The Eskom Power Plant Engineering Institute (EPPEI) and Anglo American Platinum for their support.

I also gratefully acknowledge the assistance of the following people that made it possible for me to succeed in my studies:

- My wife Diba Tshilenge Solange and children Ed, Gad and Faith Lelo for their sacrifices and encouragement throughout my studies in South Africa.
- However, most of all to God, my Creator, for keeping me alive and allowing me to reach the end of this project despite of challenges on my path.

## List of publications based on the candidate's research.

Journal papers:

1. Lelo, N.A., Heyns, P.S. & Wannenburg, J. (2022). Development of an approach to incorporate proportional hazard modelling into a risk-based inspection methodology. *Journal of Quality in Maintenance Engineering*, Vol. 29, pp.265-286.
2. Lelo, N.A., Heyns, P.S. & Wannenburg, J. (2019). Forecasting spare parts demand using condition monitoring information. *Journal of Quality in Maintenance Engineering*, Vol. 26, pp.53-68
3. Lelo, N.A., Heyns, P.S. & Wannenburg, J. (2024). The application of risk-based inspections on furnace high-pressure cooling systems incorporating proportional hazards and steam explosion consequence modelling. *Journal of Quality in Maintenance Engineering*. (Accepted for publication).
4. Lelo, N.A., Heyns, P.S. & Wannenburg, J. (2024). Risk mitigation decision based on quantified risk in industrial plant. *International Journal of Risk Assessment and Management* (Submitted).

Conference papers:

1. Lelo, N.A. (2019). A comparison between time-based and condition-based approach for spare part demand decision. Applied Reliability and Durability Conference, Berlin, Germany, April 2019.

## Notation

| | | |
|---|---|---|
| API | : | . American Petroleum Institute |
| BLEVE | : | Boiling liquid expanding vapour explosion. |
| $CoF$ | : | Consequence of failure |
| CWA: CEN | : | European committee for standardization workshop agreement |
| DRA | : | Dynamic risk assessment |
| GFF | : | Generic failure frequency |
| HP | : | High pressure |
| IMS | : | Intelligent maintenance system |
| LPG | : | Pressurized liquid gas |
| MTTF | : | Mean time to failure |
| MW | : | Molecular weight |
| NDT | : | Non-destructive testing |
| NBP | : | Normal boiling point |
| $PoF$ | : | Probability of failure |
| PFM | : | Probabilistic fracture mechanics |
| PGM | : | Platinum group metal |
| PHM | : | Proportional hazard model |
| RBI | : | Risk-based inspection |
| RIMAP | : | Risk-based inspection and maintenance procedure project |
| RMS | : | Root mean square |
| SHE | : | Safety health and environment |
| SVEE | : | Specific volume entropy and enthalpy |
| SLT | | Superheated limit temperature |
| TPM | : | Transition probability matrix |
| VCE | : | Vapour cloud explosion |

# Contents

# Chapter 1. Introduction

## 1.1 Problem statement

Failure of pressure vessels presents a major risk to many industries and therefore the design and integrity management of pressure vessels are regulated through international codes and standards. Traditionally one of the principal integrity management measures prescribed by these standards has been to perform over-pressure testing at defined intervals during the life of a vessel, which ensures that defects which may exist and do not cause failure during such a test would safely propagate without reaching critical dimensions before the next test is performed. Due to the cost of performing these tests, an alternative integrity management approach has been developed, which is called risk-based inspection (RBI).

The RBI approach replaces regulatory over-pressure testing on pressure vessels with maintenance actions such as repair and replacement based on inspection non-destructive testing (NDT) results. Because failure of pressure vessels can have catastrophic consequences, the inspection regime (where and when to do inspections) needs to be risk-based.

RBI is a methodology designed to prioritize maintenance activities. This approach is prescribed in industrial standards, such as the American Petroleum Institute (API 581) for the petrochemical industry and the European Committee for standardization Workshop Agreement (CWA 15740) standard for the power generation industry. This risk of failure of the pressure vessel is calculated as the product of the consequence of failure ($CoF$) and the probability of failure ($PoF$). Often, the $PoF$ is more difficult to determine and is the parameter that one wants to reduce through the implementation of the RBI regime and the $CoF$ is a given and easy to define.

The standards define various ways (qualitative and quantitative) to estimate risk. Quantitative methods are required for critical vessels and failure on such vessels. Preferably, the quantitative method will be based on failure models, where the relationship between the inspection results (condition parameters) and remaining useful life is known. In cases where the failure model is not known or accurate, the next best practice would be to use failure statistical methods and supplement this with Bayesian methods when data is scarce. Since RBI implies that inspections are performed and therefore that appropriate condition indicators will be available, it is argued

that it would be highly desirable to employ both statistical failure statistics, as well as the condition data, to estimate the $PoF$.

Although RBI is preferred instead of overpressure testing for pressure vessels, the following challenges remain:

- To obtain a $PoF$ that is as accurate as possible. The American Petroleum Institute which developed a well-established methodology (API 581) to implement RBI, suggests a quantitative approach based on two Weibull parameters to compute the $PoF$. However, this is fundamentally a time-based approach, which does not consider the condition of the asset. The major problem here is to have a $PoF$ as accurate as possible to be computed with the $CoF$ for a better risk assessment and inspection schedule.
- Since RBI implies that inspections are performed and therefore that condition parameters will be available, it is argued in this research that in these cases, a need exists for $a\ PoF$ estimation method, which uses both the statistical failure statistics, as well as the condition data, to estimate the $PoF$.
- Another focus of this research lies in the quantification of the consequence of failure ($CoF$), which is illustrated through a case study. This particular case study involves a complex real-world problem associated with the high-pressure cooling system of a coal-fired furnace. The failure of this system could result in a steam explosion known as a boiling liquid expanding vapour explosion (BLEVE).

The modelling of the $CoF$ will be based on BLEVE theory, as BLEVEs are of particular importance among the various major accidents that can occur in process industries and during the transportation of hazardous materials. This is due to their severity and the fact that they involve a simultaneous occurrence of diverse effects, which can have a significant impact over a large area. These effects include overpressure, thermal radiation, and missile ejection. However, in this research, we will only focus on the overpressure resulting from BLEVEs. One safety concern that will be taken into account is the mixing of water and hot molten material within the converter. The converter consists of an air-cooled hearth system, a water-cooled crucible, and a high-pressure boiling system. Ultimately, it is necessary to develop strategies for mitigating the risk in order to reduce the estimated risk to an acceptable level.

## 1.2 Literature review

A literature review is conducted to support the development of the new approach to fill the gap related to the traditional risk-based inspection methodology. The content of this section is arranged as follows: In section 1.2.1, the traditional approach for risk-based inspection is addressed, whereafter the development of an approach to a dynamic risk assessment is considered in section 1.2.2. Finally, boiling liquid expanding vapour explosion is investigated in section 1.2.3.

### 1.2.1. Risk based inspection.

Industry uses risk-based approaches to schedule inspection and maintenance programs (Giribone & Valette, 2004). Risk-based inspection is generally presented as an approach to prioritize and plan inspection. RBI has in the past been predominantly applied on pressure vessels.

#### 1.2.1.1. Probability of failure estimation in the CWA methodology

Risk assessment can generally be addressed as follows:

- Qualitative or screening level (expert judgement)
- Semi-quantitative (rule-based analysis)
- Quantitative (probabilistic, statistical, mathematical modelling)

1) Qualitative assessment (screening level)

Singh and Pretorius (2017) describe the basic steps of the CWA methodology, which address the risk analysis on multiple levels, progressing from the initial screening step to a detailed quantitative assessment.

During the screening stage, the assessment of risk consists of screening the components. The $PoF$ estimation is performed by determining several specific criteria that could influence the $PoF$.

The screening analysis is relatively fast, simple, and cost-effective. During the screening, component risks are ranked using criteria like ‘high’, ‘medium’ and ‘low’ risk levels. After screening the components, semi-quantitative analysis can be performed for components that

fall into high and medium-risk categories, while components in the low-risk category continue to be subjected to the required maintenance.

The probability of failure at the screening stage is assessed by considering criteria such as:

- Presence of degradation
- Year of the last inspection
- Component age
- Rate of degradation
- Design concerns
- Previous repairs of damage
- Rate of degradation, etc.

with each criterion having an associated weighting. The weight of each criterion is assigned according to the level of influence it has on the probability of causing failure. Furthermore, each criterion is scored relative to a qualitative measure of its influence on the component.

To produce a precise probability of failure $PoF$, the score criterion expressed by $C$ is multiplied by the weighting of the criterion expressed by $W$. The sum of that product for different components is then multiplied by the generic failure frequency $GFF$, which is a factor used based on experience to identify failure frequencies of different components. $GFF$ is typically developed using expert judgement and a history of component failure.

$$PoF = \sum_{1}^{i} \{[(C1 \times W1) + (C2 \times W2) + (C_i \times W_i)] \times (GFF)\} \quad (1)$$

2) Semi quantitative assessment (level two risk assessment)

Once the low-risk components have been screened out as described in the previous paragraph, the high and medium-risk components go to the semi-quantitative assessment (Shanil & Pretorius, 2017).

The purpose of the level two $PoF$ assessment is to determine the detailed factors that may affect the identified damage mechanisms for a given component. The generic failure frequency ($GFF$) is once again used, but for this level, actual failure frequencies obtained from industry experience, are used where available. In instances where no industrial $GFF$ data is available,

the RBI team will revert to the $GFF$ values that were used in the previous $PoF$ determination. The level two risk calculation is performed in the same manner as the level one risk calculation. However, in the level two $PoF$ assessment the number of criteria for the component under analysis is greater than the previous assessment level.

These criteria include the same as for level 1 as was listed in the previous section. But in addition to these there are now more specific criteria such as: Total starts per year, time since the last inspection, presence of hot spot, nominal operating temperature, corrosion susceptibility, Frequency of temperature excursions, the severity of temperature excursions. These additional criteria goes a level deeper than level 1 criteria, the aim of the level two $PoF$ assessment is to determine in greater detail the factors that may affect the identified damage mechanisms for the component under analysis.

3) Quantitative assessment (Level three risk assessment)

The quantitative or detailed approach is essentially based on calculating the remaining useful life for the component under analysis. No further calculation is required when the calculation indicates that there is an acceptable period before failure. Otherwise, even more, detailed calculations are performed.

In the CWA 15740, the detailed risk assessment follows almost the same rules as in the screening level, although in greater detail. For most critical components, the CWA procedure suggests a more detailed analysis where the damage mechanism can be identified, and the degradation rate obtained. The $PoF$ can then be estimated (Jovanovic, 2004).

The quantitative methods for determining the $PoF$ described above, can be divided into two discernible approaches. In the case where an accurate failure model is available and expected loading and environmental conditions are quantifiable, the life expectancy for an identified failure mode is calculated. In this calculation, the ageing damage accumulation is estimated and forms the basis of risk-based decisions in terms of inspection schedules. Such inspections monitor the damage parameters, such as crack sizes or corrosion damage and are essentially a condition monitoring activity. Depending on the observed damage found during these inspections compared to the failure model results, remaining useful life (RUL) calculations are performed to trigger repair/replacement decisions, or updated future inspection schedules. This includes the case where RBI implementation is done on existing equipment, which would already have accumulated damage. Again, future inspection schedules are based on a calculated

RUL, with a failure model being available and pre-existing damage parameters having been measured.

In the case where an accurate failure model is not available, inspection schedules are based on historical or generic failure statistics, to estimate failure rates and probabilities. In this second approach, the inspections, or condition monitoring, are also aimed at finding damage (e.g., cracking or corrosion damage), but since a failure model is not available to estimate a RUL, any indication of damage would typically lead to repair/replacement actions.

RUL and the P-F curve

1) Introduction

Condition monitoring (CM) is a practice that involves monitoring the condition of equipment through various non-intrusive testing methods, supervisory control and data acquisition , visual inspection, and other testing methods (Ochella, Shafiee & Sansom, 2021). The selection of the appropriate testing method for a particular equipment depends on the equipment's failure modes being monitored. Predictive testing and inspections play a vital role in the detection of incipient faults and performance deterioration (Square et al., 2017). These inspections include vibration monitoring, infrared thermography, ultrasonic noise (acoustics) measurements, lubricant (oil) analyses, temperature measurements, flow characteristics, ultrasonic thickness measurements, eddy current testing, and motor current signature analysis, among others (Nguyen, Fouladirad, & Grall, 2018). A detailed coverage of CM is crucial for equipment maintenance and management.

Lorenzoni et al. (2017) investigated the complexities related to logistics concerning the upkeep of offshore assets. In their study, the degradation of components was modelled using dynamic Bayesian networks, where the P-F curve represented the degradation pattern and was modelled as a reversed exponential function. The P-F curve's characteristic in the study was influenced by maintenance activities and operating conditions, which were considered in order to derive the health state of the equipment. The study employed five distinct health states to characterize operating equipment, namely: new or as good as new, very slight indication of degradation, serious degradation, stage of rapid decline, and finally, stage with very high probability of failure.

2) Potential failure curve (P-F curve)

Based on the data acquired from prognostic testing and inspection tasks, the state of an asset, when plotted against an elapsed time, manifests the potential failure or P-F curve. Figure 1 exhibits a typical P-F curve. The P-F curve derives its name from its ability to denote the exact point at which a monitored asset's failure becomes detectable. This point is referred to as the potential failure point, P. From the inception of an asset's service life to a particular point, any malfunction is indiscernible due to the monitored asset's parameters, such as temperature, vibration, lube oil analysis, etc., indicating that the asset remains in a healthy state devoid of detectable defects (Lorenzoni et al., 2017). However, incipient failure becomes detectable at a certain time when deviations start to occur. The duration from the point of actual detection of potential failure to the point of functional failure is known as the P-F interval curve (Wiseman et al., 2006). It is desirable for the P-F interval to be ample, allowing for both decision-making and maintenance as well as life-extension undertakings, to ensure the success of the entire endeavour.

A P-F curve is an important tool when managing an asset. It is a common way to represent the behaviour of an asset before a functional failure occurs. It shows the declining performance of an asset or a component over time, until it reaches a functional failure. Since failure is a process which can be caused by wear, fatigue, corrosion etc., these failure modes do not necessarily immediately cause the asset to reach the state of functional failure. In these cases the deterioration can be tracked, and the P-F interval can be used to define the inspection policy.

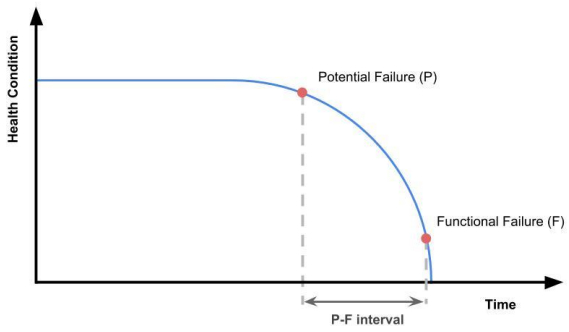


*Figure 1: P-F Curve*

P expresses the potential failure point, which is the point where it is possible to detect that failure is about to occur. The detection of P is usually done through condition indicators. F is the functional failure point or the failed state.

The P-F interval is the time between the potential failure point to functional failure, and the P-F interval length is an important key to defining the inspection frequency. The determination of P is usually flagged at the attainment of specified values of some condition indicators. This could however be challenging.

- P-F interval determination: The visual representation in figure 1 provides a clear demonstration of how equipment performance can deteriorate over time due to a single failure mode. Additionally, one must realise the varying capabilities of different condition monitoring (CM) techniques in detecting failure at different stages. Notably, it is worth mentioning that conducting a visual inspection at point P may not enable the detection of the exact size of a crack. However, deploying a more accurate inspection technique such as radiography, just after point P, might yield a range of possible P-F intervals. These intervals provide a window in which maintenance intervention can be planned and implemented. Therefore, for critical equipment, it is imperative to continuously monitor using appropriate technologies and techniques to ensure early detection (Lorenzoni et al., 2017). Furthermore, it is essential to acquire data at the appropriate frequency to facilitate the P-F curve's effectiveness in identifying equipment deterioration. In simpler terms, the inspection interval should be shorter than the P-F interval to capture faulty conditions before failure.
- Relationship between P-F interval, useful life and asset life: Lorenzoni et al. (2017) provided a definition for useful life, denoted as the duration from the commencement of service to the age at which the likelihood of failure significantly increases. This may or may not align with the emergence of incipient failure. Jardine et al. (2013) characterized RUL as "the remaining time prior to observing a failure, given the current state and age of the machine, as well as the past operational profile." In essence, the lifetime of an asset can be segregated into the useful life (normal operating state) and the faulty state during which the asset operates with an existing fault. Many articles in the literature designate these two operational zones as the "stable zone" and "failure zone," respectively. Consequently, the entire lifespan of the asset $La$, is defined as the summation of the durations in which the asset is in a satisfactory health status and the period in which it operates in an unsatisfactory state until it fails. The lifespan of the asset can be expressed using the equation: $Asset\ life = Useful\ life + Faulty\ zone\ asset$. The faulty zone comprises the P-F interval (P-F interval) and $td$, which denotes the time difference between the actual onset of incipient failure and its

detection using sensor devices. Thus, the lifespan of the asset can be represented by equation: $La = Lu + (td + PF\ interval)$. The primary aim of life-extension measures is to prolong the service life of an asset beyond its original design lifetime. When a fault is detected, a life-extension measure is implemented, and the equipment's state returns to a condition that is almost as good as new.

#### 1.2.1.2. Other risk assessment techniques

Quantitative Risk Analysis (QRA) pertains to the quantitative evaluation of risk through the application of mathematical methodologies grounded in engineering assessments, aiming to integrate estimations of incident probabilities and consequences (Song, 2018). A variety of methodologies have been devised for conducting quantitative risk analyses, with the traditional approaches such as Fault Tree (FT), Event Tree (ET), and Bow-tie (BT) standing out as the most prominent. These analyses play a crucial role in risk assessment by assessing the effectiveness of safety measures in avoiding or minimizing accident repercussions. For instance, FT, which is widely utilized, delineates the logical connections from root causes to the top event qualitatively through gates, while quantitatively revealing the potential impact of a failure.

However, these traditional risk assessment techniques are characterised by their static nature, failing to adapt to evolving operational circumstances or modifications (Khan & Abbasi, 1998). Besides, conventional risk assessment techniques, in addition to generic failure data utilization, are typically identified by their non-case-specific nature, thereby introducing uncertainty into the outcomes. The limitations associated with these techniques have spurred the emergence of dynamic risk assessment methods, which aim to provide a more refined evaluation. These methods focus on the continual reassessment of risk by updating the initial failure probabilities of events and safety barriers as new information becomes available during a specific operation.

The revision of prior failure probabilities is currently accomplished through two primary approaches. Firstly, Bayesian strategies involve the utilization of new data in the form of likelihood functions to update prior failure rates using Bayes' theorem. Secondly, non-Bayesian updating approaches rely on real-time monitoring of parameters, inspection of process equipment, and the application of physical reliability models to supply new data (Abimbola et al., 2014).

The evaluation of risk assessment techniques outlined in the preceding paragraph has revealed deficiencies in both the traditional static approaches and the dynamic method that relies heavily on expert judgment, thus hindering its fully quantitative nature.

Consequently, the present study aims to explore a dynamic risk assessment approach that is entirely quantitative and can effectively mitigate the limitations associated with current methodologies.

#### 1.2.1.3. $PoF$ estimation using failure statistics.

The quantitative approach for RBI uses also statistical models, which are based on collecting data from plant experience for given components. Generic databases often assume that the failure rate is shaped as a 'bathtub' over a component's lifetime and is divided into three zones (Jovanovic, Auerkari & Brear, 2001). If the failure rate is constant, the time to failure is exponentially distributed.

The complexity of industrial systems is a prevailing characteristic; however, repairs are possible in multiple cases. It is often challenging to obtain historical or benchmarking data regarding system failures and repair patterns, and such data can be unreliable due to practical constraints. Thus, a good reliability, availability and maintainability (RAM) analysis is crucial during the design phase and any modifications necessary to achieve optimized system performance (Afsharnia, 2017). Proper maintenance performance requires an assessment of component reliability, which is based on knowledge about component states. During the early stages of new system development, the uncertainty or unknown states of components are common. Therefore, understanding how uncertainties affect system reliability evaluation is essential. The reliability of systems depends on age, intrinsic factors such as dimensioning, component quality, and material, as well as use conditions such as environment, load rate, and stress. The failure rate $\lambda$ is the parameter that defines a machine's reliability, and it represents the frequency of breakdown occurrences. Failure rate analysis is a strategic method for integrating reliability, availability, and maintainability using techniques such as mean time to failure ($MTTF$), asset downtime, and system availability values. These methods and tools enable the identification and quantification of equipment and system failures that hinder the achievement of objectives.

1) Failure rate

The machine's reliability is determined by its ability to carry out its designated task within a predetermined time frame while adhering to certain limitations and prerequisites. The operational availability of a machine is directly proportional to its reliability; hence it can be defined as the duration during which the machine can function without any malfunctions. The reliability of equipment is contingent on the frequency of failures, which is quantified by the mean time between failures ($MTBF$). The estimation of reliability is based on failure rates (Afsharnia, 2017). The failure intensity or $\lambda(t)^2$ is defined as "the expected number of times an item will fail during a specified period, given that it was in perfect condition at time zero and is operating at time $t$." This computed value serves as a measure of equipment reliability. At present, this value is expressed as failures per million hours ($f/mh$). The calculations of failure rates are based on intricate models that integrate various component-specific data such as stress, environment, and temperature. In the prediction model the organization of assembled components follows a serial order. Consequently, the computation of failure rates for assemblies entails the summation of individual failure rates for the components within said assemblies.

$$\lambda = \frac{1}{MTBF} \qquad (2)$$

where $MTBF$ is mean time between failure.

2) Mean time between failure ($MTBF$)

The fundamental metric for assessing reliability is the $MTBF$ for an asset that can be repaired. $MTBF$ represents the duration elapsed before a component, assembly, or system failure, assuming a constant failure rate. The $MTBF$ of repairable systems refers to the estimated interval between two consecutive system failures. It is a widely employed variable in the analysis of reliability and maintainability. The $MTBF$ can be computed as the reciprocal of the failure rate λ, for systems with a constant failure rate. For example, if a component has a failure rate of 2 failures per million hours, the $MTBF$ would be the inverse of the failure rate λ.

$$MTBF = \frac{Total\ time}{number\ of\ failures} = \frac{1}{\lambda} \qquad (3)$$

According to Reiter (2017) the mean time between failures ($MTBF$) is just the sum of mean time to failure ($MTTF$) with the mean time to repair ($MTTR$). The term "repair" may be used interchangeable with other terms such as "replacement" or "replenishment," and thus, is referred to as "downtime." It is important to note that $MTBF$ includes downtime whereas $MTTF$ does not. In most cases, $MTTR$ is much smaller in comparison to $MTTF$, resulting in $MTTF$ being like $MTBF$. Nonetheless, $MTBF$ and $MTTF$ differ significantly in larger and more comprehensive systems such as production lines and aircraft since they contain numerous component parts, leading to a lower $MTBF$ and a higher downtime. As a result, industry has accepted either $MTTF$ or $MTBF$ as interchangeable terms with the same meaning. However, while functional safety engineers tend to use $MTTF$, logistics and maintenance personnel tend to prefer $MTBF$.

The second way to differentiate between $MTTF$ and $MTBF$ may not be common, but it is equally important. It has been mathematically proven (Reiter, 2017) that in redundant or fault-tolerant systems, the $MTTF$ is distinct from the $MTBF$ in steady state. This distinction between $MTTF$ and $MTBF$ becomes particularly important when the useful product life can be associated with either the "setting time" characterized by $MTTF$, or the steady state, characterized by $MTBF$.

#### 1.2.1.4. Bayesian Approach

1) Introduction

Augmenting the quantitative approach based on failure statistics can be done using Bayesian Statistics. Bayes' rule for events can be expanded to define a Bayes' rule for random variables and their distribution functions. The expanded rule can be used to combine a prior distribution and a likelihood function to produce a posterior distribution. The posterior distribution can subsequently be used as an input in risk analysis. The Bayes' rule can be written as (Guyonnet, 2009):

$$P(A|E) = \frac{P(A) \times P(E|A)}{P(E)} \quad (4)$$

where $P(A|E)$ is the Posterior: Probability distribution of the parameter (A) given data set (D); $P(E|A)$ is the likelihood. A function of the observed data (E) given a parameter (A); $P(A)$ is the prior: Probability distribution of the parameter (A) which represents our belief on the parameter before the dataset D is observed; $P(E)$ is the evidence: probability distribution of the observed data (D) which acts as a normalizing constant that ensures the cumulative posterior distribution sum to 1.

Usually, decision-making based on statistical lifetime data as well as condition monitoring data requires a large set of data which often is incomplete or missing. To overcome that problem, the use of expert judgement is accommodated using Bayesian statistics. The essential element is the revision of probabilities based on new information (Jardine & Tsang, 2013).

As previously argued, risk-based approaches for the scheduling of inspections are becoming common. The Bayesian approach is well suited for this because it allows a systematic integration of expert judgement and data obtained from ongoing inspections (Aven & Pörn, 1998).

2) Frequentist and Bayesian differences

Frequentist and Bayesian methodologies are distinguished by their varying approaches. The frequentist regards model parameters as unknown, but fixed constants, relying solely on observed data in order to estimate their values. In the context of failure time data, it is common to assume that such data is exponentially distributed.

$$f(x;\lambda) = \frac{1}{\lambda} e^{-x/\lambda} \quad (5)$$

where $\lambda$ is the parameter of interest, $MTBF$. The maximum likelihood estimator for $\lambda$ in this equation is simply the total test time divided by the number of failures which provides a point estimate for $MTBF$. To provide an account of the variability in the estimation process, a confidence interval, typically a one-sided lower bound, can be computed (Shamshoian et al., 2022). However, when the dataset is limited or no failures are observed, the bounds may be considerably wide and insufficiently informative. Additionally, in the absence of failures, a

point estimate cannot be determined due to division by zero. Furthermore, it is important to note that confidence bounds do not signify the parameter's range of values, but instead represent the uncertainty related to the sampling method (Harman, 2018). It is therefore appropriate to state that "we anticipate that 90% of the estimated intervals will encompass the population parameter."

Bayesian methods treat parameters as unknown random variables whose distribution (the prior) represents the current belief about the parameters. Bayes' rule is defined in equation 2.

The maximum likelihood estimation (MLE) serves as a tool to identify optimal parameter values that most effectively align with a given dataset, utilizing a predetermined distribution. The likelihood term serves as a representation of this form of information. It is important to note that unlike in non-Bayesian analyses, the likelihood and prior serve as inputs within Bayesian analysis, rather than outputs. In Bayesian analysis, the posterior is a probability distribution function (pdf) of the parameter given the dataset, rather than simply a point estimate. This enables the application of all pdf properties within the analysis, signifying a critical juncture in the process.

The difference between frequentist and Bayesian approaches diminish as the sample size is augmented. Nevertheless, the variances can be considerable for small datasets, with Bayesian interval evaluations frequently exhibiting narrower margins than the frequentist techniques.

Steps to implement Bayesian analysis are:

- Choose a prior distribution that describes the belief of the $MTBF$ parameter. Any prior distribution may be selected, provided it precisely characterizes the parameter information that is known and is established prior to the collection of any fresh data. For instance, in the context of failure times, we opt for an inverse gamma distribution, as it pertains to the example at hand.
- Collect failure time data and determine the likelihood distribution function: Many defence systems' failures are often assumed to conform to an exponential distribution; nonetheless, this assumption may not always hold true (Harman, 2018).
- Use Bayes' rule to obtain the posterior distribution: The posterior distribution is formed by the combination of the prior distribution and the likelihood distribution. Generally, any combination of these distributions is possible. However, in the general case, numerical methods such as Markov chain Monte Carlo (MCMC) are necessary.

Nevertheless, there exist certain combinations of distributions that lead to closed form posteriors having the same form as the prior distribution. These combinations are known as conjugate priors. For the case of exponential likelihood and inverse gamma prior, the resulting posterior distribution is an inverse gamma distribution (Shamshoian et al., 2022).

- Use the posterior distribution to evaluate the data.

#### 1.2.1.5. Framework of the existing method to estimate the $PoF$

Below is given a framework showing the existing or traditional methods to estimate the $PoF$.

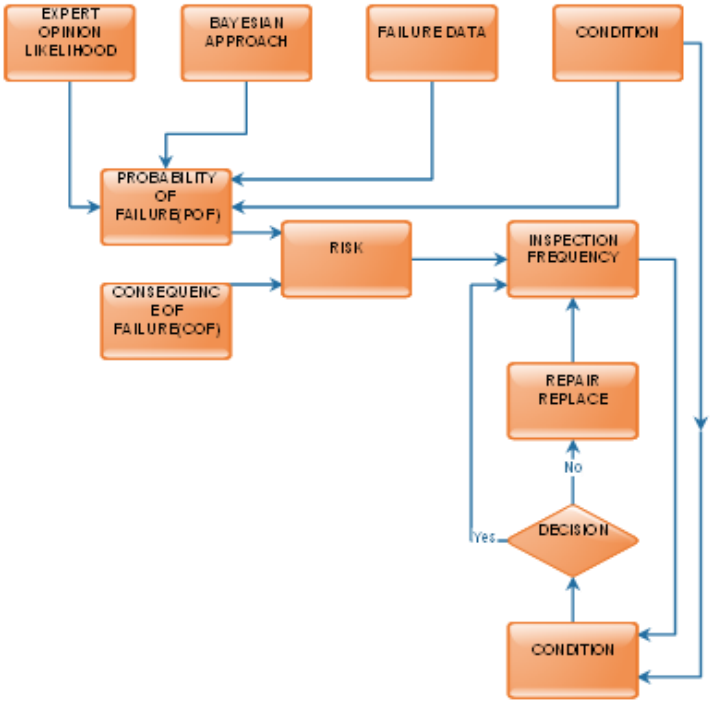


*Figure 2: Framework summarising the existing methods.*

Figure 2 represents a framework for the existing procedure to estimate the Probability of Failure ($PoF$) to assess risk. The framework is essentially constituted by four main blocks (Expert opinion likelihood block, Bayesian Approach block, Failure data block and Condition block) which are existing $PoF$ estimation methods serving respectively as input to the risk assessment in the framework. A closed loop part which captures risk indices is used to decide either to repair, replace or let the component run according to the severity of the risk index (Shamshoian et al., 2022).

In summary, Figure 2 represents the progression in risk assessment, starting from the non-quantitative approach, which is prevalent and offers no dynamic view of risk assessment, to the time-based approach, which may lead to the early replacement of components that still have a useful life. Framework describing the existing method to estimate the $PoF$ in RBI.

The traditional risk assessment addressed in this section is based on the CWA procedure and the API standard and assumes that the system or the component is still safe for operation between the planned inspection intervals. This assumption yielded many accidents (Bhatia, Khan, Patel & Abbassi, 2019). Therefore, there is a need for an innovative approach, which allows dynamic risk assessment (DRA).

### 1.2.2. Development of an approach to a dynamic risk assessment

#### 1.2.2.1. Introduction

Modern industries emphasise safety and risk prevention. This has led to the growth of risk-based inspection as one of the best approaches for scheduling inspection. Section 1.1 stated that over the two past decades, the American Petroleum Institute (API) and the Risk-based Inspection and Maintenance Procedure (RIMAP) project have published standards and guidelines to facilitate the determination of the inspection interval based on equipment life degradation rate, environmental impact, etc.

The underlying assumption of these approaches is that risk must remain acceptable between two planned inspections or maintenance intervals (Zio, 2018). This assumption may however not be suitable for degrading, fast-changing, and complex engineering systems (Bhatia et al., 2019). To deal with this challenge, researchers developed an innovative dynamic risk assessment (DRA) methodology to assess risk for a dynamically changing system. Dynamic risk can be defined as a risk profile that provides the status of risk at any given time and can be updated upon the availability of new information (Zio, 2018).

#### 1.2.2.2. Overview of the existing dynamic risk assessment methods

In his lookout on future risk assessment, Zio (2018) presents a detailed review of the recent literature related to dynamic risk assessment. From the literature, dynamic risk models can be classified into three categories.

- Data-based approach: In this approach, risk updates are based on accident or near-miss data. Also, as soon as new data are recorded, they are integrated into the model to update the risk computation. Statistical tools such as fault trees, event trees, or Bayesian networks are used in this approach to define the relationship among initiating events.
- Process-based approach: This approach is based on the fact that any change in the process parameters is likely to change the risk. All changes are monitored to update the risk calculation.
- Degradation-based approach: In this approach, the system's condition is monitored in real-time, and risk computation is updated based on continuous degradation. The degradation mechanism rate must be estimated based on experience and available data.

Meel and Seider (2006) utilised the Bayes' Theorem method to dynamically update the estimate of accident probabilities, using near misses and accident data collected from equivalent systems.

Along the same lines, Kalantarnia, Khan and Hawboldt (2009) developed a method where the Bayesian Theorem was utilised to update probability and event tree (ET) analysis was used for consequence modelling. Khakzad, Khan and Amyotte (2012) combined the Bayes' theorem with the bow-tie (BT) model. The failure probabilities of the primary event and safety barriers in the BT were continuously revised over time, and the updated BT model was used to update the risk.

The main drawback of the DRA methods as mentioned above, which is also the case for many other DRA methods, is that they use only statistical data to update the estimated risk value. Using only statistical data, updating risk indices only happens when accidents or near misses occurring.

To fill the gap identified in sections 1.2.1 and 1.2.2, a condition-based approach would resolve the shortcomings related to the non-quantitative and time-based approaches by tracking the condition of a component. Being able to estimate the remaining useful life of a component, allows inspection and replacement to be planned. However, the condition-based approach relies on the availability of an accurate failure model. When this is not available the time-based approach would be the only option, even though the inspections performed because of the RBI assessment, will continuously add information, which will be under-utilised, only being used to inform replacement/repair decisions based on conservative acceptance criteria. Hence, this

research proposes to combine the condition-based approach with component age, using a proportional hazard model (PHM). Section 1.3 addresses the suggested method to respond to the shortcomings highlighted in this paragraph.

As risk is computed based on both $PoF$ and $CoF$, the following section addresses the $CoF$ estimation.

### 1.2.3. Consequence of failure modelling

Consequences of failure are usually considered to consist of four aspects: (1) health ($CoF_{health}$), safety ($CoF_{safety}$), environment ($CoF_{environment}$), and business ($CoF_{business}$). The safety, health and environment (SHE) consequences are important in any scenario where a loss of containment takes place (Heerings & den Herder, 2004).

According to the RIMAP, the $CoF$ assessment follows the same pattern as the $PoF$, which means they are all based on a certain scenario. Section 1.2.1.1 describes the $PoF$ computation performed from the screening level known as level 1, semi-detailed known as level 2 and the detailed level, which is level 3, the consequence of failure analysis follows the same logic from level 1 to level 3 in the RIMAP approach. In the RIMAP approach, the screening level is performed by expert opinion without any numerical analysis.

However, according to API 581, the consequence of failure is presented into two categories. These are the consequences based on the affected area and financial consequences (Syawalina, Priyanta & Siswantoro, 2020).

The consequence analysis in the RBI (API 581) consists of allowing one to rank the asset items based on risk and providing a suitable inspection schedule. According to API 581, the computation of the consequences is based on empirical equations. The consequence results are expressed in terms of impact area in quantitative terms (Vianello, Guerrini, Maschio & Mura, 2014).

Loss of containment of dangerous fluids from pressurized processing equipment may result in damage to surrounding equipment, serious injury to personnel, production losses, and undesirable environmental impact (Henry & Osage, 2014). The consequences of failure are calculated using well-known consequence analysis methods and are presented as an affected

impact area or in financial terms (Shishesaz, Nazarnezhad Bajestani, Hashemi & Shekari, 2013).

The impact areas from incident outcomes such as pool fires, fireballs, and vapour cloud explosions are quantified based on the outcome of thermal radiation and overpressure on surrounding equipment and personnel. API 581 provides two levels of consequences analysis:

#### 1.2.3.1. LEVEL 1 Consequence analysis

A level 1 consequence analysis evaluates the consequence of hazardous releases for a limited number of reference fluids. The reference fluid that closely matches the normal boiling point and molecular weight of the fluid contained within the process asset should be used. The following are some reference fluids for the level 1 consequence analysis (Henry & Osage, 2014): Water; Steam; Acid; Ammonia; Chlorine; Hydrogen (H); Hydrogen fluoride (HF).

The first step is to determine the $CoF$ by selecting from the above list the reference fluid that most closely matches the normal boiling point (NBP) and molecular weight (MW) of the fluid contained within process equipment. The subsequent steps consist of calculating the release rate that depends on the physical properties of the material, the phase of the fluid and the process operating conditions and the allocated release hole size (Prayogo, Haryadi, Ismail & Kim, 2016).

#### 1.2.3.2. LEVEL 2 Consequence Analysis

Level 2-consequence analysis provides a detailed approach to determine the consequences of loss of containment of dangerous fluids from pressurized equipment.

Level 2-consequence analysis was developed as a tool to use where the assumption of level 1 consequence analysis is not valid. Examples of where level 2 calculation may be desired or necessary are cited below:

- When the stored fluid is close to its critical point, the ideal gas assumptions for the vapour release equations are no longer invalid.
- When incorporating the impact of two-phase emissions, which encompasses both jet entrainment and rainout, into the methodological framework, it becomes imperative.
- When the specific fluid is not sufficiently described in the compilation of available reference fluids, this includes situations where the fluid is a diverse combination of

substances with different boiling points or when the harmful effects of the fluid are not adequately represented by any of the reference fluids (Henry & Osage, 2014).

Since the high-pressure cooling system supporting the converter experiences multiple leaks in the case of the system under consideration, these cause safety risks because leaks on the HP are a serious problem that can result in steam explosions in the converter (which is a pyro metallurgical process devices able to transform raw material in another form of substrate). This challenge of a potential steam explosion will be the focus of the following analysis.

Consequence modelling in this work is performed according to the boiling liquid expanding vapour explosion (BLEVE) theory defined in the following section.

#### 1.2.3.3. Boiling liquid expanding vapour explosion (BLEVE)

##### 1) Definition

The definition of boiling liquid expanding vapour explosion (BLEVE) has been established by the Centre for Chemical Process Safety as the sudden release of a substantial amount of pressurized superheated liquid into the atmosphere (Abbasi & Abbasi, 2007). This sudden release can be attributed to various factors such as containment failure due to fire engulfment, missile impact, corrosion, manufacturing defects, or internal overheating. Birk et al. (2018) have defined a BLEVE as the explosive release of expanding vapour and boiling liquid when a container holding a pressure-liquefied gas fails catastrophically. They have also defined "catastrophic failure" as the sudden opening of a tank to release its contents almost instantaneously. The instantaneous and explosive boiling-vaporisation resulting from the release of previously pressurized and liquefied vapour causes a series of cataclysmic impacts.

- A boiling liquid expanding vapour explosion (BLEVE) can result in several consequences.
- The generation of short-lived pools of liquid, which may ignite if the liquid is flammable, a blast wave.
- The creation of flying fragments or missiles; and the release of fire or toxic gases. If the pressurized liquefied vapour is flammable, the BLEVE can result in the formation of a fireball. In cases where the substance undergoing a BLEVE is toxic, such as with ammonia or chlorine, the negative effects can include the dispersion of toxic gases.

## 2) Mechanism of BLEVE occurrence

Birk et al. (2018), Behrouz and Casal (2017), Birk (2008) and Abbasi (2007b) among others, have presented detailed descriptions of the events leading up to a BLEVE. Drawing from their observations a typical BLEVE can be broken down into the following steps:

- A container holding pressurized liquid gas (PLG) is subject to a heat load or experiences failure due to missile impact, fatigue, or corrosion. If a container holding pressure-liquefied gas is accidentally heated, for instance, due to nearby fire radiation, the pressure inside the container will begin to increase. Once the pressure reaches the set pressure of the pressure relief valve, the valve will open, allowing liquid vapour to escape into the atmosphere. As the liquid vaporises, the portion of the vessel wall that benefits from liquid cooling decreases. Eventually, the remaining metal may become weakened and rupture, even if the pressure relief valve is functioning correctly. A container may also fail in the absence of fire if it is struck by missiles from an adjacent exploding vessel, or due to other forms of mechanical failure such as gland/seal loss, sample line breakage, fatigue, or corrosion.
- The container ruptures. A pressure vessel is designed to withstand the pressure relief valve set pressure, but only under design temperature conditions. If the metal is heated due to a nearby fire, its strength may decrease enough to cause rupture. For example, the steel commonly used in LPG containers may fail when the container is heated to approximately 650°C and its pressure reaches approximately 15 atm. The container may also rupture due to mechanical failure, as explained in the previous paragraph.
- There is instantaneous depressurization and explosion, when a vessel experiences failure, an immediate depressurization occurs. The liquid that was previously at a high pressure and corresponding temperature is abruptly reduced to atmospheric pressure but remains at a temperature above the liquid's atmospheric pressure boiling point, resulting in superheating. However, each liquid has a different superheat limit temperature (SLT) which it can withstand. If the temperature of the liquid in the depressurized vessel exceeds its SLT, there will be instantaneous and homogeneous nucleation, leading to a violent release of a large portion of the liquid in a boiling liquid expanding vapor explosion (BLEVE) that occurs within one millisecond of depressurization. If the liquid is below its SLT but still in a state of significant superheat, a BLEVE can still occur due to factors such as depressurization waves and

the presence of likely heterogeneous nucleation sites. According to Abbasi and Abbasi (2007b) Prugh was among the first to emphasize that a BLEVE can occur even at initial temperatures below the superheat limit, but the higher TNT equivalent for BLEVE occurs near or above the SLT. BLEVEs have been observed with propane at ambient temperature, well below its atmospheric superheat limit temperature. However, for a violent and explosive boiling to occur, there must be potential for superheat in the liquid when it is suddenly exposed to a pressure below its saturation pressure due to the initial tank failure. This is particularly relevant for pressure-liquefied gases (PLGs), which are substances that are held as liquids in pressurized containers despite being in a gaseous state at atmospheric pressure. Examples of PLGs include industrial chemicals such as liquid petroleum gas, compressed natural gas, and liquefied chlorine, as well as superheated water in a boiler.

- When the vessel shatters, the liquid vaporizes suddenly and generates a powerful overpressure blast wave due to the several hundred-fold to over a thousand-fold increase in volume of the vaporizing liquid and expansion of the already existing vapour. The magnitude of the blast wave is much higher than that caused by a vapour cloud explosion occurring in an identical scenario. The quantity of substance is a critical factor in the event of a vessel shattering and its fragments being propelled in various directions. The splashing of the substance may lead to short-lived pools nearby, which may ignite if the liquid is flammable. The resulting missile fragments can cause damage to other vessels containing liquefied gas under pressure, leading to further BLEVE incidents. This chain reaction has been observed in various tragic accidents, including the one in Mexico City, which resulted in the most significant loss of life in a process industry explosion-cum-fire accident. In some cases, the vessel fragments themselves can become missiles and travel long distances, causing destruction at unexpected locations.
- Additionally, if the substance involved is not combustible or toxic, the pressure wave and missile effects are the only consequences of the explosion. However, in most cases, flammable chemicals are involved, and the explosion results in a mixture of liquid and gas, which ignites, leading to the formation of a fireball. Analysis of past BLEVE accidents has shown that over two-thirds of all incidents involve flammable chemicals, resulting in intense thermal radiation that causes massive damage. The size, shape, and heat load of the fireball are influenced by various factors, such as the presence of air

and the amount of fuel involved. Not all the fuel may burn, and some may escape through cracks or openings in the vessel. In BLEVE disasters like those in Mexico City, fragments of shattered vessels can carry flammable liquid, leading to fires in the surrounding areas and threatening other vessels.

3) Impact or consequence of BLEVE

The evaluation of the impact or the consequences of a BLEVE are determined by two essential factors: The energy of the explosion also called “burst energy**,** consists of determining the severity of the blast wave generated by and the velocity of the missiles formed out of the vessel fragments.

Generally, two treatments have been used to evaluate the burst energy related to the BLEVE: The method developed by Prugh, as documented by Abbasi is the so called “TNT equivalent method “which considers the expanding vapour as an ideal gas. The second method, also named SVEE method, is also a thermodynamic method like that of Prugh, but it is distinguished by the use of specific volume, entropy and enthalpy (SVEE).

However, this work uses the TNT method in chapter 3 to compute the BLEVE energy, overpressure and the distance from the accident epicentre (Abbasi & Abbasi, 2007).

While there exist more rigorous approaches that exhibit a greater degree of consensus regarding their applicability for the explosion of vessels containing pressurized gases, caused explosives, and vapour cloud explosions (VCE), the level of uncertainty is much higher in the context of BLEVE scenarios which involve superheated liquids and pressurized gases (Abbasi & Abbasi, 2007). In the case of a BLEVE, in which a vessel containing a superheated liquid undergoes a catastrophic failure, the "boiling liquid" and the "expanding vapour" jointly provide the burst energy. However, it becomes quite challenging to determine the contribution of each phase, since the events occurring between the initial crack and the crack's propagation up to the occurrence of the BLEVE have an impact on the state of both phases, as elaborated in the preceding section. Additionally, a certain amount of the burst energy gets expended in shattering the vessel, another portion is utilized in propelling the vessel fragments, and yet another in the generation of the blast wave. The cooling effect of the flash vaporization of the liquid and the adiabatically expanding vapour only serve to further complicate the situation. Once a vessel is shattered, some of its contents can also form transient pool fires by getting splashed on the floor before evaporating, which may reduce the quantity of the vessel contents

that form the fireball. Below, we present an overview of the state-of-the-art of BLEVE consequence assessment. Classically, two methods have been employed to estimate BLEVE energy.

#### 1.2.3.4 Analysis of risks of pressure vessel

***1) Introduction***

Wyckaert et al. (2017) conducted a study on the health and safety risk assessment of pressure vessels. They reviewed literature from the past ten years and analysed accident reports from Quebec and the United States over the past sixteen years. Despite advanced technologies and standards regulating pressure vessels and piping, serious accidents can still occur. According to Wyckaert et al. (2017), the study highlighted two major risks related to the use of pressure vessels:

- An increase of the internal fluid pressure above the burst pressure of the vessel, or
- A decrease of the resistance of the vessel material due to the operating conditions which in turns causes a decrease in the burst pressure.

Majid & Ghorba (2015) noted that technical issues are not the only factors leading to the rupture of pressure vessel. Human and organisational factors are also significant parameters to consider.

Leroux, De Marcellis-Warin & Trepanier (2010) conducted a study on the transport of dangerous materials. They identified the main risks related to the transport and storage of dangerous materials, such as explosion, fire, and emission of toxic products. The study highlighted that human error is identified as the principal causal factor in these types of accidents.

As for the material of the enclosure of the vessel, the environment has a great impact on the fragile parts of the vessel (Barbosa et al, 2006). Leaks are prone as fragile components of the pressure vessel and piping, making them more sensitive to wear, fatigue, and human error.

According to Wyckaert et al. (2017) the impact of accidents involving pressure vessels can be severe, including explosion, domino effects due to fragments, fire, creation of slick of products or gas cloud or toxic or flammable vapours and the projection of fragments.

*2) Explosion by rupture of enclosures*

With regards to the risk of rupture of pressure vessels, various authors (Ineris, 2013) have established that there are two possible causes. The first cause is an increase in the internal fluid pressure beyond the vessel's burst pressure. The second cause is a decrease in the resistance of the vessel material due to the operating conditions, which leads to a decrease in the burst pressure. However, technical issues are not the only factors that contribute to the vulnerability of pressure vessels to rupture. Human and organizational factors are also significant parameters to consider (Majid & Ghorba, 2015).

During their study of the transport of dangerous material, Leroux et al. (2010) identified the principal risks associated with the transportation and storage of dangerous materials. These risks include explosions, fires, and emissions of toxic products. The study also revealed that human error is the principal causal factor in this type of accident (Leroux et al., 2010). In the case of a rupture of the shell, pressure vessel equipment, such as gas bottles, compressors, evaporators used in many industrial applications, research, medical and household appliances, etc., are of concern. In such cases, hazards arise from the projection of fragments and impacts, as well as incidents related to pipe whipping energy. The consequences of the rupture vary depending on the phase (liquid, gas or vapour) and the product contained in the pressure device, ranging from jet of steam or superheated water to intoxication or explosion. The rupture generally occurs at the fragile parts of the pressure vessels, such as seals, welds (Barbosa et al., 2006), pipe fittings, valves, pressure reducers, etc.

*3) Leak*

Fragile components of the pressure vessel and piping are prone to leakage. They are more sensitive to wear and fatigue but also to human error. As for the material of the enclosure of the vessel, the environment has a great impact on the fragile parts of the vessel (Barbosa et al., 2006). The leak of these pressure vessel components can sometimes be classified as fugitive emissions, (i.e., “a release of pollutants to the atmosphere after an escape from the equipment after an attempt to collect them using a hood, a gasket joint or any other means which should have ensured their capture and retention”). The misuse or incorrect installation of a gasket can generate a leak of the confined fluid of the pressure vessel (Bouzid, 2014). The consequences of such leaks can be the cause of creation of a slick of flammable products or poisons, the creation of flammable or toxic gas or vapour clouds which can lead to a fire or an explosion or an asphyxiation or poisoning of workers. In the current context, terrorism spreads and gains in

extent, the intentional deterioration of an industrial installation under pressure resulting in important escape of hazardous substances cannot thus be ignored (Wyckaert et al., 2017).

*4) Risk quantification and classification of pressure vessels based on failure modes.*

The establishment of the Risk Quantification and Grading Method Based on Failure Mode (RBFM) is a noteworthy innovation. This method is highly suitable for the surface static equipment of oil and gas gathering and processing stations. It functions by analysing each failure mode and its corresponding consequences to obtain the risk grade under each respective failure mode. the present study aims to assess various failure modes and their associated risks of equipment based on field production parameters. In conjunction with API 581 Risk Based Inspection and Statistical summary pipeline transportation occurrences in 2018, typical failure modes include leakage, combustion, explosion, and the like. The primary damage mechanisms are thinning, environmental cracking, and functional or mechanical failure. The failure reasons are analysed and classified into four categories and 19 subcategories (Baru, 2016).

Of significance, the process failure mechanism of pressure vessels is innovatively introduced in the functional or mechanical failure damage mechanism, such as overpressure, gas and liquid channelling, flooding, and so forth. The corresponding risk factors gradually deteriorate the equipment over time and ultimately lead to equipment failure. The risk factors that affect pressure vessels mainly include media, operation, design, environment and man-machine factors (Singh & Pokhrel, 2018). Based on accident statistics (Pipeline Performance in Alberta, 1990–2005), the most common damage mechanism of equipment in the station is thinning, including internal corrosion and external corrosion. Internal corrosion hazards include medium components, operating parameters, and design, which ultimately affect the internal corrosion rate and lead to internal corrosion perforation (Liao et al., 2023). External corrosion is divided into soil corrosion, corrosion under the insulation layer, joint coating corrosion, among others. Therefore, the risk factors are related to soil, insulation layer, environmental parameters, and pipeline materials, which affect the external corrosion rate or potential (Shi et al., 2021). In the functional or mechanical failure damage mechanism, there are several failure reasons. Blocking hazards can be divided into three types, which are mainly related to the properties of sand gravel, wax evolution of oil products, and formation temperature of natural gas hydrate (Ke & Chen, 2019). Overpressure is related to the maximum allowable operating pressure and operating pressure. Gas and liquid channelling, tank deflection is closely related to operating parameters (temperature, pressure, flow rate, etc.). The hazards of mis-operation in improper

operation are closely related to the operators' skills and knowledge (to management and persons).

In this work we investigate only the scenario of a leaking pipe in the high-pressure (HP) cooling system which leads to water suddenly penetrating molten matte in the furnace of a converter plant in a smelter, despite the generalisation that might have been obtained from also considering all the other possible accident scenarios, such as coal explosions.

We consider the case where water accumulates on the slag crust, before the crust fails, and the water penetrates the molten matte. This may lead to a boiling liquid expanding vapour explosion (BLEVE) in the converter.

1.2.3.5. Summary and conclusion concerning BLEVE.

According to Abbasi and Abbasi (2007b), the following observations are relevant to BLEVE:

- BLEVE, which is one of the six classes of explosions that can occur in the process industry, is particularly destructive. The other five classes of explosions include vapour cloud explosion (VCE), dust explosion, condensed phase explosion, confined explosions, and 'physical' explosions. The Mexico refinery disaster of 1984, the world's second worst process industry accident, involved a chain of BLEVEs.
- Aside from producing highly destructive blast waves and fireballs, BLEVEs propel the fragments of the ruptured vessel in all directions at high velocities, and such missiles are often enveloped in fire if the ruptured vessel had contained a flammable chemical. In most BLEVE events, the greatest damage has been caused by such missiles either by directly hitting and often killing people, or by triggering fires, or by damaging other process units leading to secondary accidents.
- BLEVE can occur in any situation where a vessel or a conduit carrying a pressure-liquefied gas (PLG) is accidentally depressurized. The depressurization suddenly renders the PLG into a superheated state, leading to instantaneous nucleation and explosive flashing. However, several factors introduce complexity in this otherwise simple-looking phenomenon. For instance, the initial depressurization due to a minor crack may just cause the release of a gaseous or a liquid jet, and the crack may either not propagate further or do so after a great deal of time. However, a crack may also propagate rapidly. Abbasi and Abbasi (2007b) showed that much has been done to understand the nature and the magnitude of the forces and counterforces that are

generated in a jeopardized vessel containing a PLG. A great deal of new knowledge has been acquired, based on analysis of past accidents as well as experimental BLEVEs, but we still are not able to forecast whether a jeopardized vessel will suffer BLEVE and, if it does, when. This remains an area where a great deal of further research and development is required.

- Knowledge has been accumulated regarding the potential energy of explosion of a BLEVE, the resulting fireball size, duration, and heat load, as well as the quantity, size, orientation, and kinetic energy of projectiles generated from a shattered vessel. However, the utilization of different methods may result in significant variations in the forecasts, at times differing by several orders of magnitude.
- Despite the existence of manuals produced by coordinating agencies, such as the TNO in The Hague and the Centre for Chemical Process Safety in New York, which outline various consequence assessment methods, there is little discussion on their relative merits. This situation creates situations where the risk assessments conducted by industries and regulatory agencies may differ significantly, even though both parties have employed legitimate consequence analysis models. Therefore, there is an urgent need to standardize and codify procedures, like the approaches used in clinical and environmental analysis.
- It is surprisingly common to believe that BLEVE only occurs with flammable chemicals, even though it is a well-known and well-documented phenomenon. However, the reality is that one-fifth of all BLEVEs occur with non-flammable PLGs.
- Investigating the probability of a secondary and higher order accident (domino effect) caused by a BLEVE is one of the questions that need answers. BLEVE history indicates that it is seldom a standalone event and is frequently a trigger for other accidents. Therefore, studies on this aspect of BLEVE would refine our assessment of the risk posed by PLG-holding units.
- There is a great need for research and development to identify more reliable methods than those currently available to prevent a jeopardized vessel from undergoing BLEVE.

## 1.3 Scope of the Research

The scope of the work is divided into two sections: The work firstly proposes a new methodology to estimate $PoF$ of an asset. The method is based on PHM, which is a statistical model able to define the risk of failure for a component, subject to condition monitoring. This

is addressed in section 1.3.1. Secondly the advantages related to the proposed method is discussed in section 1.3.2.

### 1.3.1. Newly proposed method based on PHM.

It is evident from sections 1.2.1 and 1.2.2 that much research was done in the traditional risk-based inspection. Progress was also made in innovative dynamic risk assessment. However, this work proposes the incorporation of the PHM into the RBI to obtain an optimal $PoF$, which is a function not only of the time but also of asset condition.

To fill the gap related to the existing methods that use either time based statistical data or condition monitoring data, (Zeng & Zio, 2018) proposed combining statistical data with condition monitoring data to assess the risk. Their method uses a hierarchical Bayesian model to compute the reliability of the safety barriers. A Bayesian updating algorithm, which integrates particle filtering with Markov Chain Monte Carlo, is developed to update the reliability evaluations based on both the statistical and condition-monitoring data. These authors suggested that in future, models such as support vector machines, artificial neural networks, etc., may be considered for DRA.

The present research however follows a more classical approach by integrating PHM into RBI. This allows the possibility of combining both statistical failure data with condition monitoring data, in a unique model to update risk assessment while the system condition is degrading. The proportional hazards model (PHM) is based on work done by (Cox, 1972) to estimate the risk of human mortality. PHM incorporates the effects of covariates or explanatory variables on the distribution of lifetimes. Covariates are any measured parameters that are thought to be related to the lifetimes of components. For each given time, the covariate provides an increase or decrease in the hazard. proportional to the baseline hazard rate (Lelo, Heyns & Wannenburg, 2019).

PHM is now one of the most popular statistical models used for survival analysis. Its popularity arises from the fact that the proportional hazards model is part of a broader class of survival analysis which provides information on the duration of time between the identifiable start and the occurrence of an event (Carstens & Vlok, 2013). A key feature when using a proportional hazards model is that it can utilize time-series variation in the covariates. The information can be provided based on the change in explanatory variables over time, that influence the probability of the event occurring.

Figure 3 below represents a framework summarizing the proposed method described in this work.

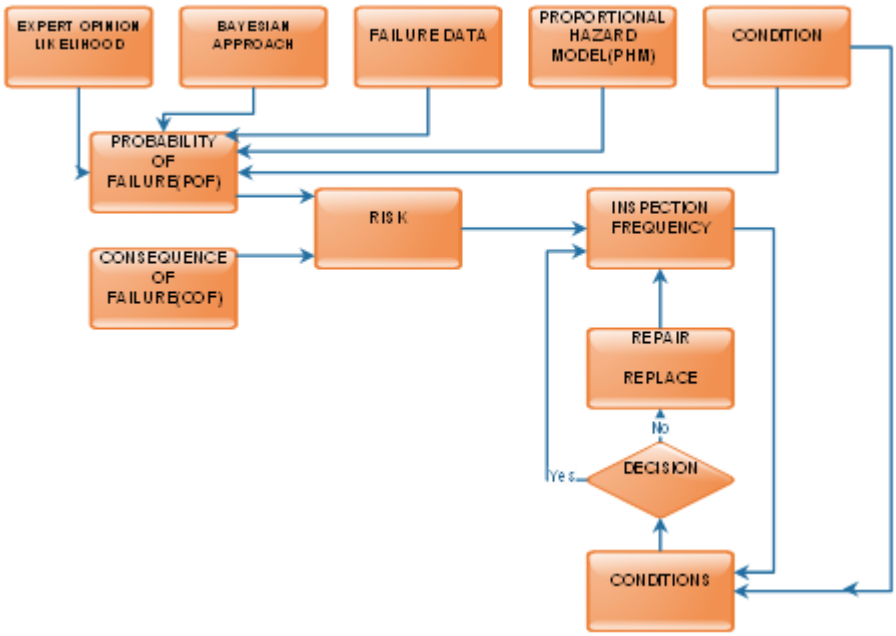


*Figure 3: Framework with the proposed method.*

The approach developed in this work consists of incorporating the proportional hazard model (PHM) into a risk-based inspection (RBI) methodology. The advantages of incorporating PHM with the RBI approach are that the PHM uses real-time condition data, allowing dynamic decision-making on inspection and maintenance.

Knowing that risk is obtained by the product of $PoF$ and $CoF$,the PHM allowed the $PoF$ computation based on failure time and covariate.

### 1.3.2. Advantages related to the suggested methods.

One of the advantages related to the application of PHM to the RBI methodology is that the PHM uses instantaneous condition data at a given time, which leads to dynamic decision-making in inspection scheduling. Another benefit is that the PHM approach is intended for situations where the covariates provide some indication of an approaching failure and, when combined with age, give an improved indication of the risk of failure, compared to using only age as an indicator. These advantages lead to an improved estimation of the $PoF$.

As risk is the product of $PoF$ and $CoF$, to model the $CoF$ in this work, the scenario that we address and present as case study 2, is that of a leaking pipe in the high pressure (HP) cooling

system which leads to water suddenly penetrating molten matte in the furnace of a converter plant in a smelter. We consider the case where water accumulates on the slag crust before the crust fails and the water penetrates the molten matte. This may lead to a boiling liquid expanding vapour explosion (BLEVE) in the converter.

## 1.4 Document overview

Traditional risk-based inspection methodology as well as the shortcomings related to it are addressed in chapter 1. To address these shortcomings it is proposed to develop a methodology that incorporates PHM into the RBI. Since this approach will be demonstrated in a high pressure cooling system where a leaking pipe can lead to boiling liquid expanding vapour explosions, the consequences of failure based on BLEVE are also introduced in chapter 1.

Chapter 2 presents the development of the PHM modelling to enhance the estimation of the $PoF$ and its incorporation into RBI, together with an illustration, using the IMS data for a bearing test rig with four test bearings on one shaft. RMS and kurtosis are used as covariates in this chapter to build the PHM and estimate the $PoF$ related. The case study described in chapter 2 also addresses the $PoF$ computation based on the time-based approach. Finally a comparison between the $PoF$ based on time-based and PHM is performed to highlight the benefits.

In chapter 3, the emphasis is on the quantification of the $CoF$, also illustrated at the hand of a case-study, which in this instance is a complex, real world problem involving a pressure vessel. The vessel is the high pressure cooling system of a coal fired furnace, where the consequence of failure would involve a BLEVE. In this chapter, the proposed methodology to estimate the $PoF$ is based on PHM with moisture and cumulative feed rate as covariates. The consequence of failure modelling in this chapter 3 is based on the BLEVE theory. The safety issues in this chapter are due to water and hot molten materials mixing within the lower part of the furnace vessel, from the HP cooling system.

Chapter 4 addresses mitigation decision making based on quantified risk. This work is concluded in chapter 5 by showing the benefits to optimize the risk policy for pressure vessels using the incorporation of PHM into RBI for improved $PoF$ quantification, together with the quantification of the $CoF$ using, in the case presented here, BLEVE principles.

# Chapter 2. Development of a model incorporating the proportional hazards model into risk-based inspection.

## 2.1 Introduction

Industry decision-makers often apply a risk-based approach to plan inspection and maintenance. Probability of failure ($PoF$) and consequence of failure ($CoF$) are the two main components involved in the risk assessment (API 581, 2016). Risk based inspection (RBI) identifies and quantifies both the $PoF$ and $CoF$ of failure to establish an inspection schedule.

Qualitative risk assessment is usually based on expert opinion and specific plant experience, while quantitative risk assessment is based on statistical computations which are based on historical data. An inspection schedule is then proposed as an outcome of the risk assessment, which is usually time-based. The need to optimize risk assessment is very critical in this research due to the gap highlighted in section 1.2.1.4.

The scope of research presented in section 1.3.1 alludes to the incorporation of the PHM into RBI to optimize the $PoF$ as well as the inspection schedule. This chapter describes the proposed model based on the PHM. The calculation of $PoF$ applying the proposed model is then illustrated by means of the IMS bearing data set.

## 2.2 Building a mixed model incorporating PHM into RBI

Over the past few decades, preventive maintenance decisions have been optimized by means of statistical analysis of failure data, while condition-based maintenance has been optimized by utilizing sophisticated methods such as vibration and oil analysis. The present research consists of building a mixed model which combines historical failure data and condition monitoring data into a mathematical model to predict the risk of failure occurrence for an asset, and then use the outcome from the prediction model to estimate the $PoF$.

Reliability analysis commonly referred to as the analysis of historical failure data exclusively, which consists of aligning historical data with a probability distribution based on time interval. The fitted distribution can be utilized for further analysis (Carstens & Vlok, 2013). However, it is postulated in this work that it would be beneficial to combine historical failure data and

condition-monitoring data by building a mathematical model that allows maintenance and inspection decision support (diagnostics or prognostics). In this thesis, a time dependent proportional hazard model (PHM), which is a popular regression model, is used. The PHM is described and utilized as a tool to optimize $PoF$ as well as inspection schedule.

Renewal theory consist of estimating the reliability of a component using the recorded time to failure and computing the renewal time that minimizes the mean life cycle cost of the future components (Carstens & Vlok, 2013). When dealing with renewal theory the reliability concepts such as failure density, cumulative failure density, reliability function and the instantaneous failure rate are important to model the history of the asset under consideration.

To model the reliability function of a renewable system, several approaches are used:

- A probabilistic modelling approaches.
- A non-probabilistic modelling approach.
- A regression modelling approach.

The following paragraph addresses the regression modelling because it involves combining both probabilistic and non-probabilistic modelling approach as specified in section 2.2.1 and particularly the proportional hazard model.

### 2.2.1. Regression modelling approach

Regression modelling entails merging probabilistic and non-probabilistic modelling approaches. The following properties define the regression modelling approach:

- Like non-probabilistic models the regression models directly recognize the existence of the survivor function or hazard rate but do not utilize the existence of an underlying failure distribution as primary assumption.
- The regression models are not only the primary use parameter modelled but also the concomitant information surrounding failure or covariates.

Several regression models have been identified in the literature for renewal theory (Vlok and Coetzee, 2012):

- Accelerated failure time models (AFTM) during 1966.
- Proportional hazard model (PHM) during 1972.
- Prentice William Peterson model (PWP model) during 1981.

- Proportional odds model (POM) during 1983.
- Additive hazard model (AHM) during 1990.

All five these named regression models have the same structure, namely a baseline function which is a time-based part estimated either using parametric or non-parametric techniques, and an explanatory part which has a direct influence on the baseline function to estimate the overall reliability of the system.

Vlok and Coetzee (2012) presented a decision matrix showing that the proportional hazard model is the most suitable out of all the named regression models. The criteria of evaluation were: (1) Theoretical foundation; (2) Previous practical success in reliability modelling; (3) Potential to lead to the dissertation objective; (4) Achievability of numerical implementation; (5) Future potential in reliability modelling.

### 2.2.2. Proportional hazard models

#### 2.2.2.1. Introduction

PHM is a statistical procedure enabling the estimation of the risk of a component failing when its condition is monitored (Jardine & Tsang, 2013). PHM models form part of a broader class of survival analysis models which estimate the risk that is incurred at a given time, given the period of operation and a measured covariate which describes the state of the machine.

When modelling the hazard function $h(t)$, the baseline hazard function $h_0(t)$ can be represented in parametric or non-parametric form. A commonly used parametric baseline hazard function is the Weibull hazard function. PHM is essentially a regression modelling analysis. A set of significant covariates is needed and only the significant covariates are inserted in the models.

The PHM with a Weibull baseline hazard function is presented in the following equation:

$$h[t, Z(t)] = \frac{\beta}{\eta}\left(\frac{t}{\eta}\right)^{\beta-1} \exp\left\{\sum_{i=1}^{m} \gamma_i Z_i(t)\right\} \qquad (6)$$

where $h[t, Z(t)]$ is the hazard function, the $Z_i(t)$ are the covariates at time t, $\frac{\beta}{\eta}\left(\frac{t}{\eta}\right)^{\beta-1}$ is the baseline hazard function with $\beta$ the shape parameter and $\eta$ the scale parameters. The Weibull

parameters, which allow the construction of the baseline part of the model, are determined by maximizing the likelihood function.

For a given PHM, the choice of the type of covariate to be used depends on the theoretical assumption about the relationship between the covariate value and the hazard function (LeClere, 2005). When the hazard function is mostly dependent on the value of the covariates at time zero or some fixed time point, then time-independent covariates are the right choice. But when the covariates change over time and the hazard function depends more on the current values of the covariates, then the time-dependent covariates are the right choice.

Considering errors yielded by the situation where covariates change over time, many studies ignore the time dependence and deal with time-dependent covariates as time-independent, by fixing its value at a given point in time or setting the value of the covariate to an average value for the period that is studied. Likely problems when using time-dependent covariates as time-independent or time-invariant covariates are:

- As several covariates are likely to change before the advent of the failure, the variation was eliminated, and important information is lost.
- Several phenomena are generated by dynamic, longitudinal processes because the value of a covariate along the time path affects the probable event happening.
- The model does not include the value of the covariate observed at the time of event occurrence, although it may be this actual value that generates the event.
- With the availability of software today, there are some programs, which directly deal with time-dependent variables, and the need for considering time-dependent variables as time-independent is reduced.

In the parametric PHM, one of the most important operations to be done is to estimate the $\gamma's$ to access the effect of the explanatory variable, the corresponding estimate parameters are determined using the maximization of the likelihood function (Vlok & Coetzee, 2012).

#### 2.2.2.2. The fully parametric PHM and maximum likelihood

Before addressing the maximum likelihood method, it is important to understand the notion of fully parametric. The PHM is parametrized by assuming a continuous distribution for the baseline (Vlok & Coetzee, 2012). For this work, the Weibull distribution is considered. This is given by expression (6).

Statistical model

Vlok and Coetzee (2012) highlighted that fewer numerical issues arise when dealing with Weibull PHM to determine the baseline parameters. Therefore, Vlok's approach to determining the three Weibull parameters in the general distribution formula for time dependence is considered here.

$$f(t) = \frac{\beta}{\eta}(\frac{t}{\eta})^{\beta-1}\exp[-(t/\eta)^{\beta}] \tag{7}$$

The hazard rate function corresponding to the probability density function (pdf) given by equation (7) is:

$$h(t) = \frac{\beta}{\eta}(\frac{t}{\eta})^{\beta-1} \tag{8}$$

with beta $(\beta)$ and eta $(\eta)$ being the shape and scale parameters of the distribution respectively. By using the Weibull distribution as the baseline hazard rate of the PHM according to equation (6), the formula becomes:

$$h\left(t, \overline{Z(t)}\right) = \frac{\beta}{\eta}(\frac{t}{\eta})^{\beta-1}\exp(\bar{\gamma} \times \overline{Z(t)}) \tag{9}$$

Considering the reliability theory, it is stated that the reliability of a component under the influence of ageing only, before the renewal at a time $T_i$ is given by:

$$R(T_i) = \exp(-\int_0^{T_i} h(t)dt) = \exp(-(\frac{T_i}{\eta})^{\beta}) \tag{10}$$

The distribution of $U_i = (\frac{T_i}{\eta})^{\beta}$ is unit negative exponential distribution, similarly for time-dependent (Jardine, 1987). As for equation (8), at the time $T_i$ the reliability of the component under the influence of time-independent covariates according to the PHM is estimated by:

$$R(t, \bar{Z}) = exp\left[-\int_0^{T_i} \frac{\beta}{\eta}(\frac{t}{\eta})^{\beta-1}\mathrm{dt}\exp(\bar{\gamma} \times \overline{Z})\right] \tag{11}$$

By solving equation (9) it follows that:

$$R(t, \bar{Z}) = exp\left[-(\frac{T_i}{\eta})^{\beta}\exp(\bar{\gamma} \times \bar{Z}\right] \tag{12}$$

Equation (12) is about the time-independent covariate. For the time-dependent $U_i = (\frac{T}{\eta})^{\beta}\exp(\overline{\gamma}, \overline{Z}_i)$, again with unit exponential distribution. When dealing with this case with time-dependent covariates, the reliability of time $T_i$ for the component, considering the time-dependent covariate will be:

$$R(t, \overline{Z(t)}) = exp\left[-\int_0^{T_i} \frac{\beta}{\eta}(\frac{t}{\eta})^{\beta-1}\exp(\bar{\gamma} \times \overline{Z(t)}dt\right] \qquad (13)$$

Equation (11) gives:

$$R(t, \overline{Z(t)}) = exp\left[-\int_0^{T_i} \exp(\bar{\gamma} \times \bar{Z}_i\,(t) d(\frac{t}{\eta})^{\beta}\right]$$

Considering the equation $U_i = \int_0^{T_i} \exp(\bar{\gamma} \times \bar{Z}_i\,(t) d(\frac{t}{\eta})^{\beta}$, with unit negative exponential distribution, in practice equations (11) and (12) are approximated by:

$$R(t, \overline{Z(t)}) = exp\left\{\sum_{k=1}^{i} \exp(\overline{\gamma} \times \overline{Z_i^*}(t_k)) \times \left[(\frac{t_{k+1}}{\eta})^{\beta} - (\frac{t_k}{\eta})^{\beta}\right]\right\} \qquad (14)$$

with $0 = t_0 < t_i < \cdots < T_i$ inspection points where covariate measurement was performed and $Z_i^* = 0.5 \times \left(\overline{Z_\iota\,(t_k)} + \overline{Z_\iota\,(t_{k+1})}\right)$.

2.2.2.3. Maximum likelihood (Parameter estimation)

As indicated in the literature, the maximum likelihood of the Cox model parameters is found by maximizing a likelihood function. The likelihood function is a mathematical expression which describes the joint probability of obtaining the data observed on the subjects in the study as a function of the unknown parameters (the $\gamma's$) in the model being considered (Vlok & Coetzee, 2012). Some literature such as the work by Vlok and Coetzee (2012), addressed the optimization of the likelihood equation to determine the Weibull parameters.

The Weibull parameters are estimated by maximizing the likelihood equation, given by:

$$L(\beta, \eta, \bar{\gamma}) = \prod_i h(T_i, \overline{Z_\iota\,(T_\iota)}) \times \prod_j R(T_j, \overline{Z_J(t))} \qquad (15)$$

with the $i$ index referring to failure times and where $j = 1,2 \ldots\ldots\ldots n$ indicate failure and suspension times. It is important to highlight that the work in this thesis deals with complete data.

The Weibull parameters $\beta, \eta, \gamma$, which maximize the likelihood in equation (15), will also maximize $\log(L(\beta, \eta, \gamma)$ or $l(\beta, \eta, \gamma)$. It is numerically appropriate to maximize $l(\beta, \eta, \gamma)$ which is given by:

$$l(\beta, \eta, \bar{\gamma}) = r ln\left(\beta/\eta\right) + \sum_i ln\left[(T_i/\eta)^{\beta-1}\right] + \sum_i \bar{\gamma} \times \overline{Z_\iota}(T_i) - \sum_j \int_0^{T_j} \exp(\bar{\gamma} \times \overline{Z}_j(t)\, d(t/\eta)^\beta \qquad (16)$$

where r is the number of failure renewals.

In this work, equations (14) or (15) are solved numerically using a Newton-Raphson optimization procedure.

$$l(\beta, \eta, \bar{\gamma}) = r(-\beta ln\eta) + r ln\beta + (\beta - 1) \times \sum_{i=1}^{r} lnt_i + \sum_{b=1}^{m} \gamma_b B_b - \left[\exp(a) \times \left(\sum_{i=1}^{n} \gamma_g Z_{jg}^i\right) \times \left(t_{i(j+1)}^\beta - t_{ij}^\beta\right)\right] \qquad (17)$$

To maximize equation (15) and estimate the three Weibull parameters, many techniques have been tested successfully (Vlok & Coetzee, 2012). Among these are:

- A Nelder-Mead method
- A BFGS Quasi-Newton method
- Snyman's dynamic trajectory method
- A modified Newton-Raphson method

The performance of the above-mentioned methods was assessed regarding their economy, which means according to the number of iterations needed to converge, the number of

objective function evaluations and the number of partial derivative evaluations, as well as robustness. The outcome from the evaluation of the above-mentioned methods was such that the Newton-Raphson method was found more suitable and economic for the optimization of the maximum likelihood function. This work uses the Newton-Raphson method to optimize equation (15).

1) Newton Raphson method for a three-parameter Weibull distribution

Vlok and Coetzee (2012) proposed a template to simplify the computation of the Newton Raphson optimization technique for vibration monitoring data for case study 1, and moisture and cumulative feed rate for case study 2. Referring to the suggested template (see table 1), $n$ expresses the number of histories, such that: $i = 1,2 \ldots . n$.

The time to failure or suspension in each history, as expressed by $T_i$, and $C_i$, are used as indications making the difference between failure and suspension. For $C_i$=1, $T_i$ is a failure and for $C_i = 0$, $T_i$ is a suspension. As indicated before we assume the data are complete, which means that there are no suspensions.

The number of inspections $k_i$ must be set to be able to model the scenario associated with the time-dependent covariate. Below in table 1, a sample of the template associated with our data, is given.

*Table 1: Template of inspection time and covariate corresponding.*

| **Inspection Time** | **Covariate** |
|---|---|
| $t_{i0}$ | $Z_{01}^{i}$ |
| $t_{i1}$ | $Z_{11}^{i}$ |
| . | . |
| . | |
| . | |
| $t_{iki}$ | $Z_{ki1}^{i}$ |

The above template is adjusted according to our data that deals with a unique covariate, as is the case in case study 1. The Weibull parameters are estimated by optimizing the objective function (15), considering the complexity of the objective function, an optimisation algorithm (fmincon) is used under MATLAB as well as opti; a free optimisation toolbox to optimize and compute the objective function given in equation (15).

2) Maximum likelihood for a simple Weibull (two parameters**)**

The simple two Weibull parameters approach is associated with the time-based approach, as recommended by API 581. while the proposed approach in this work considers three Weibull parameters, taking into consideration both historical failure data and condition monitoring data.

This section is all about determining the shape and scale parameters related to the time-based approach. Firstly, it is important to notice that the Weibull parameter estimates can be defined using different methods such as the graphical method, using probability plotting paper, or the analytical method, using either least squares or maximum likelihood (Huynh, 2011). The probability plotting method requires simpler mathematics and is suitable for a small sample

size. Furthermore, Huynh (2011) presents many advantages making the maximum likelihood method more attractive. Among its properties could be mentioned:

- It is asymptotically consistent, efficient, and unbiased.
- There is the possibility to handle survival and interval data better than rank regression.

Considering that, the lifetime $T$ follows a Weibull distribution with $\beta$ and $\eta$ parameters, the probability density function could be given by:

$$f(t) = \frac{\beta}{\eta}(\frac{t}{\eta})^{\beta-1}e^{-(\frac{t}{\eta})^{\beta}} \qquad (18)$$

with $t$, the failure time, beta the shape parameter strictly greater than zero and $\eta$ the scale parameter. the log-likelihood function is given by:

$$\Lambda = Nln(\beta) - N\beta\ln(\eta) + (\beta-1)\sum_{i=1}^{N}\ln(t_i) - \sum_{i=1}^{N}(\frac{t_i}{\eta})^{\beta} \qquad (19)$$

Referring to the Newton-Raphson method, the above equation (19) log-likelihood function maximization, gives:

$$\frac{1}{\beta} = \frac{\sum_{i=1}^{N} t_i^{\beta} lnt_i}{\sum_{i=1}^{N} t_i^{\beta}} - \frac{1}{N}\sum_{i=1}^{N} lnt_i \qquad (20)$$

As the log-likelihood function maximization is dealt with numerically, a MATLAB optimization code is used to solve (19). The estimated parameters obtained from the likelihood function maximization are utilized to build the time-based or two-parameters Weibull probability density function given in equation (18).

## 2.3 Case study 1: Illustrating the developed model.

In this section, a case study is presented to illustrate the methodology, using failure data obtained from the simple but readily available IMS bearing data set. The RBI methodology is commonly applied to pressure vessels where the need for such investigations is higher to minimize the risk of accidents. However, in this section, a simple bearing data set is used for illustrative purposes, simply because datasets like these are very well documented and well understood. A similar data set for pressure vessels is not readily available publicly.

The data for the IMS case study was generated by the NSF I/UCR Centre for Intelligent Maintenance Systems (IMS-www.imscenter.net) with support from Rexnord Corp. The following is a description of the testing configuration from which the test results were obtained.

The bearing test rig had four test bearings on one shaft. The shaft was driven by an AC motor and coupled to the shaft via rubber belts. The rotation speed was kept constant at 2000 rpm. A radial load of 6000 lbs. was applied to the shaft and bearing by a spring mechanism. All the bearings were force lubricated. An oil circulation system regulated the flow and the temperature of the lubricant. A magnetic plug installed in the oil feedback pipe, collected debris from the oil as evidence of bearing degradation. The test was discontinued when the accumulated debris adhering to the magnetic plug exceeded a certain level and caused an electrical switch to close.

Four Rexnord ZA-2115 double row bearings were installed. Each bearing had 16 rollers in each of the two rows, a pitch diameter of 2.815 in., a roller diameter of 0.331 in. and a tapered contact angle of $15.17^0$. A high sensitivity accelerometer was installed on each of the four bearings to record bearing housing vibration. Vibration data was collected every 20 minutes. The data-sampling rate was 20 kHz, and the data lengths were 20480 points.

### 2.3.1. Simulations and Results.

#### 2.3.1.1. Fault diagnosis of bearings

For this case study1, the root mean square (RMS) and kurtosis of the measured acceleration signals are used as covariates for the proportional hazards model. The RMS value is associated to the energy of the signal. Usually, the appearance of a defect is detected by an increase of the vibration level. The RMS values were compared with levels while the bearing is still undamaged.

Kurtosis is the fourth statistical moment of the vibration signal, normalized by the standard deviation raised to the fourth power.

RMS and kurtosis were used in this work for condition monitoring because of their simplicity of application and interpretation.

### 2.3.1.2. Graphical representation of the data (RMS and kurtosis)

The bearing test RMS and kurtosis results are depicted below for bearings 3 and 4. The interest in bearings 3 and 4 is justified by the fact that at the end of the test-to-failure experiment, defects occurred for bearings 3 and 4.

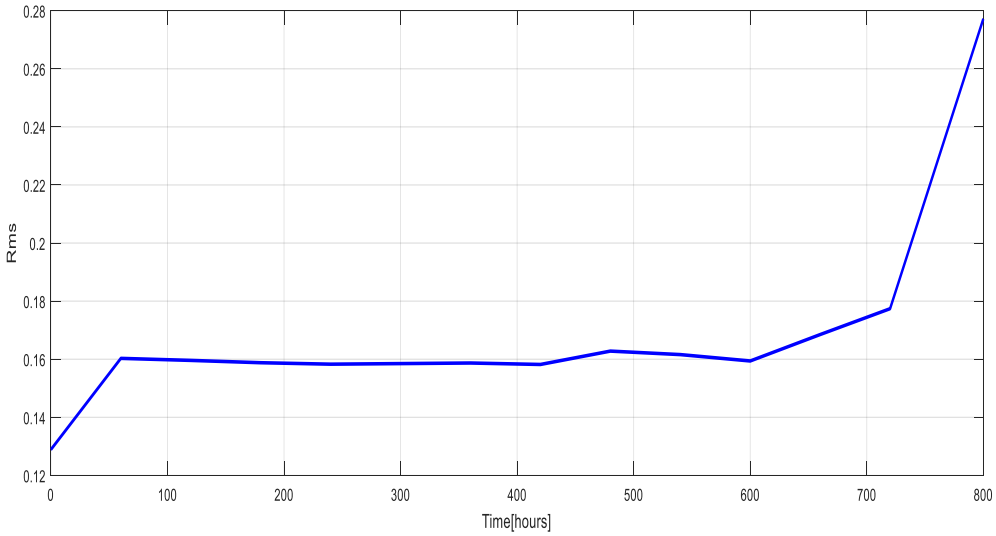


*Figure 4: RMS as function of time for bearing 3*

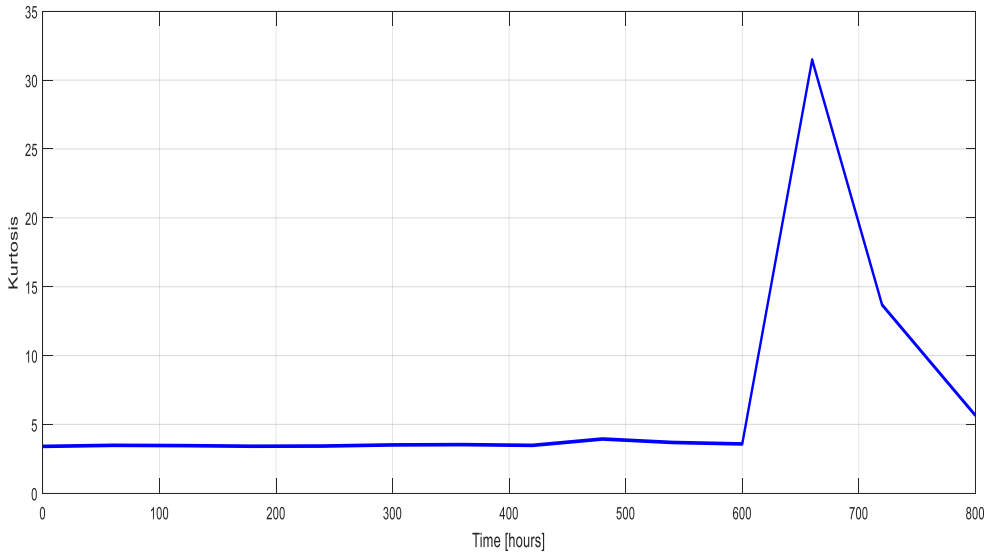


*Figure 5: Kurtosis as function of time for bearing 3*

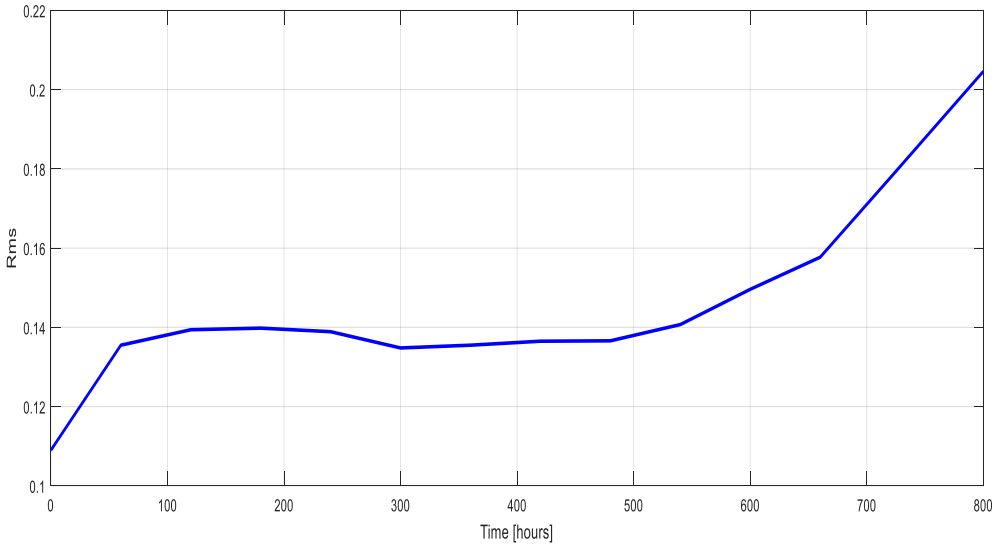


*Figure 6: RMS as function of time for bearing 4*

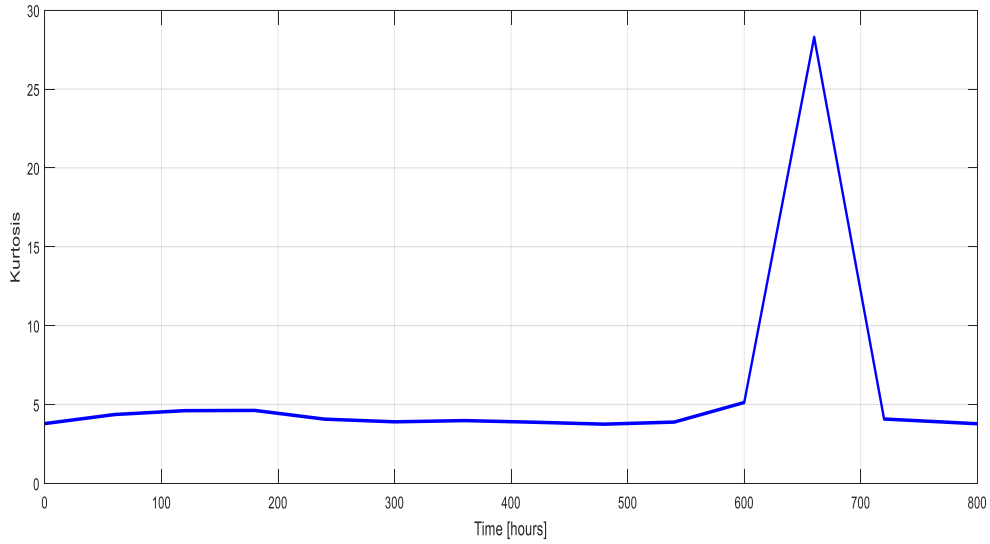


*Figure 7: Kurtosis as function of time for bearing 4*

Figures 4 and 6 are RMS vibration trends for bearings 3 and 4 respectively. Both figures reveal that the change of RMS can be divided into two phases for the inner race defect. In the first phase, during the first 600-700 hours of operation, no underlying trend was observed. However, after the test had been running for 600-700 hours, the RMS increased significantly. The increased RMS can be explained by the propagating damage. As the damage spreads over an increased area, the RMS vibration level rises.

Figures 5 and 7 depict the kurtosis for bearings 3 and 4 respectively. The peaks in the kurtosis show the characteristic behaviour of kurtosis where peak levels of vibration are initially

important but as the damage spreads over a larger area, become less important compared to the growing RMS value.

#### 2.3.1.3. Kurtosis and RMS as condition indicators

Kurtosis is a useful feature to indicate an initially localised failure in a bearing with the kurtosis rising suddenly as the failure occurs. As the failure propagates around the bearing the fault becomes more distributed, the kurtosis generally drops (Randall & Antoni, 2011) and kurtosis loses some of its value as fault indicator.

Therefore, while kurtosis and RMS are both indeed useful condition indicators, they nevertheless provide only partial information on the condition of the component. It is therefore proposed here to combine failure time information with the condition information to enhance the risk assessment. As previously discussed, the combination of age and condition information is enabled by the application of PHM. This is shown later in figure 10.

### 2.3.2. Time based approach and risk assessment

This section addresses the time-based approach for RBI. The previous section highlighted that the condition indicators kurtosis and RMS alone are not always adequate for identifying machine condition. This can in some cases be dealt with by either applying more sophisticated signal processing to find better condition indicators, but in the absence of this, a time-based approach could also be followed.

The same steps undertaken in section 2.2.2.3 to estimate the regression coefficients required to build the PHM, are also needed for the two parameter Weibull, or time-based approach. Equation (21) below, which is the log likelihood function for the parameter Weibull distribution, must be maximized to determine the regression parameters.

$$\Lambda = Nln(\beta) - N\beta \ln(\eta) + (\beta - 1)\sum_{i=1}^{N} \ln(t_i) - \sum_{i=1}^{N} (\frac{t_i}{\eta})^{\beta} \qquad (21)$$

The maximum of the log likelihood function given by equation (21) gives the following equation:

$$\frac{1}{\beta} = \frac{\sum_{i=1}^{N} t_i^{\beta} lnt_i}{\sum_{i=1}^{N} t_i^{\beta}} - \frac{1}{N}\sum_{i=1}^{N} lnt_i \tag{22}$$

The determination of the shape parameter $\beta$ in equation (22) is normally dealt with numerically. Using a MATLAB code, the output gave a shape parameter $\beta = 4$ for the bearing data.

The differentiation of equation (21) with respect to $\eta$ gives:

$$\eta = (\frac{1}{N}\sum_{i=1}^{N} t_i^{\beta})^{1/\beta} = \frac{1}{4}\sum_{i=1}^{4} t_i^4 = 360\ hours \tag{23}$$

With $\beta$ and $\eta$ known, the hazard or risk of failure for the time-based approach is:

$$h(t) = \frac{4}{360}(\frac{t}{360})^{4-1} \tag{24}$$

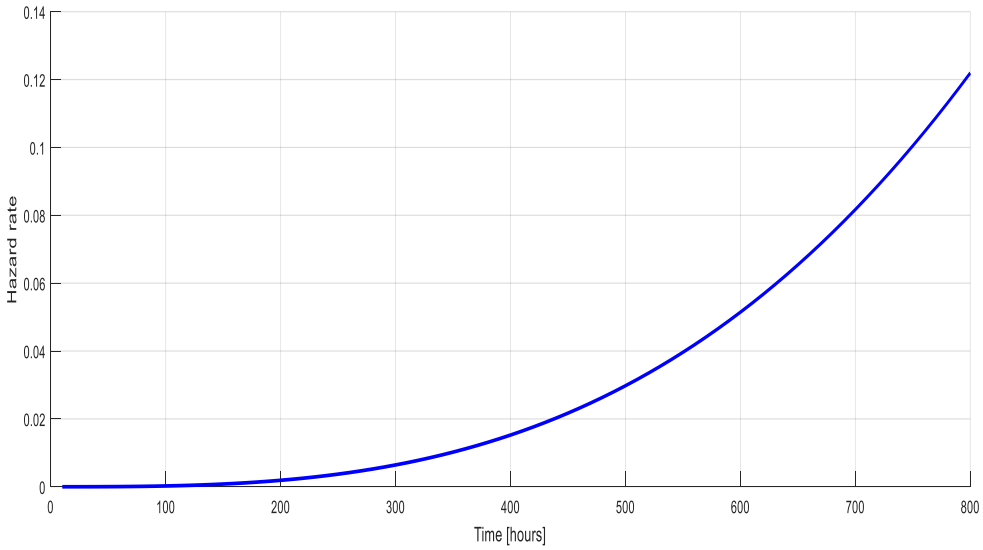


*Figure 8: Time-based hazard rate*

The cumulative distribution function (cdf) or probability of failure curve related to the hazard represented in figure 8, is given in figure 9 below.

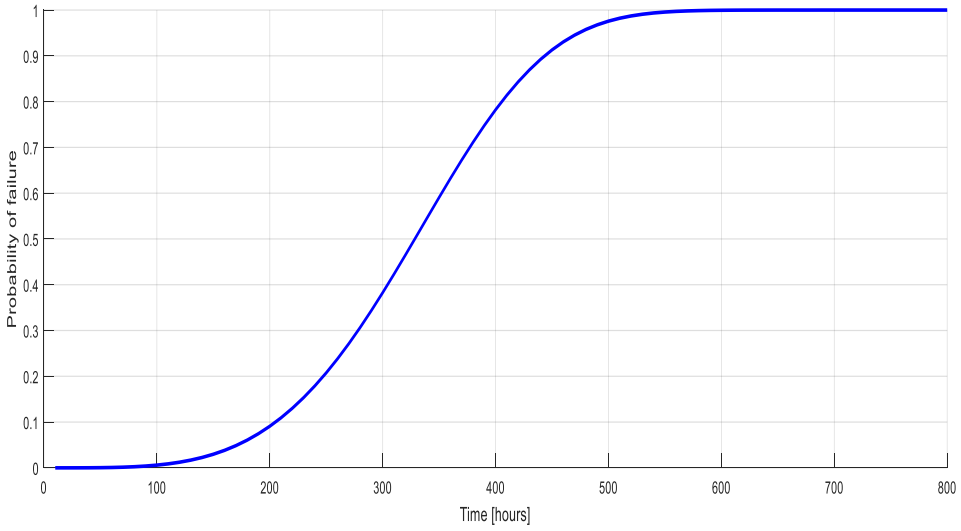


*Figure 9: Time-based Weibull cumulative distribution function*

The economical approach for the time-based approach consists of finding an optimal time of replacement which minimizes the cost per unit time. Referring to Jardine et al. (2013), the optimal preventive replacement time of a component subject to breakdown, is given by:

$$C(t_p) = \frac{C_p \times R(t_p) + C_f \times (1 - R(t_p))}{t_p \times R(t_p) + M(t_p)(1 - R(t_p))} \qquad (25)$$

We consider a three to one cost ratio, so that the failure cost $C_f$ in South African Rands (ZAR) is three times the preventive cost $C_p$. If we further assume that $C_p = 2000\ ZAR$ and $C_f = 6000\ ZAR$, the results after computation are given below:

*Table 2: Table of results for time-based approach.*

Considering Table 2, the optimal expected replacement cost per unit time is 13,13 ZAR/day.

| | Time (hours) | Reliability $R(t)$ | Probability of failure $F(t)$ | Cost per unit time $C(tp)$ |
|---|---|---|---|---|
| 1 | 0 | 1 | 0 | inf |
| 2 | 60 | 0.999 | 0.001 | 33.41 |
| 3 | 120 | 0.987 | 0.0123 | 17.2743 |
| 4 | 180 | 0.9394 | 0.0606 | 13.1416 |
| 5 | 240 | 0.8208 | 0.1792 | 13.1323 |
| 6 | 300 | 0.6174 | 0.3826 | 16.2892 |
| 7 | 360 | 0.3679 | 0.6321 | 24.5829 |
| 8 | 420 | 0.1568 | 0.8432 | 49.355 |
| 9 | 480 | 0.0424 | 0.9576 | 154.5658 |
| 10 | 540 | 0.0063 | 0.9937 | 893.1391 |
| 11 | 600 | 0.0004 | 0.9996 | 11228 |
| 12 | 660 | 0.0004 | 0.9995 | 364330 |
| 13 | 720 | 0 | 1 | 74051000 |

The following section consists of estimating the expected optimal cost based on Risk (PHM) instead of time as it is the case in this section. The cost per unit time obtained for time-based will be compared to the cost per unit time for PHM to evaluate the advantages of PHM over the time-based approach.

### 2.3.3. PHM Approach

#### 2.3.3.1. Building the PHM

The PHM model incorporates both the kurtosis and the RMS as covariates. The first step of this investigation consists of estimating the regression coefficients $\beta, \eta, \gamma$ required to build the PHM. (Carstens & Vlok, 2013) argue that the log-likelihood function represented by equation (17) should be maximised:

$$l(\beta,\eta,\bar{\gamma}) = rln\left(\beta/\eta\right) + \sum_i ln\left[(T_i/\eta)^{\beta-1}\right] + \sum_i \bar{\gamma} \times \overline{Z_i}(T_i) - \sum_j \int_0^{T_j} exp(\bar{\gamma}\,\overline{Z}_j(t)\, d(t/\eta)^{\beta} \quad (26).$$

The outcome from this optimisation renders a shape parameter β=4, a scale parameter ή=800 hours the weight of the covariate γ1= 0.4952 (weight of the RMS) and γ2= 0.5 (for the kurtosis)

The above regression parameters are obtained from the maximum likelihood equation (13):

The hazard rate equation corresponding to the above parameters with kurtosis and RMS as covariate, is given by:

$$h[t,z(t)] = \frac{4}{800}\left(\frac{t}{800}\right)^{4-1} exp[0.4952\ RMS + 0.5\ KURT] \quad (27)$$

A graphical representation of this equation for the PHM with RMS and kurtosis as covariates is given as figure 10 below.

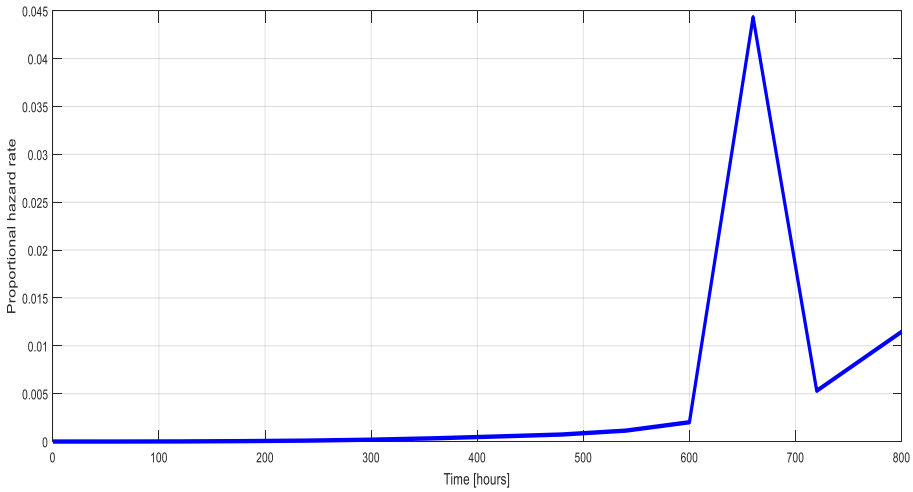


*Figure 10: Proportional hazard rate (PHM)*

2.3.3.2. Probability of failure estimation using the PHM

The probabilistic hazard rate $h(t)$, without considering that the condition of the component, is defined as the instantaneous failure rate at time $t$, therefore the probability of a failure event at time $T$, occurring during an arbitrarily small time period $dt$ after $t$, given that the component has not failed before time $t$, divided by $dt$.

$$h(t) = \lim_{dt\to 0} \frac{\Pr(t \le T < t + dt | T \ge t)}{dt} \quad (28)$$

The probability of failure during the time period $dt$ will equal $dt$ and the probability of not failing before time $t$ is by definition equal to the reliability R(t), which reduces to:

$$h(t) = \frac{f(t)}{R(t)} \tag{29}$$

The reliability $R(t)$ and therefore also the $PoF = F(t)$, can be determined from the hazard rate $h(t)$ and the probability density function $f(t)$, which will all be functions of the fitted failure time distribution parameters in a time-based approach.

However, such probabilistic approach is limited because it is only time-based. The PHM addresses this by assuming that the hazard rate of an item is the product of a baseline hazard rate $h_0$(t) and a functional term, which is function of time and covariates.

$$h\left[t, \overline{Z(t)}\right] = h_0(t) \times exp\left(\gamma, \overline{Z(t)}\right) \tag{30}$$

which is the general form of the problem to calculate the corresponding $PoF$ is now that only the modified hazard rate will be known and not the probability density function$f(t)$. Further manipulation of Equation 29 is required. By definition:

$$R(t) = \int_t^{\infty} f(t)dt$$
$$= \int f(\infty)dt - \int f(t)dt$$
$$= -\int f(t)dt$$
$$f(t) = -\frac{dR(t)}{dt}$$

which means

$$h(t) = -\frac{1}{R(t)}\frac{dR(t)}{dt}$$
$$= -\frac{d\ln(R(t))}{dt}$$

so that

$$-\int_0^t h(t)dt = \ln(R(t))$$

and

$$R(t) = e^{-\int_0^t h(t)dt}$$

This can be discretised:

$$R(t_i) = e^{-\sum_{k=1}^{i} h(t_k)\Delta t}$$

and

$$R(t_{i-1}) = e^{-\sum_{k=1}^{i-1} h(t_k)\Delta t}$$

then

$$\ln[R(t_i)] - \ln[R(t_{i-1})] = -h(t_i)\Delta t$$

giving.

$$R(t_i) = e^{\ln[R(t_{i-1})] - h(t_i)\Delta t}$$

This makes it possible to recursively calculate $R(t_i)$, only as a function of $R(t_{i-1})$ and this $h(t_i)$ will be valid for the PHM:

$$R(t_i) = e^{\ln[R(t_{i-1})] - h(t_i)\Delta t} \qquad (31)$$

with $t_1 < t_2 \ldots \ldots < T_i$ inspection times, when covariate information is updated.

If the cumulative distributive function cdf is defined as the probability of failure at each inspection time, it could then be calculated as:

$$R(t_i) = e^{\ln[R(t_{i-1})] - h(t_i)\Delta t}$$

$$F[t, Z(t)] = 1 - R[t, Z(t)] \qquad (32)$$

The $PoF$ related to the condition of the bearings (in this case bearing #4) at a given time is given in figure 12.

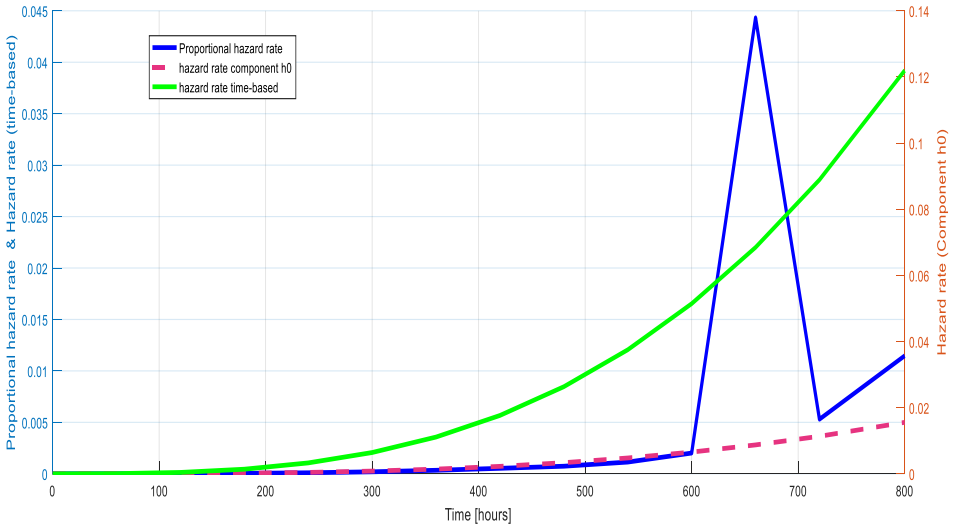


*Figure 11: Comparison of hazard rate*

2.3.3.3. Interpretation of the results

The hazard rate and $PoF$ results obtained for the time-based and the proportional models are respectively plotted in figure 11 and figure 12.

As it is always the case with hazard rate plots, the values are difficult to interpret, but the trends are insightful. For the time-based model figure 8, the hazard rate is smoothly increasing with time (age) to the power of three (β-1). For the proportional model, both the proportional hazard rate, as well as the time-based component (factor $h_0$) of it, are plotted in figure 11. It may be observed that this time-based component $h_0$, although it is smoothly increasing with age to the power of three (β-1), is significantly lower than the time-based hazard rate, due to a smaller η. This means that the over-all proportional hazard rate, up to when the covariates start to increase, is significantly lower that the time-based hazard rate. It is also having a relatively small contribution to the over-all proportional hazard rate, when the covariates start to increase, showing the dominance of the covariates (kurtosis) later in the life of the bearings, closer to the failure time.

The influence of the kurtosis covariate on the proportional hazard rate may be observed starting at 600 hours but decreasing soon after a while, the RMS influence is significantly smaller.

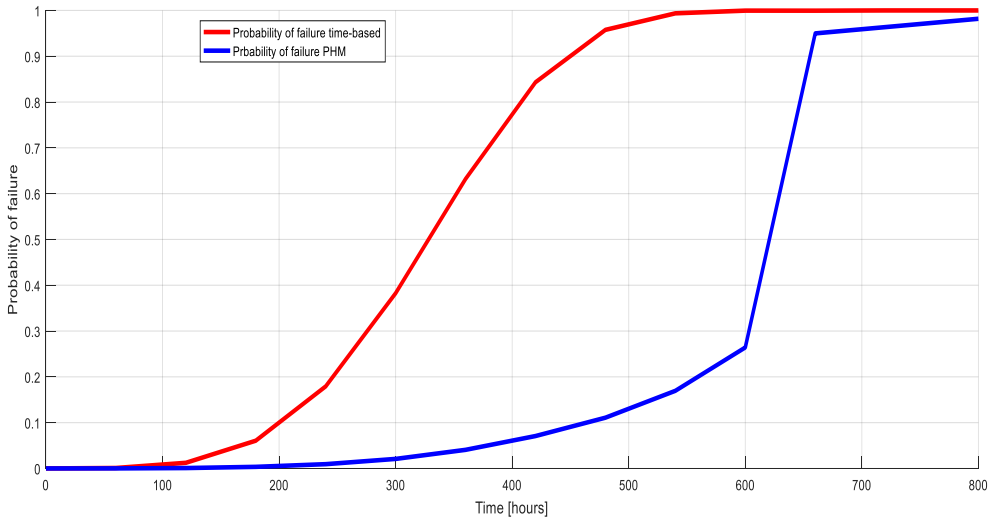


*Figure 12: Comparison of time-based and PHM probability of failure results*

Similarly, the comparison of the probabilities of failure ($PoF$) shown in figure 12, is insightful. It should be noted that the proportional $PoF$ can only be derived from the proportional hazard rate results. The proportional $PoF$ curve is lower than the time-based $PoF$ curve for a major part of the life of the bearing. It reaches a $PoF$ value of only 20% at 550 hours, driven up to that point only be the age of the bearing (implying the usefulness of the age component of the PHM), whereas the time-based $PoF$ reached 20% already at 250 hours and are close to 100% at 500 hours. This is a very significant demonstration of the benefit of the PHM method for more realistic $PoF$ estimation, compared to the time-based model, which is the main reason for this approach.

The proportional $PoF$ rises sharply just at 600 hours due to the kurtosis spike, which demonstrates an insightful way of interpreting kurtosis results in terms of $PoF$. After the dying away of the kurtosis peak, the $PoF$ does not decrease, due to the cumulative nature of the $PoF$ calculation, which makes intuitive sense.

### 2.3.3.4. Optimal decision making based on PHM

The PHM provides an approximate risk of failing for the component based on the age and covariates (RMS and kurtosis for the case study presented here). The information, which is made available by the PHM, should be utilized to obtain economic benefits.

For optimal replacement decision making with the PHM in reliability, Makis and Jardine (2013) made a model available. The model specifies the optimal renewal policy in terms of an

optimal hazard leading to the minimum life cycle cost (LCC). To be able to determine the hazard rate that leads to the minimum LCC it is needed to predict the behaviour of covariates.

Makis and Jardine's model assumes the covariate behaviour to be stochastic and approximating it by a non-homogeneous Markov chain in a finite space. Referring to that model, the expected average cost per unit time is a function of the threshold risk level given by:

$$\emptyset(d) = \frac{C_p + KQ(d)}{W(d)} \tag{33}$$

where, $Q(d) = P(T_d \geq T)$ represents the probability that failure replacement will occur and $W(d)$ the expected time until replacement and $K = C_f - C_p$.

For the bearings case, the prediction of the covariates (RMS) behaviour was performed using a Markov chain and the following transition probability matrix (TPM) with five states was found. Each state expresses a given range of the covariate. For example, the case below is a sample for rms, with:

State 1: from 0.10 to 0.12

State 2: from 0.12 to 0.14

State 3: from 0.14 to 0.16

State 4: from 0.16 to 0.18

State 5: from 0.18 to 0.30

The optimal average cost per unit time found after computation using equation 15 is 6.92 ZAR/day, which is less than the 13.13 ZAR/day for the time-based approach. This is one of the important benefits related to the use of PHM compared to the time-based approach.

### 2.3.4. Benefits of incorporating PHM into RBI

Quantitative risk-based inspection decisions are time-based (having to decide on time-based inspection frequencies) and are therefore normally based on only time-based failure data to estimate the time progression of the $PoF$. RBI, also by definition, incorporates a condition-

based approach, to guide decisions based on inspection (condition) results. These decisions may include keeping a component in operation, but changing future inspection frequencies, or replacing/repairing the component.

As was argued in section 2.3.3.3, that the PHM approach offers significantly better insight into the progression of the $PoF$ with age, than the time-based approach. In the case of the bearings, initial inspection frequency decisions would be based on the concept of a quantified PF-interval (i.e., the time it takes for a bearing to fail from the first onset of damage indication due to the kurtosis covariate contribution). No such insight is available when only observing the time-based $PoF$ curve, which shows only a smooth increase of the $PoF$ over time. It is therefore argued that the PHM approach would lead to both economic and safer inspection frequency decisions.

In terms of the decisions made, based on inspection results (in this case, the RMS and kurtosis measurements), section 2.3.3.4 demonstrates the economic benefits of using the PHM method, compared to only the time-based data. Obviously, should the RBI inspection include condition monitoring where the relation between the condition monitoring parameter(s) have a known and accurate relation to the remaining useful life through a failure model, then this benefit of using PHM for replacement decisions, would not realise. We however argue that the PHM approach will still have economic benefits insofar as replacement decisions are concerned, should the condition monitoring used during RBI not have a known and accurate remaining useful life model available, for example, when the condition indicators do not vary monotonically with the remaining useful life.

A third, most important benefit of incorporating the PHM approach into RBI processes, is derived from the fact that it allows the use of real time condition monitoring data and therefore allows dynamic risk-based decisions, for inspection and maintenance planning. Again, this benefit will also be applicable only to cases where the condition monitoring results cannot be combined with an accurate remaining useful life model.

As mentioned before, PHM does have limitations for situations where the failure manifestation is easily measurable, such as crack growth of an accessible crack, meaning that the condition of the component can easily be quantified, and a condition-based approach would be more appropriate. Another limitation of the PHM is that when covariate data as not available, time-based approaches might be more appropriate.

A decision process identifying the right situation to use the PHM method could be based on the following components:

- The failure mode relevant to the PHM use (e.g., corrosion, wear, inaccessible fatigue damage, etc.).
- The availability of failure and condition data is an important component in the decision process.
- The relative significance of condition versus age data in the PHM computation.
  The relevance of this work is that an enhanced $PoF$ estimation leads to a dynamic risk assessment.

The benefits are:

- The improvement of decision-making support.
- The $PoF$ estimation is enhanced to optimize inspection and maintenance policies leading to a cost-effective approach.
- Where traditional techniques might not give an accurate estimation of the remaining useful life, to plan inspection, the PHM gives a better estimation of the remaining useful life by combining age and condition data for incorporation into RBI, to allow for a better risk-based inspection schedule.

# Chapter 3. Application of PHM model and BLEVE theory on a real-world case study.

## 3.1 Introduction to Case Study 2

The previous chapter comprised the development of a modelling approach that integrates the proportional hazard model into risk-based inspection. The chapter was concluded by a simple case study applying the model. However, this chapter aims to apply the approach to a real risk-based inspection case, which is a HP cooling system for a platinum converting process.

The platinum group metals (PGMs) consist of platinum, palladium, ruthenium, osmium, rhodium and indium (Viviers & Hines, 2005). The process for the extraction of PGMs includes different steps such as smelting, converting, refining etc. At the centre of this process can be found furnace, boiler, high pressure cooling system.

This chapter presents the application of RBI to a furnace high pressure cooling system by incorporating PHM and steam explosion consequence modelling.

The following sections address the risk assessment on the HP cooling system by means of a model that combines historical data with condition data in a unique statistical model.

## 3.2 Problem description

Water coming in contact with liquid metal is well known in the metallurgical industry to be dangerous and has been at the base of many fatal incidents worldwide (Kennedy et al., 2013). During the converting process of the platinum group metals (PGMs), water leaking from a cracked pipe in the HP cooling system, may accumulate on the slag crust on top of a pool of molten matte. This can cause a boiling liquid expanding vapour explosion also called “BLEVE” when sufficient water has accumulated over time. Definitions for BLEVE are proposed in section 1.2.3.3.

Figure 13 schematically depicts water leaking from a HP pipe, at a mass flow rate $\dot{m}_1$, and then accumulating on the slag crust at a mass flow rate $\dot{m}_2$, before the slag fails under the weight of the accumulated water, the water penetrates the matte and then flashes.

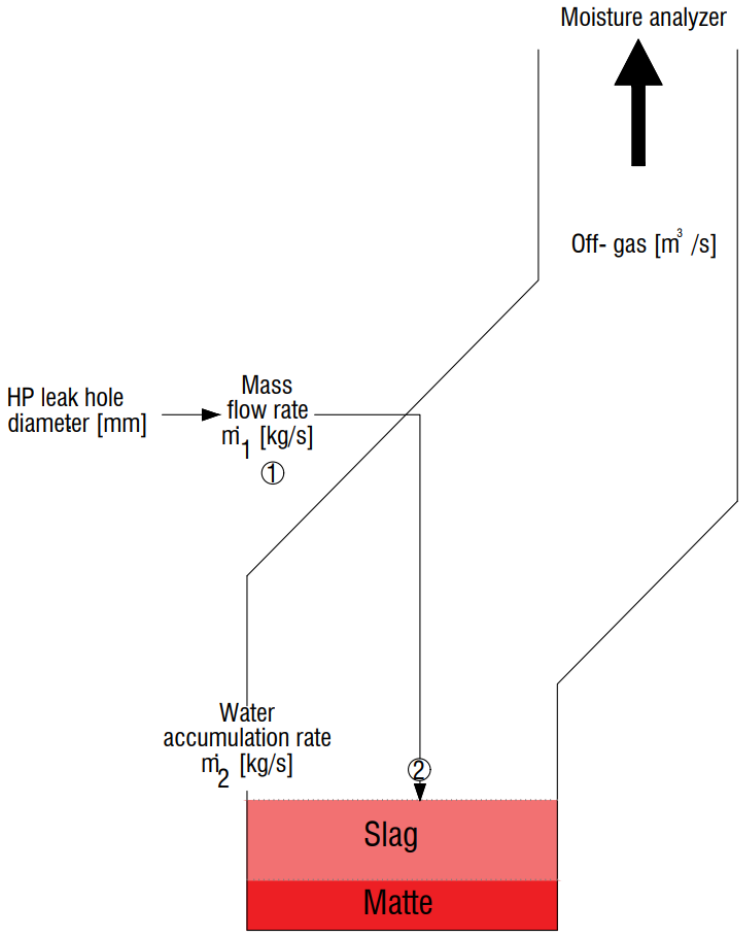


*Figure 13: Overview of the model describing the HP water leak accumulation on the slag*

To address the risk assessment in this chapter a case study is proposed in the following section**.**

## 3.3 Case study 2 details

We consider the closed-circuit high-pressure (HP) cooling system on an Amec Foster Wheeler converter plant. The system is constructed out of SA-192 boiler tubes with a total surface area of 628 square meters in contact with the converter off-gas. The system is designed to cool the converter plant off-gas from the processing temperature of approximately 1400°C degrees down to less than 800°C.

The operating parameters of the HP system are:

- System temperature: 220-250°$C$
- System pressure: 50-70 bar

- Circulating water flow: 1600 ($m^3/hr$)
- Inlet gas temperature: 1200-1400°$C$
- Outlet gas temperature: 600-800 °$C$
- Exit water temperature limit: 275°$C$

The downtime hours experienced due to HP leaks from 2017 until 2020 have been recorded and are shown in table 3. The moisture of the off-gas and the cumulative feed-rate corresponding to the cumulative operating times (age), have also been recorded as condition and usage indicators. It is argued that increasing moisture in the off-gas would indicate the development of leaks in the cooling system.

Table 4 illustrates an example of data featuring moisture and cumulative feed-rate as a covariate for the HP cooling system. The standardization of the measured covariate values is conducted to alleviate the computational burden during parameter fitting, considering that these values may vary significantly in magnitude. The comprehensive data pertaining to tables 3 and 4 can be found in the appendix. The standardized values in table 4 are unitless, and inspection values in the same table are explained in section 2.2.2.3 and table 1.

*Table 3: Sample of downtime hours experienced due to HP leak*

| Year | Date and time start | Date and time stop | Duration (Hours) | Description | Reason |
|---|---|---|---|---|---|
| 2017 | 22 Sept | 23Sept | 11.7 | B/maker patched HP leak | 323-HP cooling system |
| 2017 | 23 Sept | 23Sept | 2.1 | Melting down solids | 323-HP cooling system |
| 2017 | 23Sept | 23Sept | 2 | Melting down solid | 323-HP cooling system |
| 2017 | 12 Oct | 13Oct | 22.8 | HP leak on the west side | 323-HP cooling system |
| 2018 | 08 May | 08May | 1.28 | Melting down solids | 323-HP cooling system |
| 2018 | 13 May | 13May | 1.18 | HP leak | 323-HP cooling system |
| 2018 | 18 May | 18May | 9 | Plant off for HP leak repair | 323-HP cooling system |
| 2020 | 28 Oct | 09Nov | 277 | HP cooling system leak | 323-HP cooling system |
| 2020 | 07 Dec | 07Dec | 1.01 | HP cooling system leak | 323-HP cooling system |
| 2020 | 08 Dec | 08Dec | 4.88 | HP cooling system leak | 323-HP cooling system |

*Table 4: Sample of history*

| Inspection Time | Moisture | Feed rate | Standardized moisture | Standardized feed rate |
|---|---|---|---|---|
| 50 | 3.200 | 2066.500 | 10.917 | -1.864 |
| 100 | 0.073 | 4321.678 | -0.312 | -1.821 |
| 450 | -0.019 | 11576.624 | -0.648 | -1.681 |
| 500 | -0.019 | 13724.506 | -0.648 | -1.640 |

### 3.3.1. Simulation and results for $PoF$ computation based on failure data (Weibull time-based approach).

This section addresses the time-based approach for RBI that involves determining the $PoF$ related to the HP cooling system failure data. The historical failure data employed for this purpose was recorded over a period of three years, and consisted of leaking incidents due to cracking of the piping at various locations in the cooler system. It was assumed that each such incident represented a new independent failure of the cooler, considered to be one non-repairable system, with one Weibull failure distribution, for our purposes. Even though the leaks causing the various incidents had been repaired, it was assumed that no repeat failures occurred at the same location, making this assumption viable.

We first estimate the regression coefficients required to build a time-to-failure two-parameter Weibull equation. Equation (18), which is the log likelihood function for the two parameters Weibull distribution, is maximized to determine the regression parameters.

The maximum likelihood of the log-likelihood function given by equation (19) leads to the outcome, which is equation (20).

The estimation of the shape parameter $\beta$ in equation (20) is performed numerically using a MATLAB code, the result is such that the shape parameter $\beta = 1.5$ for the HP cooling system.

Differentiation of equation (20) gives the shape parameter $= 1.5$ and $\eta$

$$\eta = (\frac{1}{N}\sum_{i=1}^{N} t_i^{\beta})^{1/\beta} = 5180.4\ hours \tag{34}$$

With $\beta$ and $\eta$ known, the hazard rate for the time-based approach is:

$$h(t) = \frac{1.5}{5180.4}(\frac{t}{5180.4})^{1.5-1} \tag{35}$$

Since the HP-cooling system is complex and has multiple failure modes, it is to be expected that the shape parameter will be close to unity. This would indicate a near constant failure rate and hazard rate. Figure (14) below depicts the actual hazard rate related to the failure data for the HP cooling system.

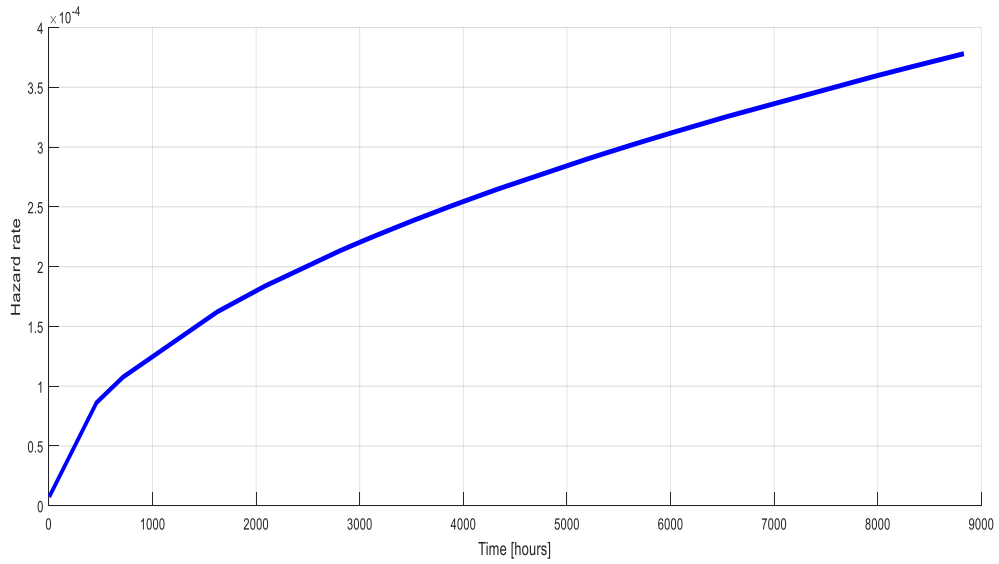


*Figure 14: Hazard rate time-based on the HP cooling system*

The hazard rate in figure 14 is increasing, but gradually tends towards a constant rate. The mean time to failure ($MTBF$) is given by:

$$MTBF = \frac{\text{Operating time}}{\text{Number of failures}} = \frac{8850}{32} = 276 \text{ hours}$$

This means that at each 276 hours or at each 11 to12 days there is a probability of having a leak in the HP cooling system. The probability of failure corresponding to the time-based approach for the HP cooling system is given in figure 15 below. The hazard rate, $MTBF$ and risk calculations are based on operating time and number of failures only, and does not consider the covariates.

From the data under analysis in this work the Laplace trend value is 0.2737 which is between -1 and +1. This means that the data is noncommittal and as a result, the data set is independent and identically distributed, hence renewal theory is applicable.

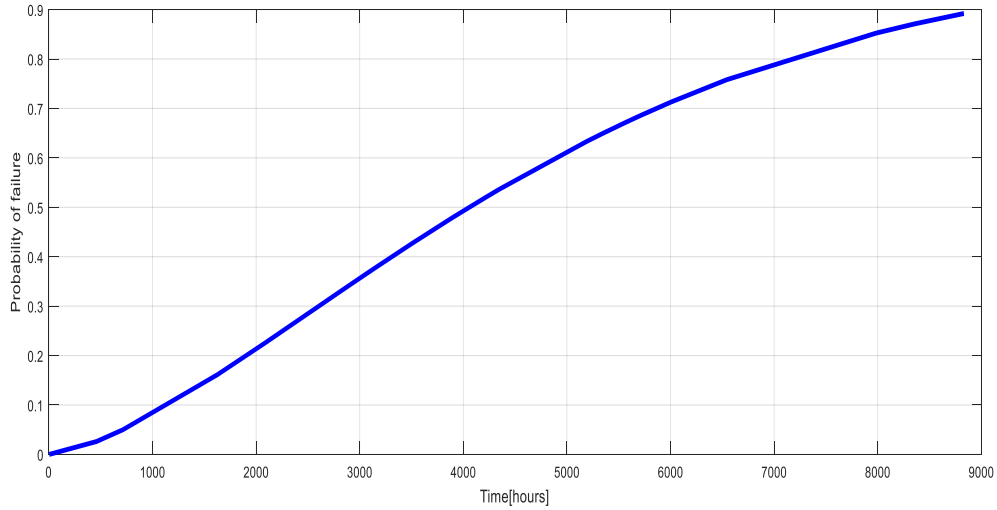


*Figure 15: Probability of failure for the HP cooling system (Time-based)*

*Table 5: Summarized results corresponding to the time-based approach*

| Failure time | Hazard-rate | Probability of failure |
|---|---|---|
| 3.5 | 7.526e-06 | 1.756e-05 |
| 459.5 | 8.623e-05 | 0.0260 |
| 8825 | 0.00037 | 0.891 |
| 8832 | 0.00037 | 0.892 |

### 3.3.2. Simulation and results for *PoF* computation based on the incorporation of covariates into the hazard computation using the PHM.

#### 3.3.2.1. Introduction to the proportional hazard model (PHM)

Referring to section 2.2.2, PHM was defined as a statistical procedure that enables the estimation of the risk for a component or system to fail when its condition is monitored (Jardine & Tsang, 2013). PHM models are part of a broader class of survival analysis models

that enable estimation of the risk of failure at a given time, given the period of operation (age), and any measured covariates that describe the state (condition or usage) of the component or system.

The PHM with a Weibull baseline hazard function is presented in the following equation (36). This equation is the same as equation (6), and is reintroduced here for convenience:

$$h[t, Z(t)] = \frac{\beta}{\eta}\left(\frac{t}{\eta}\right)^{\beta-1} \exp\left\{\sum_{i=1}^{m} \gamma_i Z_i(t)\right\} \tag{36}$$

where $h[t, Z(t)]$ is the hazard function, $Z_i(t)$ are the covariates at time $t$, $\frac{\beta}{\eta}\left(\frac{t}{\eta}\right)^{\beta-1}$ is the baseline hazard function with $\beta$ the shape parameter and $\eta$ the scale parameter, which allow the construction of the baseline part of the model. These parameters are determined by maximizing the likelihood function, based on the historical data.

3.3.2.2. Probability of failure for HP cooling system based on the PHM.

For the sake of convenience, it is important to repeat that the PHM model uses both the moisture and cumulative feed rate as covariates. They are indications of failure available for the system. The first step of this investigation consists of estimating the regression coefficients β, η, γ required to build the PHM (Carstens & Vlok, 2013). After computation, the outcome from equation (26) is described in the following paragraph.

The result from the optimization of equation (26) gives a shape parameter $\beta = 4$, a scale parameter $\eta = 8850$ hours the weight of the covariate $\gamma_1 = 0.0100$ (weight of the moisture parameter) and $\gamma_2 = 0.5281$ (weight of the cumulative feed rate parameter). The regression parameters are obtained from the maximum likelihood equation (26). The hazard rate equation corresponding to the above parameters with moisture and cumulative feed rate as the covariate is given by:

$$h[t, z(t)] = \frac{4}{8850}\left(\frac{t}{8850}\right)^{4-1} \exp[0.0100\,\text{Moisture} + 0.5281\,\text{Feed rate}] \tag{37}$$

A graphical representation of this equation for the PHM with moisture and cumulative feed

rate as covariates is given in figure 16 below.

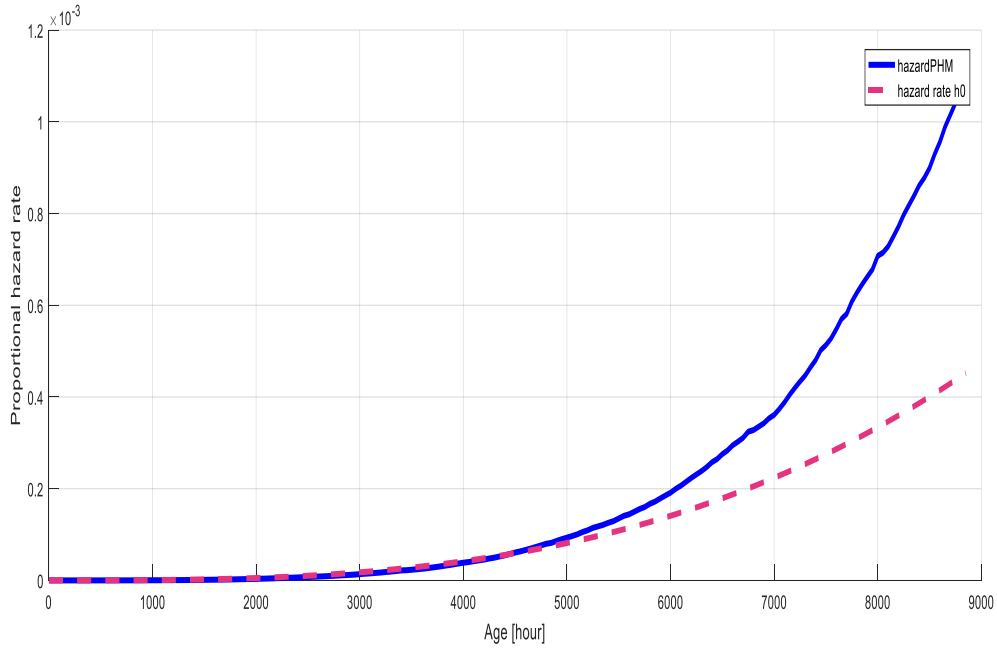


*Figure 16: Proportional hazard rate for HP cooling systems*

Figure 16 shows both the proportional hazard rate, as well as the time-based component (factor $h_0$) of it. It may be observed that this time-based component $h_0$ , is smoothly increasing with age according to a power of three ($\beta - 1$) rule. It is also important to observe that the trend of the time-based component $h_0$ means that covariates influence the proportional hazard rate.

The probability of failure corresponding to the proportional hazard approach for the HP cooling system is given in figure 17 below:

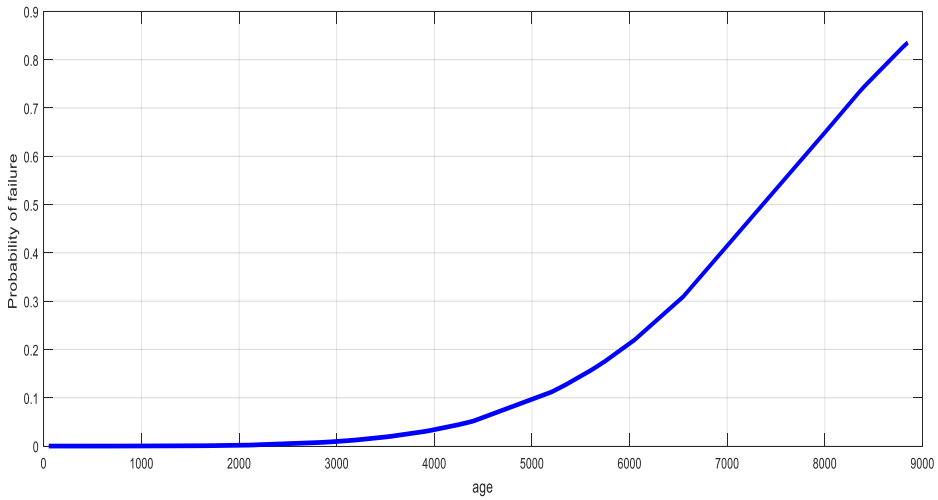


*Figure 17:Probability of failure for HP cooling system (covariatees included)*

3.3.2.3. Comparison between the time-based hazard rate and proportional hazard rate and the $PoF$ related to both.

Figures 18 and 19 below display respectively the hazard-rate related to the time-based and the proportional hazard rate and the $PoF$ related to both, the time-based and PHM approach.

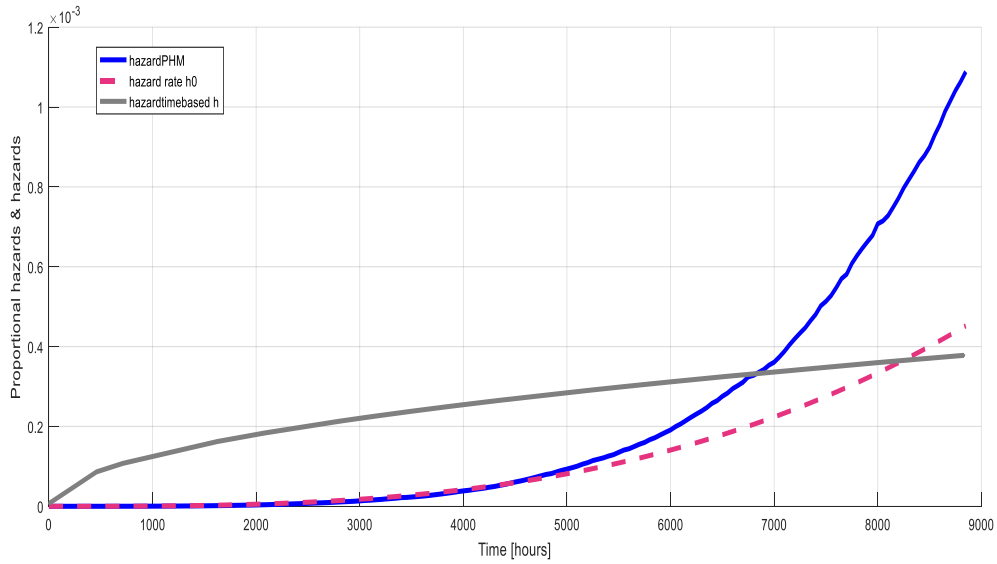


*Figure 18: Comparison of hazard rate*

The hazard rate and $PoF$ results obtained for the time-based and the proportional models are respectively plotted in figure 18 and figure 19.

Normally, the hazard rate values are difficult to interpret, but the trends are insightful as the hazard rate expresses an instantaneous rate of failure. The time-based hazard rate $h$ in figure 18, is slightly increasing with time (age) to the power of 0.5 ($\beta - 1$). However, by inserting covariates in the hazard computation using the proportional model, both the proportional hazard rate, as well as the time-based component (factor $h_0$) of it, as plotted in figure 6, are showing a significantly increasing hazard rate.

This indicates that the incorporation of the covariate information yields a lower initial hazard rate that increases exponentially to a similar value than the time-based hazard rate towards the end of the period. The comparison of the cumulative distribution functions ($PoF$) shown in figure 19 shows a similar result.

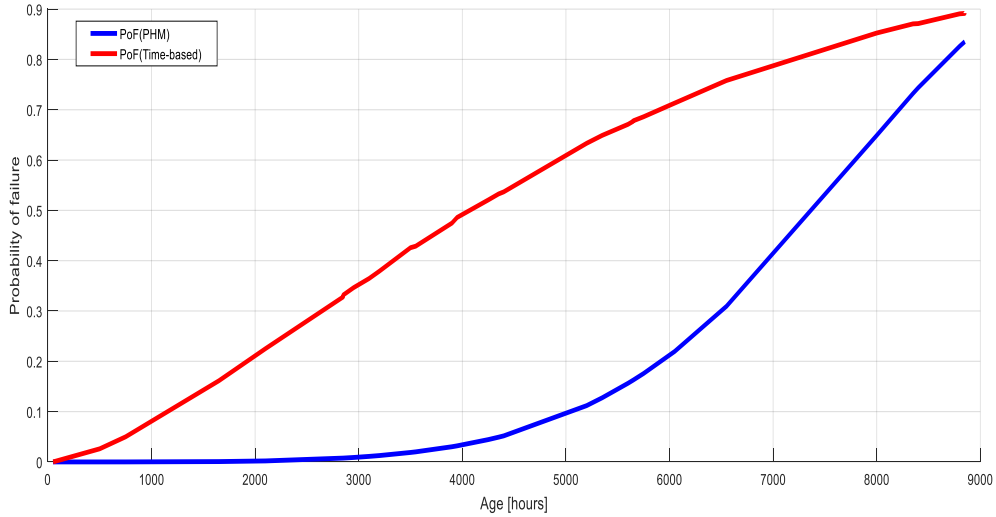


*Figure 19: Comparison of time-based and PHM probability of failure results*

The proportional $PoF$ curve is lower than the time-based $PoF$ curve for the major part of the life of the HP cooling system. It reaches a $PoF$ value of only 20% at 6000 hours, whereas the time-based $PoF$ reached 20% already at 2000 hours and is close to 70% at 6000 hours. This is a very significant demonstration of the benefit of the PHM method for more realistic $PoF$ estimation, compared to the time-based model.

### 3.3.3. Consequence of failure for HP cooling system based on the BLEVE.

#### 3.3.3.1. Introduction

Current furnace designs often integrate extensive use of cooling elements to accomplish long service lives at high operating intensities. However, contact between water and high-temperature fluids can provoke boiling liquid expanding vapour explosions (BLEVEs) (Kennedy et al., 2013). There are several types of explosion, such as deflagration, detonation, dust explosion, vapour cloud explosion, and boiling liquid expanding vapour explosion (Kumar Malviya & Rushaid, 2018). However, for the purposes of this work, consequence of failure modelling refers to the impact or consequences of BLEVE. Contact between water and high temperature fluids can result in powerful BLEVE.

BLEVEs are important due to their severity and the fact that they simultaneously involve diverse effects which can cover a large area: overpressure, thermal radiation, and missiles ejection (Planas-Cuchi, Salla, & Casal, 2004).

3.3.3.2. Impact or consequence of BLEVE

The evaluation of the consequences of a BLEVE pivots on two parameters:

- The burst energy determines the severity of the blast overpressure generated by the BLEVE (Abbasi & Abbasi, 2007).
- The impact of the blast on structures and injuries on persons.

The calculation of a BLEVE incident severity consists of a stepwise procedure. One of the first steps is to calculate the energy associated with the BLEVE. According to the TNT equivalency method, the energy or the effects of physical explosion can be expressed as TNT equivalent mass by using the appropriate energy conversion factor ($approximately\ 4680\ \frac{\mathrm{J}}{\mathrm{kg}}$ of TNT) where $M_{TNT}$ is the equivalent mass of TNT ($kg$). The equation is provided by the API 581 document:

$$M_{TNT} = C_{30} n_v R T_s \ln\left[\frac{P_s}{P_{atm}}\right] \qquad (38)$$

with $T_s$ the storage or normal operating temperature, $R$ is the universal gas constant which is 8.314 J/(kg-mol), $n_v$ is the moles (kg-mol) that flash from liquid to vapour upon release at $t_0$ atmosphere, $P_s$ (kPa) is the storage or normal operating pressure, and $P_{atm}$ is the atmospheric pressure.

Abbasi and Abbasi (2007) proposed equation (39) to calculate the energy associated with the BLEVE, if the flashing fraction of the liquid and the pressurized gas expand isentropically as an ideal gas.

$$M_{TNT} = \frac{2.4 \times 10^{-4} \times PV^*}{k-1}\left[1 - \left[\left[\frac{101}{P}\right]^{k-1/k}\right]\right. \qquad (39)$$

with P (kPa) the pressure in the vessel at the time of burst, $V^*$ ($m^3$) is the total vapour volume $k$ ratio of specific heats at constant volume, and $M_{TNT}$ is the equivalent mass (kg) of TNT of the explosion energy.

Once the explosion energy of a BLEVE is estimated, overpressure can be determined by employing the correlations available in literature, which link overpressure with explosion energy, and the distance from the accident epicentre.

Overpressure (or blast overpressure) is the pressure caused by shock waves over and above a normal atmosphere. Kumar and Rushaid (2018) suggested an equation to calculate the overpressure:

Assume the equivalent TNT mass (kg):

$$M_{TNT} = \frac{f_E \, \Delta H_c M_G}{\Delta H_{TNT}} \qquad (40)$$

with $M_G$ (kg) the mass of the gas that participates in the explosion, $\Delta H_c$ is the heat of combustion of the gas (kJ/kg), and $\Delta H_{TNT}$ is the heat of combustion of TNT (kJ/kg).

The scaled distance $Z$ in (m/$kg^{1/3}$):

$$Z = \frac{x}{{M_{TNT}}^{1/3}} \qquad (41)$$

where $M_{TNT}$ is the equivalent TNT mass, and $x$ is the distance from the centre of the explosion. The overpressure of the shock wave is given by:

$$PS = \frac{80.800[1 + [\frac{Z}{4.5}]^2}{\sqrt{1 + [\frac{Z}{0.045}]^2}\sqrt{1 + [\frac{Z}{0.32}]^2}\sqrt{1 + [\frac{Z}{1.35}]^2}} \qquad (42)$$

3.3.3.3. Impact modelling

After defining the reference fluid, which is steam in our case, the next step is to assess the consequences of incident outcomes on workers and structures utilizing impact modelling.

It is well known that overpressure, thermal radiation, etc. cause damage according to the exposure level, however, mathematical modelling is needed to predict the impact and risk associated with the BLEVE (Ahumada, 2016).

To assess the consequences of an accident on people and structures, a probit model is often used (Mustapha & El-Harbawi, 2016). The word probit relates to ‘probability plus unit’. In statistics the probit variable Y is a measure of the percentage of a population submitted to an effect with a given intensity ($V$). The probit variable $Y$ therefore represents a dose-response relationship and provides a measure of having certain damage as a function of the intensity of the $V$ dose through a linear correlation. As it is usually the case that this variable follows a normal distribution, with an average value and a standard deviation of The probit function is usually of the form:

$$Y = a + blnV \qquad (43)$$

where $Y$ represents the probit function or variable, and $a$ and $b$ are constants obtained from best fitting response data or are experimentally determined from information on accidents, etc. $V$ is the causative factor whose definition changes according to the associated hazard, it is also a measure of the intensity of the damaging effect. It can be overpressure, thermal radiation, or any other parameter (Mustapha & El-Harbawi, 2016). For this research, overpressure is used as a measure of the damaging effect.

In this thesis, the dose has been considered as the overpressure whereas the effect is considered as the damage on the structure as well as lung haemorrhage on the people. The variable Y can be directly compared with the actual failure probability (Salzano, 2001).

The relationship between the probit variable $Y$ and the probability of fatality $P$ is given by

$$P = 50[1 + \frac{Y-5}{|Y-5|}\text{erf}\left(\frac{|Y-5|}{\sqrt{2}}\right) \qquad (44)$$

with $P$ the probability of fatalities due to BLEVE and erf; the error function.

3.3.3.4. BLEVE impact estimation for the HP cooling system

1) Overpressure estimation

Consequence of failure in this thesis is related to the BLEVE effects. However, the literature describes three types of BLEVE effects: the shock wave or overpressure , the thermal radiation, and the fragment projection (Shariff, Wahab & Rusli, 2016). Here we deal with overpressure as the causative factor of damaging effect. In fact, overpressure is the pressure caused by a shock wave over and above normal atmospheric pressure (Kumar Malviya & Rushaid, 2018). To estimate the overpressure given in equation (42), the equivalent TNT mass equation (40) is first needed. However, equation (40) includes an important parameter $M_G$ which is the mass of the explosive material which will be based on leak rate modelling. For the purposes of leak modelling, we use the Bernoulli equation for fluid flow through a pipe with a given diameter. (Saqib, Mysorewala & Cheded, 2017)

$$\dot{m} = \dot{V} \times \rho \tag{45}$$

with $\dot{V}$ the flow rate and $\rho$ the water density.

The mass is a function of the flow rate $\dot{V}$ given by:

$$\dot{V} = C \times A \sqrt{\frac{2\Delta P}{S\rho}} \tag{46}$$

with $C$ the discharge coefficient. For an orifice in pipe, it varies between 0,60 to 0,80. $A$ is the crack area, the specific gravity equals that of water, $\rho$ water density = 1000 kg/cube meter, and $\Delta$P is the pressure drop.

From equations (45) and (46) which compute respectively the mass and flow rate of the material flowing through the pipe crack to mix with the molten matte and slag in the furnace, the equivalent mass of the TNT given in equation (40) is obtained. Together with the scaled distance, the following graph is obtained:

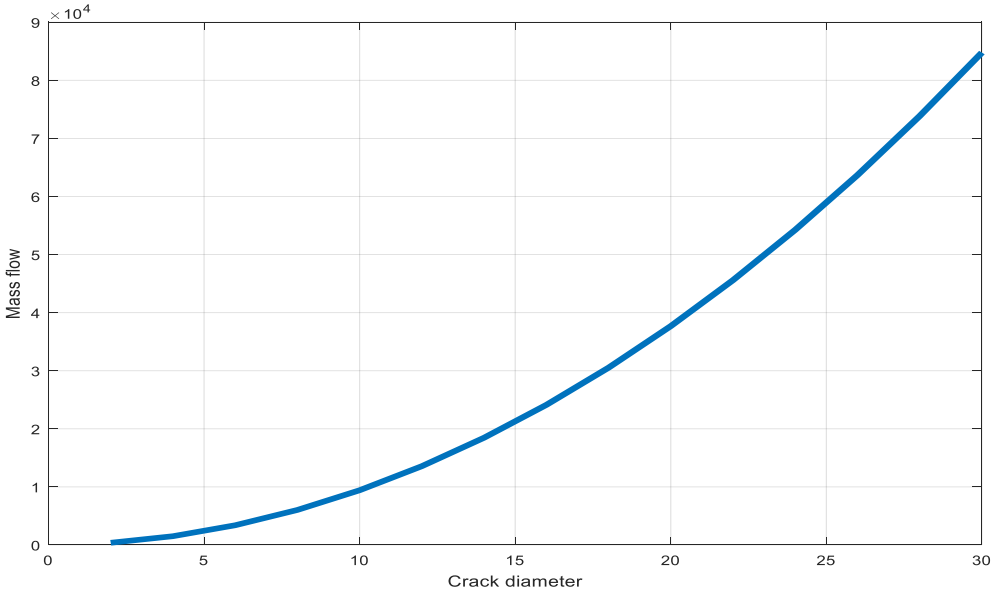


*Figure 20: Mass flow versus crack diameter*

The overpressure related to the explosion is given by figure 21 below:

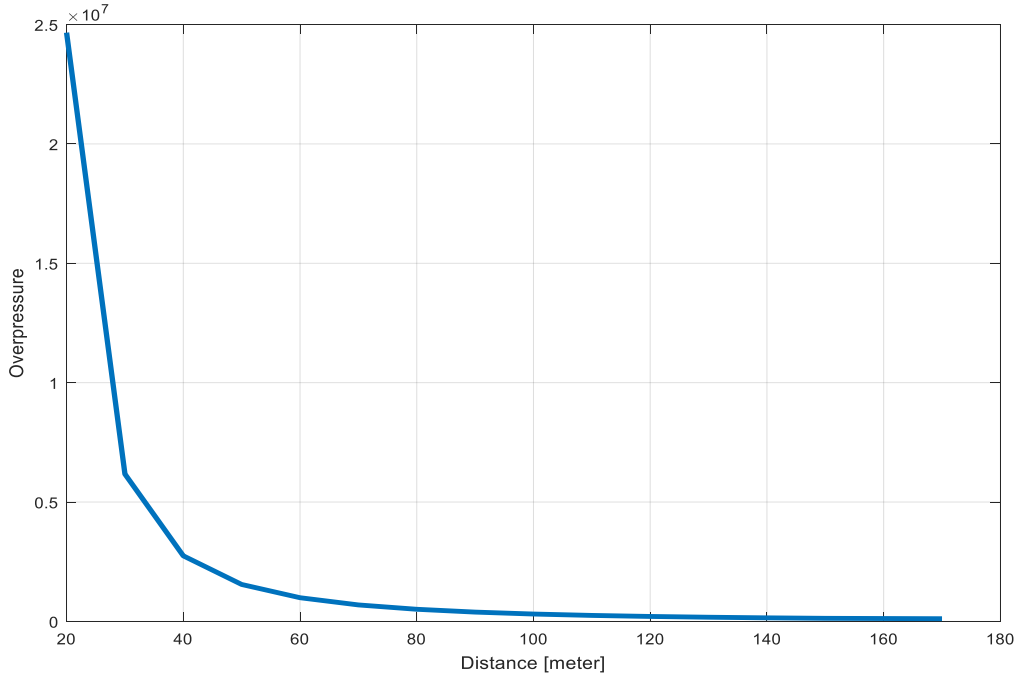


*Figure 21:Overpressure in kPa versus distance in meter*

To estimate the consequences of an accident on people, we will refer to the probit function defined in equation 43. The following section evaluate the effects of overpressure on humans and constructions.

2) Effects of overpressure on human and constructions

The direct effects of overpressure on humans are eardrum rupture, lung haemorrhage, whole body displacement injury and injury from shatter glasses. It is also important to notice that the most likely harm to people during the explosion comes also from the indirect effects of people being inside or close to the building when it collapses (Mustapha & El-Harbawi, 2016).

The typical consequences from an explosion are burning, fragments hitting the people, building or structure failing down, people falling, etc.

Sharrif, Wahab and Rusli (2016) provide probit correlations for a variety of causes and their corresponding effects:

The probit equation for an eardrum exposed to overpressure is given by:

$$Y1 = -15.6 + 1.93\ln P_{ovr} \qquad (47)$$

The probit equation relating death from lung haemorrhage to overpressure is given by:

$$Y2 = -77.1 + 6.91\ln P_{ovr} \quad (48)$$

There have been several experimental and theoretical studies of the behaviour of shattering and flying glass and studies of glass breakage following accidental explosions. The probit equation relating glass breakage to overpressure is given by:

$$Y3 = -18.1 + 2.79\ln P_{ovr} \quad (49)$$

and the probit equation relating structural damage to overpressure, by:

$$Y4 = -23.8 + 2.92\ln P_{ovr} \quad (50)$$

As stated previously, in this research we consider the BLEVE effect based on probit function equation (43) using overpressure as a causative factor $V$.

3) Probability of fatalities

The probability of fatalities due to BLEVE can be obtained using equation (41), leading to the following curves:

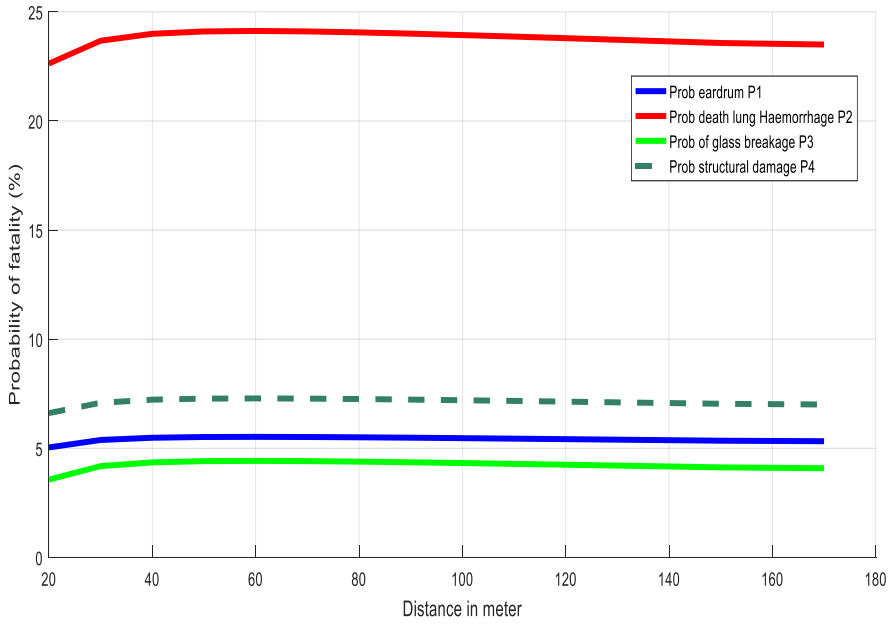


*Figure 22: Probability of fatality versus distance*

### 3.3.4. Summary of the chapter

In this chapter, a case study was undertaken, utilizing data obtained from a closed-circuit high-pressure (HP) cooling system on an Amec Foster Wheeler converter plant. The crucial elements

necessary for risk computation were defined namely, the probability of failure and the consequence of failure. The quantification of the $PoF$ was first based solely on historical failure data, adhering to the approach prescribed by API 581, subsequently, the quantification was further enhanced by employing the PHM, which represents the proposed method. The computational results, as depicted in figure 19, clearly demonstrated the added value associated with the proposed methodology. Additionally, this chapter introduced the computation of the $CoF$ by means of probability of fatalities resulting from a BLEVE, a notion that had not been addressed in chapter 2. The following chapter will place considerable emphasis on the crucial importance of risk mitigation, while also presenting a number of viable mitigation options that can be quantifiably effective in achieving said mitigation.

# Chapter 4. Mitigation decisions based on quantified risk in industrial plant.

## 4.1 Introduction

Risk mitigation is the strategic approach employed by industries to minimize the impacts of business risks. The process of risk mitigation entails understanding specific risks and threats, acknowledging their existence, and making appropriate decisions to minimize their effects (Ni, Chen & Chen, 2010). This chapter addresses the decision-making process of risk mitigation based on quantified risk for a high-pressure cooling system in a furnace.

It is important to note that risk mitigation does not follow a universal model, as different industries adopt their own approaches to mitigating the effects of particular threats. Nevertheless, there are some common techniques employed for risk mitigation, including risk transfer, risk acceptance, risk avoidance, and risk monitoring (Wyckaert, Nadeau & Bouzid, 2017). However, in this work risk is dynamically monitored and mitigated when reaching a threshold value.

Furthermore, as risk mitigation is an integral component of the risk management process, it necessitates a comprehensive risk assessment that culminates in a quantitative risk assessment. This work primarily focuses on developing a methodology to optimize quantitative risk assessment by employing proportional hazards model and the consequence of failure quantification based on BLEVE theory in order to establish an optimal inspection strategy aimed at mitigating the risk in the furnace high pressure cooling system.

Qualitative methods for assessing risk that are susceptible to CWA the European standard, encompass techniques for identifying hazards such as risk checklists, qualitative risk analysis, preliminary hazard analysis (PHA). Hadj-Mabrouk (2017) list inspections, hypothetical accident and consequence analysis, failure mode and effect analysis (FMEA) (Liu et al , 2013), hazard and hazard regulation studies (HAZOP), as well as other methods (AlKazimi & Grantham, 2015).

Experts' opinions are used in qualitative methods to provide relative levels of high, medium, and low risks that are convenient and quick to operate. However, the frequency and consequences of hazardous accidents cannot be quantified. Semi-quantitative risk assessment,

on the other hand, is a risk analysis technique based on quantitative risk indicators. Quantitative risk analysis (QRA), also known as Probability Risk analysis which is addressed in API 581, is a rigorous mathematical and statistical method employed to quantify absolute accident frequency (Steijn, Van Kampen, Van der Beek, Groeneweg & Van Gelder, 2020). This evaluation and analysis method is widely utilized in the nuclear, aviation, and petrochemical industries.

However, despite the inclusion of qualitative and quantitative evaluations in the CWA and API 581 respectively, there remains a gap in the quantification of risk. The calculation of probability of failure ($PoF$) primarily relies on historical failure data considerations only, while the quantification of Consequence of Failure ($CoF$) is often approached qualitatively. This work aims to address both the $PoF$ and $CoF$ quantification in order to enhance risk assessment and subsequently improve risk mitigation strategies.

The assessment of asset risk can have significant consequences. Singh and Pokhrel (2018) argue that the risk assessment method provided by RBI can guide inspections of stations and improve economic benefits. However, while RBI includes risk assessments of corrosion thinning failure modes, its focus is primarily on oil refining, petrochemical, and chemical plants, which are not always applicable to the working conditions of oil and gas processing plants. Furthermore, the application of RBI requires a substantial amount of data collection, and the accuracy of evaluation results is often difficult to guarantee.

Additionally, the existing asset integrity management process fails to integrate with pipeline and pressure vessel integrity management in the application of oil and gas stations, which makes implementation of asset integrity management challenging. Moreover, the risk management link relies on multiple parameters, such as failure data, which do not facilitate pre-emptive risk assessment and cannot effectively support preventive maintenance elements. As such, Liao et al. (2023) propose an innovative risk assessment method. By analysing various failure modes of pressure vessels, they created risk quantification and classification of pressure vessels based on failure modes (RBFM), which can quickly prepare risk assessments for pressure vessel failure modes. Unlike RBI, RBFM circumvents the need for extensive failure data statistics, combines failure mechanisms, starts from the failure development trend, establishes relevant factors and indicators, and identifies the likelihood of failure.

The main innovations of RBFM risk assessment method are as follows: (1) They undertake an assessment of the risks associated with diverse failure modes. That exercise has provided a firm grounding for future detection and maintenance activities. (2) By means of comparing various standards, specifications, and literature studies, a sound methodology has been established to avoid the pitfalls of an invalid database. Further, they have developed indices and value ranges under different failure modes, considering the influence of medium and working conditions on the incidence of failure. The correlation between detection methods and risk levels has been enhanced. Drawing on failure mode, failure probability, and risk level, a detection strategy that encompasses a detection method and detection cycle has been devised, thereby improving the accuracy rate of equipment inspection.

The integrity management of pressure vessels has been improved through this strategy, rendering the risk assessment of pressure vessels more precise. This approach has also led to an improvement in the integrity management level of pressure vessels at the station. However, unlike Liao et al. (2023) who considered different failure modes to investigate the risk assessment, this work considers only a unique failure mode as it serves as an illustrative case to support the proposed methodology. Furthermore, this work demonstrates the application of risk management of a high-pressure (HP) cooling system for a metal smelting furnace, as water ingress into the furnace from leaks due to cracks, can cause a steam explosion. The proposed risk management methodology incorporates a quantitative assessment of the Probability of Failure ($PoF$), based on proportional hazard modelling (PHM), and the consequence of failure ($CoF$), of an explosion event as was proposed in chapter 3.

The unmitigated risk is thereby quantified by means of a risk matrix which enables evaluating and deciding on suitable risk mitigation strategies. Probable risk mitigation strategies are such as using risk based inspection principles to define the inspection frequency sufficient to ensure that repair actions are taken before leaks occur, or to shorten the furnace campaign duration before swapping out and performing major rebuild or replacement, to lower the risk to an acceptable level.

## 4.2 Objectives of risk assessment

Risk assessment may target three objectives: evaluation, forecast and understanding with the latter one being the most demanding (Ryser, 2021). The first objective is to quantify the risk the assets are exposed to, considering that a risk quantification measure has been precisely

defined. The second objective is to forecast potential losses, including. social, economic, regulatory factors. The latter and most demanding objective is to understand why potential losses occur and why historical losses have occurred. In this work more attention is given to the first objective which consist of quantifying the risks. To analyse and quantify risks, various methodologies are available, including qualitative and quantitative methods (Gebremeskel & Gebregziabher, 2021). The following section addresses risk quantification with particular emphasis on both qualitative and quantitative method.

## 4.3 Risk quantification

Risk quantification is a crucial component of the decision-making process within all organizations. The act of risk quantification entails the assignment of numerical values or the measurement of potential risks that an organization may encounter. The quantification of risks encompasses two fundamental aspects: the probability of a risk event taking place and the potential financial repercussions that may arise if the risk event indeed occur (Gebremeskel & Gebregziabher, 2021). This serves as the foundation for conducting risk assessments, enabling businesses to comprehend the risk landscape in which they operate.

The key difference between qualitative and quantitative risk analysis is that qualitative risk is based on subjective judgement, while quantitative risk analysis is objective based on verified and specific data. Qualitative risk assessment may rank the risk from one scenario or group of scenarios to be greater than some other scenario or group of scenarios. When all the scenarios from a system are included in the ranking, the ranking can only be done subjectively. In contrast, for quantitative risk assessment, the risk from each scenario is estimated numerically, allowing the analyst to determine not only risk relative to all scenarios in the system, but absolute risk measured on whatever scale of units is chosen, this determination can be made objectively using numerical scale (Andreis & Florio, 2019).

### 4.3.1. Qualitative risk assessment

#### 4.3.1.1. Introduction

Qualitative risk analysis is a process of assessing the impact of identified risk factors. Through this process, the priorities are determined for solving potential risk factors, depending on the impact they could have. The main characteristic of the qualitative risk assessment method is

the use of subjective indexes, such as ordinal hierarchy: Low-medium-high (Ryser, 2021). The following are steps for qualitative risk analysis:

- Step 1 is to identify risk. In this step a master list of risks is created.
- Step 2 is to classify risk, there are several techniques for classifying risks, with one popular technique being the risk matrix which combines the consequence and likelihood of a risk occurring. The following subsection will describe the risk matrix.
- Step 3 is to control risk; this step is generally divided into two categories. The first category is focused on targeting the root causes of risks such as hazard or inefficient management processes. The second category is geared towards mitigating the negative impact of the risk through corrective actions.
- Step 4 is to monitor the risks.

#### 4.3.1.2. Introduction to the risk matrix

Plotting $PoF$ and $CoF$ values on a risk matrix is a productive method of representing risk graphically. $PoF$ is plotted along one axis, increasing in magnitude from the origin, while $CoF$ is plotted along the other axis (API RP 581, 2016). It is important to notice that it is the responsibility of the owner (user) to define and document the basis for $PoF$ and $CoF$ category ranges and risk targets used.

A risk matrix can be defined as a mechanism to characterize and rank process risks that are typically identified through one or more multifunctional reviews (e.g. process hazard analysis, audit or incident investigation) (Markowski & Mannan, 2008).

Plotting the risk results in a matrix is an efficient way of presenting the distribution of risks for components in a processing unit without using numerical values (API RP 581, 2016). There are two dimensions to a risk matrix, which consist of evaluating how severe and likely an unwanted event is. The combination of these two dimensions creates a matrix. The risk matrix is known as the simplest and easy-to-apply semi-quantitative risk assessment tool (Ni et al., 2010). In this work risk quantification is performed referring to the risk matrix taken from API RP 581(2016).

1) Traditional risk matrix approaches

The traditional risk matrix also called the original risk matrix (ORM) was introduced by the Electronic System Centre and developed by US Air Force and MITRE corporation (Li, et al.,

2014). In the traditional risk matrix, two key metrics for risk are the probability of occurrence and the severity of consequences illustrated in the subsequent bullets.

- Probability of occurrence

Probability of occurrence capture the likelihood that an identified risk could happen. The probability of occurrence in table 6 uses a rating and value scale ranging from inconceivable or not present (1) to very likely (5).

The probability of occurrence table with a standard linear scaling chart includes a per-cent probability that an issue will occur. Note that this chart is done in accordance to normal practice scaled from 1 to 5 with 5 being the highest probability.

*Table 6: Probability of occurence table (From API 581)*

| Likelihood | Description | Rating Value | Per cent |
|---|---|---|---|
| Very likely | The most likely result of the hazard | 5 | Above 0.1 |
| Possible (Likely) | Has a good chance of occurring and is not unusual | 4 | 0.1 |
| Conceivable | Might occur at some time in future | 3 | 0.01 |
| Remote | Has not been known to occur after many years | 2 | 0.001 |
| Inconceivable | Is practically impossible and has never occurred | 1 | 0.0001 |

- Severity of consequences

There are several ways of considering severity: An event could be very severe from the perspective of people's life or the perspective of damage to a facility. More often four perspectives are used (people, environment, safety, and health). Any event can be judged against these four categories.

The severity of consequences in table 8 assigns a rating based on the impact of an identified risk to safety, resources, property, and environment. Each rating is then assigned a value (for example" No risk "may be assigned a value of 1 and a "High" rating may be assigned a value of 5).

The severity of consequences with a standard linear scaling chart evaluates impacts on people, safety, environment, and health associated with each rating.

*Table 7: Severity of consequences table (from API 581)*

| Severity | Description | Rate |
|---|---|---|
| Catastrophic | Numerous fatalities irrecoverable property damage and productivity | E |
| Fatal | Approximately one single fatality major property damage if the hazard is realised | D |
| Serious | Non-fatal - injury, permanent disability | C |
| Minor | Disabling but not permanent injury | B |
| Negligible | Minor abrasions, bruises, cuts, first aid type injury | A |

- Low probability, high severity

The complexity of the events that have very low frequency, but a catastrophic severity is that if the risk matrix categories are not set up correctly, these types of events tend to fall off the grid and get less attention than they deserve.

This is the problem with historical frequency scales, where an event will get the lowest possible score just because it has never occurred. A possible solution is to make the worst severity category the highest priority category, regardless of the probability.

2) Types of risk matrix according to API 581

Referring to the API RP 581(2016), two risk matrix examples are provided in figure 23 and figure 24. In both figures, probability of failure $PoF$ is expressed in terms of number of failures over time $P(t)$or damage factor ($DF$). Consequence of failure $CoF$ is expressed in the area or financial terms in the examples. According to the examples, two types of risk matrix can be described:

- Unbalanced risk matrix

$PoF$ and $CoF$ value ranges are allocated numerical and letter categories, respectively, increasing in order of magnitude (API RP 581, 2016). Risk categories (high, medium-high, medium and low) are allocated to the boxes with risk matrix shading asymmetrical.

For example, using table 6 and 7, the 3C box is medium risk category when plotted in figure 23.

Figure 23 below expresses the unbalanced risk according to API 581.

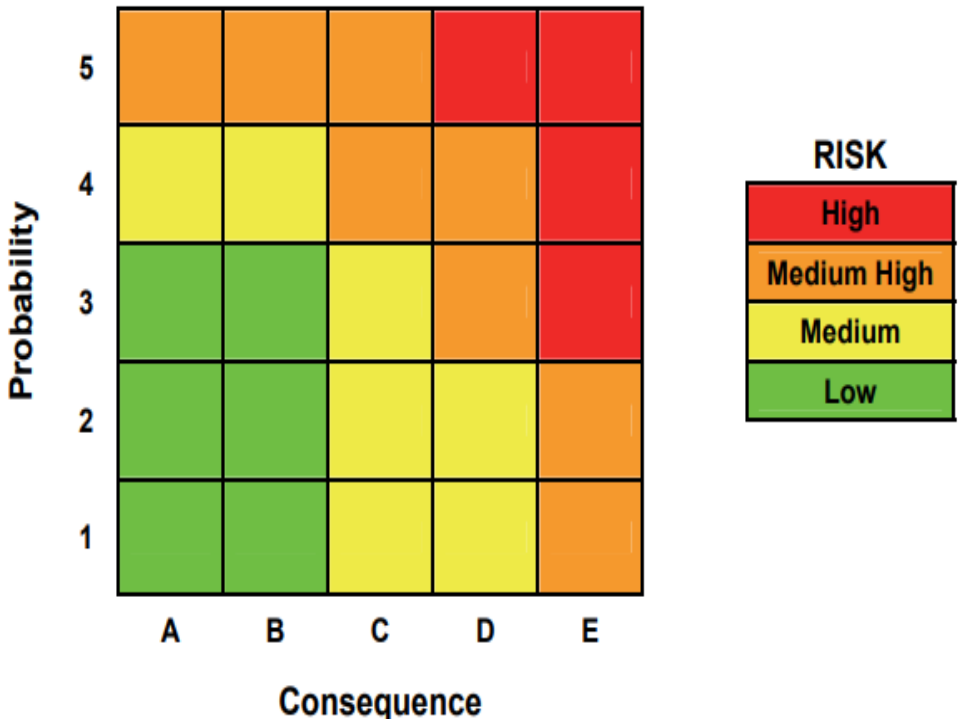


*Figure 23: Unbalanced Risk matrix (Figure taken from API 581)*

- Balanced risk matrix

The $PoF$ and $CoF$ value range are allocated numerical and lettered categories as in the previous section. However, for this case risk categories (High, Medium, low) are allocated symmetrical to the boxes, when values from table 6 are used. However, the 3C box in figure 24 example corresponds to a medium risk category.

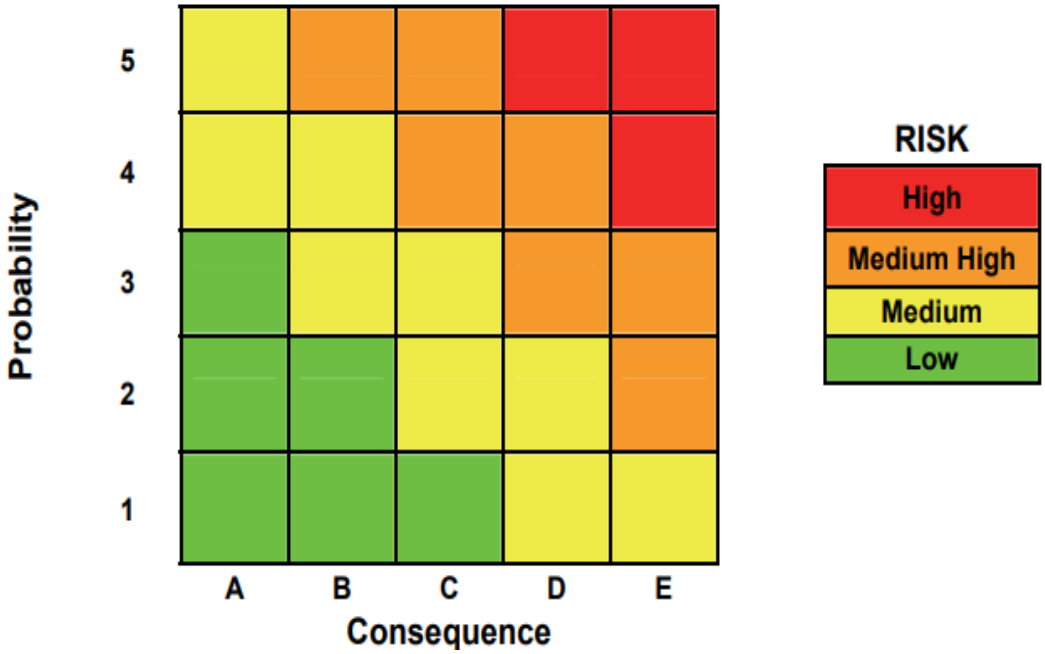


*Figure 24: Balanced risk matrix* (API RP 581, 2016).

All ranges and risk category shading given in table 11, as well as in figures 23 and 24 are examples of dividing the plot into risk categories and are not recommended risk targets and thresholds (API RP 581, 2016). It is the responsibility of the owner (user) to established the range values for their risk-based.

3) The design of the risk matrix

The risk matrix is a very important tool for risk assessment, although the design of the risk matrix is a topic that has not reached a consensus, despite its widespread use in practice (Bao et al., 2017). Many methods have been proposed to help design a risk matrix, such as fuzzy risk matrix proposed by Markowski & Mannan (2008). Bao et al.(2017) compared two risk matrix design methods from the perspective of applicability. Duijm (2015) investigated and explored the weaknesses related to the risk matrix and provided a recommendation for the use design of the risk matrix.

According to Markowski and Mannan (2008), to produce or design a risk matrix, some basic rules should be followed:

- The basis for the risk matrix is the standard definition of risk as a combination of the severity of the consequences occurring in a certain accident scenario and its probability. That means only two input variables are needed to construct a risk matrix. The output risk index id determined only by the severity of the consequences and their probability.
- The severity of consequence, probability and output risk index can be divided into different levels, respectively, with qualitative description and scales.
- The calculation process of matrix producing is presented by the logic implication if the probability is $p$ and the severity of consequence is $c$ than $r$ is the risk.

### 4.3.2. Quantitative risk assessment

Quantitative risk assessment (QRA) is a systematic approach implemented to calculate risks arising from hazardous events (Declerck, 2002). This technique involves the calculation of potential consequences associated with a hazard, as well as the frequency at which the hazard may occur. These factors are then combined to quantify the risk in numerical values, typically pertaining to the risk of fatality. QRA encompasses the evaluation of all identified hazardous events to assess the overall risk levels (Declerck, 2002). Often, similar hazardous events are aggregated and evaluated together as bounding or representative events.

Quantitative risk assessment is a systematic approach to evaluating and managing risks by assigning numerical values to the likelihood and consequences of potential hazards (Rodolfo, Mason & Nassivera, 2011). In the case of pressure vessel as the case of this work quantitative risk assessment involves estimating the probability of failure and the potential consequences of failure. This is typically done by analysing historical and condition monitoring data, using a statistical model. This will be described in section 4.4.

## 4.4 Case study 3: Risk assessment of the HP cooling system

This particular case study bears corresponds to the case study 2, but with the probability of failure ($PoF$) and the consequence of failure ($CoF$) calculation which were already calculated in chapter 3.

In chapter 4, our focus shifts towards risk analysis and the subsequent decision-making process of risk mitigation, ultimately culminating in the formulation of an inspection schedule.

As in the preceding case study, the design characteristics and processing temperature, along with the dimensions of the surface that comes into contact with the exhaust gas from the metal smelting furnace related to the closed circuit high pressure cooling system, remain unchanged. The operational variables of the high-pressure system, including system pressure, temperature of the gas at the inlet and outlet, and other parameters, remain the same.

The moisture of the off-gas and the cumulative feed-rate corresponding to the cumulative operating times (age), have been recorded as condition and usage indicators. It is argued that increasing moisture in the off-gas would indicate the development of leaks in the cooling system. A case study is presented in this section to illustrate the risk assessment implementation conducting to the risk mitigation for the HP cooling system.

As emphasized previously in this section, the two components referred to as the probability of failure and the consequence of failure are necessary for the quantification and mitigation of risk, which serves as the primary aim of this chapter 4 and has already been computed in the preceding chapter. The subsequent sections will refer to the calculated component in order to analyse the risk.

### 4.4.1. Probability of failure

This section describes the probability of failure computation, which is function of downtime hours experienced due to the HP cooling system leak, during the cumulative operating time going from 2017 to 2020. Tables 3 and 4 in section 3.3 serve as illustrations of a subset of historical failure data and the condition monitoring data, respectively. A comprehensive link to the complete dataset is available in the appendix.

Referring to section 3.3.1, the maximum likelihood estimation, which is a well-known method to estimate the regression coefficients as defined in equation (20), allowed determining the shape parameter $\beta$. The characteristic life from equation (23) together with the computed shape parameter allowed determining the probability of failure using the two-parameter Weibull distribution method given by equation (51):

$$PoF = 1 - \exp[-\left(\frac{t}{\eta}\right)^{\beta}] \quad (51)$$

where the Weibull shape parameter $\beta$ is unit-less, it shows how the failure rate develops over time, the Weibull characteristic life parameter, $\eta$, in years, and $t$ is the independent variable time in years. The $PoF$ versus time in hours refers to figure 15 in section 3.3.1.

The cumulative distribution function in figure 15 shows a smooth increase of the probability of failure over time, whereas this work uses an approach based on the proportional hazard model PHM (with the moisture of the gas off and cumulative feedrate as covariate) which optimizes the $PoF$ estimation compared to the traditional method such as time-based (Lelo, Heyns & Wannenburg, 2022). $h[t, Z(t)]$ is the hazard rate based on the PHM :

$$h[t, Z(t)] = \frac{\beta}{\eta}\left(\frac{t}{\eta}\right)^{\beta-1} \exp\left\{\sum_{i=1}^{m} \gamma_i Z_i(t)\right\} \tag{52}$$

Referring to section 3.3.2.1, the covariates $Z_i(t)$ in equation (52), are monitored parameters that either relate to usage of the system, or condition of the system. Their influence on the hazard rate, and therefore on the $PoF$, are signified by weight factors ($\gamma_i$), which are estimated, together with the Weibull shape and scale parameters, based on a statistical maximum likelihood method, using historical data of the monitored parameters, as well as failure data. In this case study, the monitored cumulative feed rate throughput of the smelter was used as a usage covariate and the monitored moisture content in the off-gas was used as a condition parameter.

Comparative curves of the $PoF$ based on the two parameter Weibull versus the $PoF$ based on the PHM was previously given in figure 19. Examining figure 19, it can be observed that during the primary span of the HP cooling system's lifespan, the value derived from the PHM approach is lower than that determined by the time-based approach. This disparity highlights the substantial advantage of employing the PHM method for more realistic estimation, when compared to the time-based model.

### 4.4.2. Consequence of failure evaluation

Section 3.3.3 provides calculations of the consequence of failure for the HP cooling system based on the BLEVE, as current furnace designs often integrate extensive use of cooling elements to accomplish long service lives at high operating intensities. Therefore, contact between water and high temperature fluid can provoke explosion.As highlighted in section 3.3.3.2 concerning the impact of the BLEVE on human and construction, Abbasi and Abbasi

(2007) state that the assessment of the impact (consequence) of the overpressure due to BLEVE is determined by two factors :

- The energy of the explosion, or "burst energy". This determines the severity of the blast wave produced by the BLEVE. When a vessel containing a superheated liquid fails in a BLEVE, the “boiling liquid” as well as the “expanding vapour” together produce the burst energy.

- The manner of release of the vessel contents. This determines the size, duration, and heat flux of the fireball, if the contents are flammable.

In this chapter, the impact or consequence of a BLEVE will be estimated based on the overpressure. The overpressure related to the explosion versus the crack size refers to figure 21 in section 3.3.3.4. Figure 21 showed a rapidly decreasing pressure at increasing distances from the centre of the explosion. In the case study, this result is used to estimate the effect of the overpressure on humans at 20 m.

To estimate the impact of an accident on humans and structures, Section 3.3.3.4 introduced the probit equation, which evaluated the effects of overpressure on humans and constructions. The direct consequences of overpressure are lung haemorrhage on people and structural damage. The measure of the percentage of a population subjected to an effect with the intensity $(V)$ is performed by the probit variable Y. This variable follows a normal distribution, with an average value and standard deviation of 1. As was previously indicated the probit function is typically of the form:

$$Y = a + b \ln V \qquad (53)$$

Section 3.3.3.4 provides detailed calculations related to equation (53) presenting the effect of overpressure on human and construction. It is then important to evaluate the potential consequences and effects of overpressure caused by explosions on people and structures. The probit and probability equations were used to estimate lung haemorrhage damage and structure. Table 8 shows the probability of lung haemorrhage and damage impact on the structure. The probabilities in the table are based on the direct effect of overpressure only according to the equation (53). Table 8 provides detailed values of overpressure received by the surface at a distance X in meter.

*Table 8: Probability effect of overpressure on humans and structures.*

| Distance (X) in meter | Overpressure | Lung Haemorrhage (Y2) | Structural (Y4) | P2 | P4 |
|---|---|---|---|---|---|
| 20 | 2.466e+07 | 40.514 | 25.901 | 18.195 | 10.854 |
| 30 | 6.172e+06 | 30.941 | 21.856 | 13.390 | 8.814 |
| 40 | 2.746e+06 | 25.346 | 19.491 | 10.575 | 7.617 |
| 50 | 1.547e+06 | 21.380 | 17.815 | 8.573 | 6.767 |
| 60 | 9.915e+05 | 18.306 | 16.516 | 7.017 | 6.107 |
| 70 | 6.896e+05 | 15.798 | 15.456 | 5.741 | 5.566 |
| 80 | 5.075e+05 | 13.679 | 14.561 | 4.657 | 5.109 |
| 90 | 3.893e+05 | 11.845 | 13.786 | 3.712 | 4.712 |
| 100 | 3.081e+05 | 10.230 | 13.104 | 2.871 | 4.361 |
| 110 | 2.501e+05 | 8.787 | 12.494 | 2.109 | 4.047 |
| 120 | 2.071e+05 | 7.483 | 11.943 | 1.396 | 3.762 |
| 130 | 1.743e+05 | 6.295 | 11.441 | 0.701 | 3.502 |
| 140 | 1.489e+05 | 5.203 | 10.979 | 0.439 | 3.262 |
| 150 | 1.286e+05 | 4.193 | 10.553 | 1.080 | 3.039 |
| 160 | 1.223e+05 | 3.255 | 10.156 | 2.008 | 2.832 |

Figure 28 below expresses the percentage of people and structures affected by different effects and causes at a given point (overpressure effect).

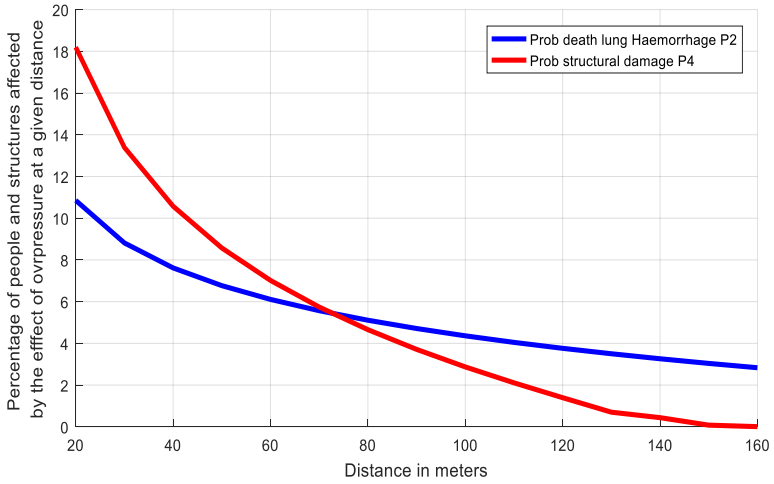


*Figure 25:Percentage of people and structures affected by effect and causes at a given point.*

Figure 25 shows the percentage of people and structures affected by overpressure. The results in table 8 reveal that at 20 meters distance, the probability of fatality is 18.195 % due to lung haemorrhage and 10.854% due to structure damage. These values can be used to define further risk mitigation strategies in the discussion section.

### 4.4.3. Risk computation

This section consists of rating risks using probability of occurrence and severity of consequence scale. Risk assessment consists of a series of procedure related to risk analysis, assessment of the degree of risk, judgement on whether the risk is acceptable or unacceptable (Embry et al., 2014)

In this, risk assessment will use probability of occurrence and severity of consequence scales to rate risk associated with the BLEVE effect in the system under analysis.

#### 4.4.3.1. Probability of occurrence

The probability of occurrence in this work corresponds to the probability of having an explosion, $PoF_{expl}$ explores the likelihood that the risk could occur. Probability of occurrence uses a rating and value ranging from inconceivable (1) to very likely (5). For the purposes of this paper, the probability of occurrence includes two probabilities:

- The probability of failure calculated from the history of failure - $PoF_h$
- The probability that the leak is at critical crack size - $PoF_{cra}$.

Then the probability of occurrence or the probability of having an explosion will be:

$$PoF_{expl} = PoF_h \times PoF_{cra} \qquad (54)$$

The only data set available to estimate $PoF_{cra}$, is the fact that a catastrophic steam explosion has occurred twice during the twelve-year life of the system. We therefore estimate that the event of the crack failure large enough which causes water accumulation occurred twice in twelve years, i.e. $(1/6$ yearly). The probability of a crack, if it occurs, being large enough to cause a steam explosion hence can thus be estimated as:

$$PoF_{cra} = (1/6)/PoF_h \text{ (at end of year)} \qquad (55)$$

From figure 19 it can be seen that $PoF_h(\text{at end of year}) = 0.83$. This means that we can estimate $PoF_{cra} = 1/6/(0.83) = 0.2 = 20\%$.

Failure probabilities of reactor pressure vessels have attracted significant attention in recent years. Extensive efforts have been dedicated to converting statistical evidence of conventional high pressure vessel integrity and findings from surveillance testing into failure probabilities specific to nuclear pressure vessels. Investigations on vessels comparable to nuclear vessels have been conducted both in the United Kingdom and in Germany. These investigations encompassed a total of approximately 100,000 and 1,000,000 vessel years, respectively. The overall number of failures relevant to nuclear vessel services corresponded to failure rates of $10^{-3}$ to $10^{-4}$ per year, Xiao, Shi, Cao, Xu, & Hu (2018) recently investigated the safety and reliability of pressure vessels considering various uncertain factors. The outcome from the investigation was that when the crack is shallow, the failure probability is less than $10^{-3}$. For the case of this work considering the scenario of having cracks in the piping circuit of the HP cooling system and based on the experience on the ground we assumed that failure happened twice every twelve years which justify the incorporation of $1/6$ in the probability calculation.

In the above it is useful to realise that the difference between the two probabilities $PoF_h$ and $PoF_{expl}$ is that ,$PoF_h$ denotes the calculated probability of failure based on historical failure data (which is either time-based or condition-based (PHM) as outlined in Table 9), whereas, $PoF_{expl}$ represents the probability of having an explosion in the event of the crack failure becoming large enough to cause a steam explosion.

4.4.3.2. Total probability of fatalities $Tpf$ (likelihood)

Risk measures the likelihood and severity of the accident to evaluate the magnitude and prioritize the hazard as shown in table 6. After the total probability of fatality and degree of harm is determined, the risk is assessed.

$$Tpf = PoF_h \times PoF_{cra} \times \text{Probit} \quad (\text{at end of year}) \qquad (56)$$

It is important to highlight that the introduction of the parameter ($PoF_{cra}$), is required to take account of the fact that not all HP system water leaks would cause a steam explosion. Historical incident investigations have concluded that steam explosions occur only when sufficient liquid-

phase water accumulates on the crust of the molten metal in the furnace, to break through the crust and then to come into direct contact with the molten metal below the crust. For this to happen, the rate of water leakage needs to be high enough and this will depend on the size of a pipe crack.

The result obtained from the total probability of fatality equation is considered as the likelihood or the y-axis in the risk matrix.

#### 4.4.3.3. Severity of Consequences

Severity of consequences assessments assign a rating based on the impact of an identified risk to safety, economic, persons and environment (Zakaria, Ismail, Rani, Amat, & Wahab, 2018). The severity of consequence assesses impacts in table 7 in the form of:

- Single fatality (Lung haemorrhage)
- Multiple fatality (Structural damage)

Table 9 Risk computation

| Age [hours] | PoF [Time-Based] | PoF [PHM] | Lung Haemor-rhage Probit $Y2$ | Structural Probit $Y4$ | Lung Ha. Probability of occurence [time-based] Likelihood | Lung Haemorrhage Probability of occ [PHM] Likelihood | Structural Probability of occurrence [ Time-based] Likelihood | Structural Probability of occurrence [PHM] Likelihood |
|---|---|---|---|---|---|---|---|---|
| 3.5 | 1.76e-05 | 1.7e-09 | 0.241 | 0.074 | 8.46e-07 | 8.18e-11 | 2.60e-07 | 2.51e-11 |
| 459 | 0.026 | 5.02e-06 | 0.241 | 0.074 | 1.25e-03 | 2.42e-07 | 3.85e-04 | 7.42e-08 |
| 2083 | 0.225 | 0.002 | 0.241 | 0.074 | 1.08e-02 | 9.64e-05 | 3.33e-03 | 2.96e-05 |
| 3519 | 0.429 | 0.02 | 0.241 | 0.074 | 2.07e-02 | 9.64e-04 | 6.35e-03 | 2.96e-04 |
| 4220 | 0.521 | 0.044 | 0.241 | 0.074 | 2.51e-02 | 2.12e-03 | 7.71e-03 | 6.51e-04 |
| 5191 | 0.633 | 0.112 | 0.241 | 0.074 | 3.05e-02 | 5.40e-03 | 9.37e-03 | 1.66e-03 |
| 5559 | 0.671 | 0.156 | 0.241 | 0.074 | 3.23e-02 | 7.52e-03 | 9.93e-03 | 2.31e-03 |
| 6542 | 0.758 | 0.309 | 0.241 | 0.074 | 3.65e-02 | 1.49e-02 | 1.12e-02 | 4.57e-03 |
| 7985 | 0.852 | 0.648 | 0.241 | 0.074 | 4.11e-02 | 3.12e-02 | 1.26e-02 | 9.59e-03 |
| 8798 | 0.89 | 0.826 | 0.241 | 0.074 | 4.29e-02 | 3.98e-02 | 1.32e-02 | 1.22e-02 |
| 8825 | 0.892 | 0.835 | 0.241 | 0.074 | 4.30e-02 | 4.02e-02 | 1.32e-02 | 1.24e-02 |
| 8832 | 0.892 | 0.835 | 0.241 | 0.074 | 4.30e-02 | 4.02e-02 | 1.32e-02 | 1.24e-02 |

### 4.4.4. Risk mitigation strategies and interpretation of the results

4.4.4.1. Introduction

1) Risk matrix for single fatality

For the lung haemorrhage, the likelihood (y-axis) is 0.040, which is rated 5 referring to table 6, while the single fatality is rated D according to table 7. To assess the risk for the lung haemorrhage we therefore obtain the couple (D,5) on the risk matrix, meaning severity (consequence) rated at D and likelihood at 5 (most likely), section 4.4.4.2 explains the meaning (D,5).

For the probability of fatality due to the structural damage, the likelihood value is 0.01, which is rated 4 in table 6, while the single fatality is rated to D according to table 7. Section 4.4.4.2 explains the meaning of (D,4) which is the couple severity and likelihood respectively.

2) Risk matrix for multiple fatality

Multiple fatality analyses consider the number of persons exposed in the risk and how far they should be moved away this would be the focus of our next chapter dealing with risk mitigation strategies.

4.4.4.2. Interpretation of the results

For the fatality occurring due to lung haemorrhage, a total probability value of 0.04 was calculated (in Table 9). This could be understood to mean that, if there existed a hundred such identical plants, it is to be expected that every year 4 explosions which will cause single fatality would occur, or alternatively, during a hundred years of operating one plant, there is an expectation of four fatalities. caused by explosions, would occur. The assessed risk for this situation at (D,5) on the risk matrix. The risk matrix in figure 24, from which the results are interpreted, has four coloured zones and our lung haemorrhage result falls in the red zone. The red zone generally means that a high risk exists that management's objectives would not be achieved and that it therefore needs to be mitigated immediately.

For the structural the total probability of fatality value is 0.01 which falls at 4 (likely) in the y-axis and the severity at D (a single fatality). The assessed risk of (D,4) in figure 24 falls in the

orange zone, which is called “medium high” in the API 581. At this level of risk, management’s objectives may not be achieved and there is a need to mitigate the risk as soon as possible.

#### 4.4.4.3. Suggested mitigation strategies

Considering the previous section showing risk at the red zone (D,5), there is necessity for risk mitigation strategies**.** Possible risk mitigating actions, to lower these risks to acceptable levels, include the following:

- Introducing inspections for cracks at frequencies sufficient to ensure repair actions are taken before leaks occur. This is the major objective of the RBI approach. The PHM method introduced in this paper, ensures more accurate quantification of the risk as it evolves over time, which implies a less onerous schedule.
- Shortening the duration of the campaigns of the furnace before swapping out and performing major rebuilds or replacements, whilst the assessed risk is still low enough. Again, the introduction of the PHM approach, makes this a viable mitigation action, since the risk increases rapidly towards the end of a campaign. It is important to note that the probability of failure results used to assess the risk, were end-of-campaign values.
- Making the end-of-campaign decision risk-based, implying that the furnace would be taken out of operation at an acceptable risk level, which will be dynamically calculated, using the PHM introduction of the covariates as inputs.
- Introducing controls, acting on the moisture measurement, to shut down the water-feed to the HP system as soon as any indication of leaking is noticed, to avoid the accumulation of sufficient water to cause the major explosion (ie, reducing the $PoF_{cra}$ parameter).

The following chapter will address each of the mitigation options suggested in this section by quantifying and interpreting them in the context of industrial plant.

#### 4.4.4.4. Risk mitigation based on probabilistic fracture mechanics analysis.

During the integrity assessment of a structure by fracture mechanics analysis, the goal is to determine critical crack sizes as well as fatigue crack propagation rates. Wannenburg (1994),

describes an analytical method to estimate the probability of failure of structure containing defects (Deng et al., 2021).

The probability that, if a defect exists, it is critical and remains in the structure after inspection and repair, is calculated as:

$$P_{fd} = P(a_c < a)(1 - P_d) \quad (57)$$

where $P_d$ is the probability that a defect will be detected by non-destructive inspection exercises.

The probability that a structure contains a critical defect after inspection and repair is given by:

$$P_f = 1 - (1 - P_{fd})^N \quad (58)$$

Where N is the number of defects before inspection. To define the detection probability $P_d$, Matzkanin and Yolken (2001) state that it is a function of crack size and depth of the crack (a larger crack would be more easily detectable). Wannenburg (1994) and other recent researchers use constant numbers for probability of detection (0.6 for limited inspection and 0.95 for good inspection).

The UK Health and Safety Executive (2017) gives values of the tolerable probability of failure arising from a calculated assessment of the integrity of a high quality fabrication as follows:

- Upper value: $6 \times 10^{-6}$
- Median value: $4 \times 10^{-6}$
- Lower value: $2 \times 10^{-6}$

In this chapter we consider the medium value of $4 \times 10^{-6}$ to implement a measure which would control the probability of failure in an effective manner. Inspection and repair schedules are the most common fracture control measures used in industry.

After each inspection, the number of defects remaining in the vessel would be reduced

to (1-$P_d$)× $N$. The probability of failure should therefore be reduced by a factor $(1 - P_d)$ after each inspection to keep the total probability of failure below $4 \times 10^{-6}$.

$$4 \times 10^{-6} > P_f(year) \times (1 - P_d)^i \quad (59)$$

where $i$ is the inspection number, and $P_f(year)$ is the largest possible original probability of failure, as a function of years in service, as determined.

#### 4.4.4.5. Risk mitigation through inspection

Section 4.4.4.3 considered implementation of the inspection based on mitigation strategy. In order to implement the outlined mitigation strategies equation (59) was solved to determine when each inspection should take place to keep the total probability of failure below $4 \times 10^{-6}$.

This probability value is the medium acceptable probability of failure, arising from a calculated assessment of the integrity of high -quality fabrication such as pressure vessel according to HSE - U.K. Health and Safety Executive.(2017). The results of this calculation are presented in table 4 and figure 28, which provide the recommended number of inspections, their frequencies, and the time at which each inspection should occur. These results can be used to effectively implement the mitigation strategies outlined in section 4.4.4.3.

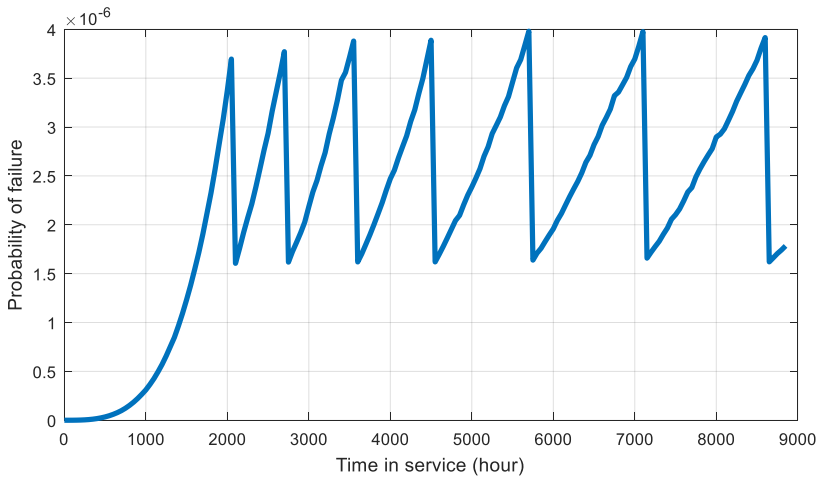


*Figure 26: Probability of failure versus time in service*

Considering the detection probability of 0.6 and the acceptable probability of failure arising from the assessment of the integrity of a high -quality pressure vessel, figure 26 and table 10 can be interpreted as follows:

Comparing figure 26 with figure 27, it can be observed that the probability of failure is very sensitive to the assumption concerning the detection probability.

Table 10 and figure 26 show that the probability of failure would therefore rise to $3.695 \times 10^{-6}$ at the end of 2050 hours of the HP cooling system life, at which time the first inspection would be performed. After inspection and repair the lowered probability of failure would then rise again to reach $3.771 \times 10^{-6}$ after 2700 hours when the second inspection would be performed. After 3550 hours, a third inspection would be required, thereby lowering the probability of failure again, etc.

For the detection probability of 0.9, figure 26 becomes:

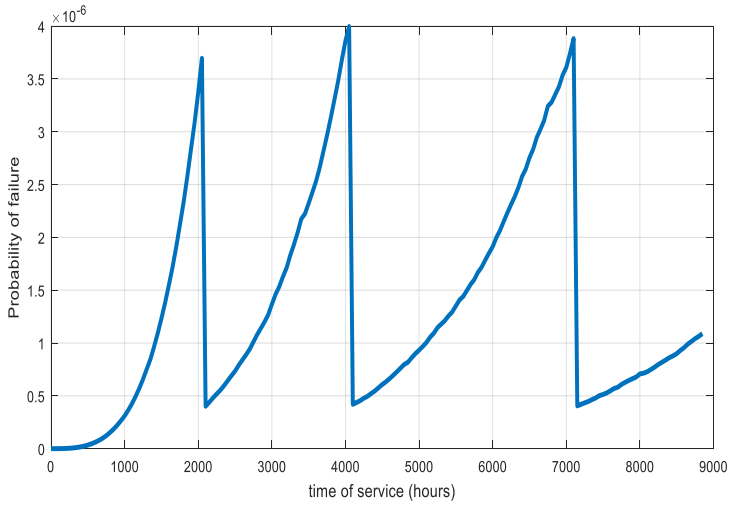


*Figure 27: Probability of failure versus time in service for detection probability of 0.9*

*Table 10: Inspection Schedule*

| Inspection number | Hours (Year) Inspection interval | Pf (year) Hours | Pf (year)$\times (1 - Pd)^{i-1}$ |
|---|---|---|---|
| 1 | 2050 | $3.695 \times 10^{-6}$ | $3.695 \times 10^{-6}$ |
| 2 | 2700 | $9.427 \times 10^{-6}$ | $3.771 \times 10^{-6}$ |
| 3 | 3550 | $2.424 \times 10^{-5}$ | $3.879 \times 10^{-6}$ |
| 4 | 4500 | $6.075 \times 10^{-5}$ | $3.888 \times 10^{-6}$ |
| 5 | 5700 | $1.555 \times 10^{-4}$ | $3.980 \times 10^{-6}$ |
| 6 | 7100 | $3.883 \times 10^{-4}$ | $3.976 \times 10^{-6}$ |
| 7 | 8600 | $9.559 \times 10^{-4}$ | $3.912 \times 10^{-6}$ |

The results presented in figure 26 and table 10 successfully address the mitigation strategies suggested in section 4.4.4.3. The first strategy involved implementing inspection for cracks, and the results recommend seven inspections at specific interval as shown in table 10. The other strategy involved shortening the duration of the furnace campaigns, and the results suggest setting the campaign duration at 2025 hours, which is the time to the first recommended inspection.

Considering the detection probability of 0.6 and the acceptable probability of failure arising from the assessment of the integrity of a high -quality pressure vessel, figure 26 and table 10 can be interpreted as follow:

Comparing figure 26 with figure 27, it can be observed that the probability of failure is very sensitive to the assumption concerning the detection probability.

Table 10 and figure 27 show that the probability of failure would therefore rise to $3.695 \times 10^{-6}$ at the end of 2050 hours of the HP cooling system life, at which time the first inspection would be performed. After inspection and repair the lowered probability of failure would then rise again to reach $3.771 \times 10^{-6}$ after 2700 hours when the second inspection would be performed. After 3550 hours, a third inspection would be required, thereby lowering the probability of failure again, etc.

#### 4.4.4.6. Shortening campaign duration

The results presented in figure 26 and table 10 also successfully address the shortened campaign duration mitigation strategy, suggested in section 4.4.4.3. The results suggest setting the campaign duration at 2025 hours, which is also the time to the first recommended inspection, since currently, the target maximum risk is exceeded.

#### 4.4.4.7. Risk based campaign duration.

Since the PHM method, used for calculating the $PoF$, can be updated during the campaign, using the monitored covariates as inputs, the risk assessment can also be dynamically updated. This implies that the end of campaign decision (and in fact, also the inspection frequencies), can be updated accordingly.

# Chapter 5. Conclusion and recommendations

The risk based inspection (RBI) methodology is an ideal tool for asset management because of its ability to optimize the inspection schedule and extent of inspection, which contribute to the saving of cost and prioritize inspection on important components.

When the potential consequences of failure ($CoF$) are high, it becomes imperative to perform quantified probability of failure ($PoF$) calculations. In cases where an accurate relationship between inspection or condition monitoring results and the remaining life, based on failure models, are not known, these calculations are based on statistical methods, using historical failure data, specifically time-based data.

With this research a case is made to introduce the utilization of proportional hazards modelling (PHM) in the realm of RBI. This has not been done before but it is demonstrated that the approach offers significant benefits. These benefits include:

- Time-based probability of failure calculations seems to be overly conservative compared to the PHM-based calculations.
- Dynamic condition and usage data is incorporated in the calculation, thereby enabling dynamic risk assessment.

It is therefore recommended that PHM methods are more generally applied in RBI programs. Similarly, the $CoF$ estimation in RBI programs are often done in qualitative manner (in fact, the RBI standard do not require quantified $CoF$ calculation in high risk situations, such as it does for ($PoF$).

Using a real-world case study as an example, this work illustrates the complexity of such quantification by considering one potential consequence of failure, by considering boiling expanding vapour explosions (BLEVEs). Although the work only considers this one potential consequence of failure, a methodology to deal with such consequences is illustrated in the context of the methodology that is presented earlier in the work. The work also illustrates the importance of considering such consequences. Although only considering the BLEVE situation, the point is strongly made that such analysis should be part of high-risk pressure vessel RBI programs.

Furthermore, due to the fact that the $CoF$ calculation for the case study, introduced statistical parameters such as the probit variable and the probability of fatalities. The possibility of complex interaction between $CoF$ (which is typically only seen as static, deterministic evaluation) and $PoF$ (where the statistical nature of the problem is quantified), is highlighted.

Based on the above, it is recommended that the RBI methodology should incorporate such situations where $PoF$ and $CoF$ are well quantified as illustrated in chapter 3. It was demonstrated that failure in the management of a high pressure (HP) cooling system for a metal smelting furnace, as water ingress into the furnace from leaks due to cracks, can cause a steam explosion. The risk management methodology incorporated a quantitative assessment of the Probability of Failure ($PoF$), based on Proportional Hazard Modelling (PHM), and the Consequence of Failure ($CoF$), using BLEVE methods, of an explosion event. Finally, risk mitigation strategies, such as using Risk Based Inspection principles to define the inspection frequency sufficient to ensure that repair actions are taken before leaks occur, or to shorten the furnace campaign duration before swapping out and performing major rebuild or replacement, to lower the risk to an acceptable level have been defined.

This study demonstrated the application of the RBI approach on a furnace high pressure cooling systems, incorporating the PHM and steam explosion consequence modelling, and demonstrated in terms of its application in risk assessment and mitigation, as well as the associated decision-making that it enables.

It is concluded that the research may contribute towards more effective and practical integrity management of pressure vessels using RBI principles.

From the observations made during this study, the following was highlighted as limitations and recommendations for future work:

- This study provides a foundation for the $PoF$ computation for the dynamic risk assessment (DRA) based on PHM. While the current API 581 standard relies on time-based analysis, the proposed methodology has the potential to be integrated into the API framework in the future.
- The estimation of PHM parameters requires enough lifetime data as well as condition monitoring data, which often is incomplete or missing, therefore, the use of knowledge elicitation (expert opinion) can be applied to determine Weibull parameters when there is not enough lifetime data.

- In the present work, a particular application and a specific type of accident have been considered, leading to the suggestion that future research should be conducted to explore various accident types.
- In this work, we have considered initially a simple application on experimental bearing data, followed by the validation of the method, and subsequently expanded to encompass the HP cooling system.

# Appendix

The downtime caused by the leakage of the HP cooling system facilitated the determination of the operating time required for the compilation of the historical failure data. In the second link, there are 32 histories, which present a connection between a specific age and the respective covariates, namely moisture and cumulative feed rate.

See the data available in the following link below:

Historical failure data for High-pressure cooling system

Downtime hours experienced due to HP leaks from 2017 until 2020 have been recorded

https://docs.google.com/spreadsheets/d/1KvEeE4eE00Nb8wWUFWIouDR1E4rKa-RiHkt7O_6CnsI/edit?usp=sharing

Campaign 1 prepared data (32 histories)

https://docs.google.com/spreadsheets/d/1Ski88ej2RWFlTJxB8QKFdwtIcvBqwaY0GMIYCTTPETs/edit?usp=sharing

# Bibliography

Abbasi, T., & Abbasi, S. A. (2007a). The boiling liquid expanding vapour explosion ( BLEVE): Mechanism , consequence assessment , management. Journal of loss Prevention in the Process Industries, *141*, 489–519. https://doi.org/10.1016/j.jhazmat.2006.09.056

Abimbola,M.O,Faisal K, Khakzad N (2014), Dynamic safety risk analysis of offfshore drilling, *Journal of Loss Prevention in the Process Industries*,30(5),74-85.

Ahumada, C. B. (2016). Probabilistic Risk Assessment Tool Applied in Facility Layout Optimization, (August). Retrieved from http://oaktrust.library.tamu.edu/handle/1969.1/157941

AlKazimi, M. A., & Grantham, K. (2015). Investigating new risk reduction and mitigation in the oil and gas industry. *Journal of Loss Prevention in the Process Industries*, *34*, 196–208. https://doi.org/10.1016/j.jlp.2015.02.003

Andreis, F. De, & Florio, M. (2019). Risk Management Instruments, Strategies and Impacts in the Complex Organizations. *American Journal of Industrial and Business Management*, *09*(05), 1157–1167. https://doi.org/10.4236/ajibm.2019.95078

API RP 581. (2016). *Risk-Based Inspection Methodology*. *American Petroleum Institute* (Vol. 3rd Ed.).

Aven, T., & Pörn, K. (1998). Expressing and interpreting the results of quantitative risk analyses. Review and discussion. *Reliability Engineering and System Safety*, *61*(1–2), 3–10. https://doi.org/10.1016/S0951-8320(97)00060-4

Bao, C., Wu, D., Wan, J., Li, J., & Chen, J. (2017). Comparison of Different Methods to Design Risk Matrices from the Perspective of Applicability. *Procedia Computer Science*, *122*, 455–462. https://doi.org/10.1016/j.procs.2017.11.393

Bhatia, K., Khan, F., Patel, H., & Abbassi, R. (2019).Dynamic risk-based inspection methodology. *Journal of Loss Prevention in the Process Industries*, *62*(October), 103974. https://doi.org/10.1016/j.jlp.2019.103974

Birk, A. M. (2008). Review of expanded aluminum products for explosion suppression in containers holding flammable liquids and gases. *Journal of Loss Prevention in the Process Industries*, *21*(5), 493–505. https://doi.org/10.1016/j.jlp.2008.04.001

Birk, A. M., Heymes, F., Eyssette, R., Lauret, P., Aprin, L., & Slangen, P. (2018). Near-field BLEVE overpressure effects: The shock start model. *Process Safety and Environmental Protection*, *116*, 727–736. https://doi.org/10.1016/j.psep.2018.04.003

Carstens, W.& Vlok, P. . (2013). Through-life diagnostic information using the Proportional Hazards Model. *South African Journal of Industrial Engineering*, *24*(August), 59–68.

Declerck, L. (2002). Quantitative risk assessment. *Topics in Modelling of Clustered Data*, 157–172. https://doi.org/10.26634/jfet.6.1.1292

Deng, F., Li, S. Q., Zhang, X. R., Zhao, L., Huang, J. B., & Zhou, C. (2021). An intelligence method for recognizing multiple defects in rail. *Sensors*, *21*(23). https://doi.org/10.3390/s21238108

Duijm, N. J. (2015). Recommendations on the use and design of risk matrices. *Safety Science*, *76*, 21–31. https://doi.org/10.1016/j.ssci.2015.02.014

Embry, M. R., Bachman, A. N., Bell, D. R., Boobis, A. R., Cohen, S. M., Dellarco, Doe, J. E. (2014). Risk assessment in the 21st century: Roadmap and matrix. *Critical Reviews in Toxicology*, *44*(SUPPL.3), 6–16. https://doi.org/10.3109/10408444.2014.931924

Gebremeskel, N. H., & Gebregziabher, H. F. (2021). Developing guideline for risk management of tunnel construction in Ethiopia. *Open Journal of Safety Science and Technology*, *11*(04), 171–183. https://doi.org/10.4236/ojsst.2021.114012

Giribone, R., & Valette, B. (2004). Principles of failure probability assessment (PoF). *International Journal of Pressure Vessels and Piping*, *81*(10-11 SPEC.ISS.), 797–806. https://doi.org/10.1016/j.ijpvp.2004.07.010

Guyonnet, D. (2009). Bayesian methods in risk assessment Prepared for by. *Report*, 1–58.

Hadj-Mabrouk, H. (2017). Preliminary Hazard Analysis (PHA): New hybrid approach to railway risk analysis. *International Refereed Journal of Engineering and Science*, *6*(2), 51–58. Retrieved from www.irjes.com

Harman, M. (2018). Practical Bayesian Analysis for Failure Time Data, (June). Retrieved from www.afit.edu/STAT.

Heerings, J. H. A. M., & den Herder, A. J. (2004). Consequence of failure for RBMI 29th MPA Seminar, Stuttgart, October 9 and 10, 2003. *International Journal of Pressure Vessels and Piping*, *81*(10-11 SPEC.ISS.), 787–796. https://doi.org/10.1016/j.ijpvp.2004.07.011

Hemmatian, B., Planas, E., & Casal, J. (2017). Comparative analysis of BLEVE mechanical energy and overpressure modelling. *Process Safety and Environmental Protection*, *106*, 138–149. https://doi.org/10.1016/j.psep.2017.01.007

Henry, P. A., & Osage, D. A. (2014). Recent developments and technology improvements in api risk-based inspection planning technology. *10th Process Plant Safety Symposium, Topical Conference at the 2008 AIChE Spring National Meeting*, (January), 175–203.

HSE - U.K. Health and Safety Executive. (2017). Failure Rate and Event Data for use within Risk Assessments. *Health & Safety Executive Offshore Safety Division*, *1*(1), 1–96.

Jardine, A. K. S., Tsang, A. H. C. (2013). *Maintenance, Replacement, and Reliability*. *Maintenance, Replacement, and Reliability*. https://doi.org/10.1201/b14937

Jardine A.K.S, Tsang A.H.C. (2013). *Maintenance,Replacement,and Reliability(Theory and applications)* (Taylor and). Boca Raton: CRC pRESS.

Jardine A.K.S , Anderson P.M, Mann D.S. (1987). *Application of the weibull proportional hazards model to aircraft and marine engine failure data* .Quality and reliability engineering international. Vol 1, (77-81).

Jovanovic, A. (2004). Overview of RIMAP project and its deliverables in the area of power plants. *International Journal of Pressure Vessels and Piping*, *81*(10-11 SPEC.ISS.), 815–824. https://doi.org/10.1016/j.ijpvp.2004.07.001

Jovanovic, A. S., Auerkari, P., & Brear, J. (2001). Risk-related issues in life management of power plant components : inspection , monitoring , code-based analysis, (June).

Kalantarnia, M., Khan, F., & Hawboldt, K. (2009). Dynamic risk assessment using failure assessment and Bayesian theory. *Journal of Loss Prevention in the Process Industries*, *22*(5), 600–606. https://doi.org/10.1016/j.jlp.2009.04.006

Kennedy, M. W., MacRae, A., Jones, R. T., Kolbeinsen, L., Nos, P., & Filzwieser, A. (2013). Some considerations for safer furnace cooling. *Com 2015*, *53*(9), 1689–1699.

Kennedyl, M. W., Nos, P., Bratt, M., Weaver, M., & States, U. (2013). SAFER FREEZE LINED FURNACE OPERATION, 299–300.

Khakzad, N., Khan, F., & Amyotte, P. (2012). Dynamic risk analysis using bow-tie approach. *Reliability Engineering and System Safety*, *104*, 36–44. https://doi.org/10.1016/j.ress.2012.04.003

Kumar, R. & Rushaid, M. (2018). Consequence Analysis of LPG Storage Tank. *Materials Today: Proceedings*, *5*(2), 4359–4367. https://doi.org/10.1016/j.matpr.2017.12.003

LeClere, M. J. (2005). Time-Dependent and Time-Invariant Covariates Within a Proportional Hazards Model: A Financial Distress Application. *SSRN Electronic Journal*, (April). https://doi.org/10.2139/ssrn.311301

Lelo, N. A., Heyns, P. S., & Wannenburg, J. (2019). Forecasting spare parts demand using condition monitoring information. *Journal of Quality in Maintenance Engineering*, *26*(1), 53–68. https://doi.org/10.1108/JQME-07-2018-0062

Lelo, N. A., Stephan Heyns, P., & Wannenburg, J. (2022). Development of an approach to incorporate proportional hazard modelling into a risk-based inspection methodology. *Journal of Quality in Maintenance Engineering*,. https://doi.org/10.1108/jqme-04-2021-0030

Li, Z. P., Yee, Q. M. G., Tan, P. S., & Lee, S. G. (2014). An extended risk matrix approach for supply chain risk assessment. *IEEE International Conference on Industrial Engineering and Engineering Management*, 1699–1704. https://doi.org/10.1109/IEEM.2013.6962700

Liao, K., Qin, M., He, G., Chen, S., Jiang, X., & Zhang, S. (2023). Improvement of integrity management for pressure vessels based on risk assessment - A natural gas separator case study. *Journal of Loss Prevention in the Process Industries*, *83*(May), 105087. https://doi.org/10.1016/j.jlp.2023.105087

Liu, H. C., Liu, L., & Liu, N. (2013). Risk evaluation approaches in failure mode and effects analysis: A literature review. *Expert Systems with Applications*, *40*(2), 828–838. https://doi.org/10.1016/j.eswa.2012.08.010

Lorenzoni, A., Kempf, M., & Mannuß, O. (2017). Degradation model constructed with the aid of dynamic Bayesian networks. *Cogent Engineering*, *4*(1). https://doi.org/10.1080/23311916.2017.1395786

Markowski, A. S., & Mannan, M. S. (2008). Fuzzy risk matrix. *Journal of Hazardous Materials*, *159*(1), 152–157. https://doi.org/10.1016/j.jhazmat.2008.03.055

Matzkanin, G. A., & Yolken, H. T. (2001). *A Technology Assessment of Probability of Detection (POD) for Nondestructive Evaluation*. *Ntiac*. Retrieved from http://oai.dtic.mil/oai/oai?verb=getRecord&metadataPrefix=html&identifier=ADA3982

Meel, A., & Seider, W. D. (2006). Plant-specific dynamic failure assessment using Bayesian theory. *Chemical Engineering Science*, *61*(21), 7036–7056. https://doi.org/10.1016/j.ces.2006.07.007

Mustapha, S., & El-Harbawi, M. (2016). Capability of GIS in the analysis of explosion hazard from BLEVE event in LPG Terminal. *American Academic Scientific Research Journal for Engineering, Technology, and Sciences*, *26*(4), 343–363. Retrieved from https://asrjetsjournal.org/index.php/American_Scientific_Journal/article/view/2463

Narain Singh, S., & Pretorius, J. H. C. (2017). Development of a sem-quantitative approach for risk based inspection and maintenance of thermal power plant components. *SAIEE Africa Research Journal*, *108*(3), 128–137.

Nguyen, K. T. P., Fouladirad, M., & Grall, A. (2018). New Methodology for Improving the Inspection policies for degradation model selection according to prognostic measures. *IEEE Transactions on Reliability*, *67*(3), 1269–1280. https://doi.org/10.1109/TR.2018.2829738

Ni, H., Chen, A., & Chen, N. (2010). Some extensions on risk matrix approach. *Safety Science*, *48*(10), 1269–1278. https://doi.org/10.1016/j.ssci.2010.04.005

Ochella, S., Shafiee, M., & Sansom, C. (2021). Adopting machine learning and condition monitoring P-F curves in determining and prioritizing high-value assets for life extension. *Expert Systems with Applications*, *176* (March), 114897. https://doi.org/10.1016/j.eswa.2021.114897

Planas-Cuchi, E., Salla, J. M., & Casal, J. (2004). Calculating overpressure from BLEVE explosions. *Journal of Loss Prevention in the Process Industries*, *17*(6), 431–436. https://doi.org/10.1016/j.jlp.2004.08.002

Prayogo, G. S., Haryadi, G. D., Ismail, R., & Kim, S. J. (2016). Risk analysis of heat recovery steam generator with semi quantitative risk based inspection API 581. *AIP Conference*

*Proceedings*, *1725* (April 2016). https://doi.org/10.1063/1.4945516

Randall, R. B., & Antoni, J. (2011). Rolling element bearing diagnostics: A tutorial. *Mechanical Systems and Signal Processing*, *25*(2), 485–520. https://doi.org/10.1016/j.ymssp.2010.07.017

Rodolfo, B., Mason, M. C., & Nassivera, F. (2011). Green marketing and renewable energy: evidence on motivations and behaviour in the aquacultural market. *Chinese Business Review*, *10*(12). https://doi.org/10.17265/1537-1506/2011.12.003

Ryser, G. R. (2021). Qualitative and quantitative approaches to assessment. *Identifying Gifted Students*, 33–57. https://doi.org/10.4324/9781003235682-2

Salzano, E., Iervelino, I., Fabbrocino. (2001). Seismic risk of atmosphericstorage tanks by probit analysis.University of Naples.

Shamshoian, J., Şentürk, D., Jeste, S., & Telesca, D. (2022). Bayesian analysis of longitudinal and multidimensional functional data. *Biostatistics*, *23*(2), 558–573. https://doi.org/10.1093/biostatistics/kxaa041

Shariff, A. M., Wahab, N. A., & Rusli, R. (2016). Assessing the hazards from a BLEVE and minimizing its impacts using the inherent safety concept. *Journal of Loss Prevention in the Process Industries*, *41*, 303–314. https://doi.org/10.1016/j.jlp.2016.01.001

Shishesaz, M. R., Nazarnezhad Bajestani, M., Hashemi, S. J., & Shekari, E. (2013). Comparison of API 510 pressure vessels inspection planning with API 581 risk-based inspection planning approaches. *International Journal of Pressure Vessels and Piping*, *111–112*, 202–208. https://doi.org/10.1016/j.ijpvp.2013.07.007

Singh, M., & Pokhrel, M. (2018). A Fuzzy logic-possibilistic methodology for risk-based inspection (RBI) planning of oil and gas piping subjected to microbiologically influenced corrosion (MIC). *International Journal of Pressure Vessels and Piping*, *159* (November 2017), 45–54. https://doi.org/10.1016/j.ijpvp.2017.11.005

Square, W., Kingdom, U., Gini, A., Cornia, A., Fields, G., Lustig, N., & Subramanian, S. (2017). L aurence R oope 2, (4), 661–684.

Steijn, W. M. P., Van Kampen, J. N., Van der Beek, D., Groeneweg, J., & Van Gelder, P. H. A. J. M. (2020). An integration of human factors into quantitative risk analysis using Bayesian Belief Networks towards developing a 'QRA+.' *Safety Science*, *122*(February

2019), 104514. https://doi.org/10.1016/j.ssci.2019.104514

Syawalina, K. M., Priyanta, D., & Siswantoro, N. (2020). Inspection scheduling programs analysis of amine reboiler heat exchanger using risk-based inspection API 581 Method. *International Journal of Marine Engineering Innovation and Research*, *5*(4). https://doi.org/10.12962/j25481479.v5i4.7574

Saqib, N., Mysorewala, M. F., & Cheded, L. (2017). A multiscale approach to leak detection and localization in water pipeline network. *Water Resources Management*, *31*(12), 3829–3842. https://doi.org/10.1007/s11269-017-1709-3

Vianello, C., Guerrini, L., Maschio, G., & Mura, A. (2014). Consequence analysis: Comparison of methodologies under API standard and commercial software. *Chemical Engineering Transactions*, *36* (August 2015), 511–516. https://doi.org/10.3303/CET1436086

Viviers, P., & Hines, K. (2005). The new anglo platinum converting project. *Australasian Institute of Mining and Metallurgy Publication Series*, (November), 101–108.

Vlok, P.-J., & Coetzee, J. L. (2012). Advances in renewal decision-making utilising the Proportional Hazards Model With Vibration Covariates. *The South African Journal of Industrial Engineering*, *11*(2), 99–111. https://doi.org/10.7166/11-2-367

Wannenburg, J. (1994).The determinationof cost-effective NDE inspection schedule structure containing defect based on probabilisticfailure mechanics, *International Journal of Pressure Vessel 59, 259–269.*

Wiseman, M., Lin, D., Gurvitz, N., & Dundics, M. (2006). The Elusive P-F Interval, *2016*(28 August), 1–13. Retrieved from http://www.omdec.com/articles/reliability/ElusivePF.php

Wyckaert, P., Nadeau, S., & Bouzid, H. (2017). Analysis of Risks of Pressure Vessels. *Kongress Der Gesellschaft Für Arbeitswissenschaft FHNW Brugg-Windisch, Schweiz*, (February). Retrieved from https://www.researchgate.net/publication/313985693%0Ahttp://www.iaeng.org/publication/WCE2010/WCE2010_pp1120-1123.pdf

Xiao, Z., Shi, J., Cao, X., Xu, Y., & Hu, Y. (2018). Failure probability analysis of pressure vessels that contain defects under the coupling of inertial force and internal pressure. *International Journal of Pressure Vessels and Piping*, *168* (September), 59–65. https://doi.org/10.1016/j.ijpvp.2018.09.005

Zakaria, Z., Ismail, S., Rani, W. N. M. W. M., Amat, R. C., & Wahab, M. H. (2018). Fire Hazard assessment during construction of a mixed-use development project in Kuala Lumpur. *International Journal of Engineering and Technology (UAE)*, *7*(3), 5–10. https://doi.org/10.14419/ijet.v7i3.9.15262

Zeng, Z., & Zio, E. (2018). Dynamic Risk Assessment Based on Statistical Failure Data and Condition-Monitoring Degradation Data. *IEEE Transactions on Reliability*, *67*(2), 609–622. https://doi.org/10.1109/TR.2017.2778804

Zio, E. (2018). The future of risk assessment. *Reliability Engineering and System Safety*, *177* (April), 176–190. https://doi.org/10.1016/j.ress.2018.04.020